ГІРНИЧИЙ ВІСНИК

Заснований у 1966 році
Періодичність випуску: 2 рази на рік

Том 59, № 2

Кривий Ріг
2025

ISSN 2306-5435
УДК 622
DOI: 10.31721/2306-5435-2025-2

Засновник:
Криворізький національний університет

Рекомендовано до друку та поширення
через мережу Інтернет Вченою радою
Криворізького національного університету
(протокол № 5 від 24 грудня 2025 р.)

Державна реєстрація:
Ідентифікатор медіа R30-04964.
Рішення Національної ради України з питань телебачення
і радіомовлення № 1501, протокол № 15 (09.05.2024 р.)

Науковий журнал включено до категорії «Б» Переліку наукових фахових видань України.
Спеціальності: 121 – Інженерія програмного забезпечення, 122 – Комп'ютерні науки, 123 – Комп'ютерна інженерія, 131 – Прикладна механіка, 133 – Галузеве машинобудування, 136 – Металургія, 151 – Автоматизація та комп'ютерно-інтегровані технології, 183 – Технології захисту навколишнього середовища, 184 – Гірництво, 192 – Будівництво та цивільна інженерія, 193 – Геодезія та землеустрій, 263 – Цивільна безпека, 274 – Автомобільний транспорт, 275 – Транспортні технології (за видами)
(наказ МОН України від 17 березня 2020 року № 409)

Журнал індексується в наукометричних базах даних:
Національна бібліотека України імені В. І. Вернадського (НБУВ), Google Академія, Інститут проблем реєстрації інформації Національної академії наук України, Dimensions, Бібліотека Університету Осло, Litmaps, Ulrichsweb, Open Ukrainian Citation Index (OUCI), J-Gate

Контактна адреса:
Криворізький національний університет
50027, вул. В. Матусевича, 11, м. Кривий Ріг, Україна
E-mail: info@mining-journal.com.ua
https://mining-journal.com.ua/uk

MINING JOURNAL
of Kryvyi Rih National University

Founded in 1966
Frequency: 2 times a year

Volume 59, No. 2

Kryvyi Rih
2025

ISSN 2306-5435
UDC 622

DOI: 10.31721/2306-5435-2025-2

Founder:

Kryvyi Rih National University

Recommended for printing and distribution
via the Internet by the Academic Council
of Kryvyi Rih National University
(Minutes No. 5 of December 24, 2025)

State Registration:
Media identifier R30-04964.
Decision of the National Council of Television
and Radio Broadcasting of Ukraine No. 1501, Minutes No. 15, dated 09.05.2024

The scientific journal is included in category "B" of the List of scientific specialised publications of Ukraine.
Specialties: 0532 – Earth sciences, 0613 – Software and applications development and analysis,
0712 – Environmental protection technology, 0714 – Electronics and automation, 0715 – Mechanics
and metal trades, 0724 – Mining and extraction, 0732 – Building and civil engineering,
1032 – Protection of persons and property, 1041 – Transport services
(Order of the Ministry of Education and Science of Ukraine No. 409, dated 17.03.2020)

The journal is indexed in databases:
Vernadsky National Library of Ukraine (VNLU), Google Scholar, Institute of Information Registration Problems
of the National Academy of Sciences of Ukraine, Dimensions, University of Oslo Library, Litmaps, Ulrichsweb,
Open Ukrainian Citation Index (OUCI), J-Gate

Address for contacts:
Kryvyi Rih National University
50027, 11 Vitalii Matusevich Str., Krivyi Rih, Ukraine
E-mail: info@mining-journal.com.ua
https://mining-journal.com.ua/en

Редакційна колегія

Editorial Board

Зміст / Contents

Journal homepage: https://mining-journal.com.ua/en
ISSN 2306-5435
MINING JOURNAL
of Kryvyi Rih National University
Vol. 59, No. 2, 2025
Received: 30.06.2025; Revised: 01.12.2025; Accepted: 24.12.2025; Published: 05.01.2026

UDC 622.272/.271:622.83
DOI: 10.31721/2306-5435-2025-2-10-20

Oleksandr Shepel*
PhD in Technical Sciences, Associate Professor
Kryvyi Rih National University
50027, 11 Vitalii Matusevich Str., Kryvyi Rih, Ukraine
https://orcid.org/0000-0003-4581-5441

Stress-strain state research of rock mass during open-pit mining of minerals

Abstract. Sustaining the stability and load-bearing capacity of open-pit mine slopes is a critical and complex condition for the transition to open-pit-to-underground mining methods. For this reason, the research in this study aimed to provide a geomechanical justification for the stability of the technological elements of the open-pit-to-underground mining complex. This justification, conducted using a developed model, aimed to determine the influence on the formation of the rock mass's stress-strain state, exemplified by the quarries of the Kryvyi Rih mining and processing plants. In this work, mathematical and numerical methods were applied to predict the influence of the open pit on subsequent underground extraction, including the finite element method, as well as statistical and factor analysis. Additionally, to investigate the stress-strain state of the rock mass surrounding the depleted open pit, the software "Ansys, Inc. Products 2019 R3" was used. It was established that the magnitude of the maximum vertical displacements of the pit slope increases from 13-14 mm on the upper benches at depths of 30-45 m from the ground surface to 60-63 mm on the lower benches at depths of 270-300 m at the bottom of the depleted pit. The dependence of the magnitude of the maximum vertical displacements of the pit slope elements on the depth of excavation is described by a logarithmic function. It was also established that the stress magnitude ranges from 0.7-1.2 MPa at the pit bottom to 4.6-4.9 MPa beneath the pit floor at the depth of the future underground stopes. The dependence of the magnitude of the maximum stresses in the rock mass beneath the pit floor on depth is described by an exponential function. The calculations made it possible to obtain quantitative data on the change in the stress state of the rock mass depending on depth. The practical significance of the work lies in using these indicators to ensure a safe and effective transition to underground mining technology

Keywords: open-pit mine; geomechanical justification; integrated mining; dependence; modelling

Introduction

Safe and efficient transition from open-pit to open-pit-to-underground and purely underground mining technology depends on geomechanical processes within the rock mass. An understanding of these processes is crucial for ensuring accident-free mineral extraction in open-pit mines where underground operations are conducted beneath them. The most complex and difficult-to-predict phenomena are deformations of the open-pit fields, which are worked using the open-pit-to-underground method. The presence of open-pit slopes

Suggested Citation:
Shepel, O. (2025). Stress-strain state research of rock mass during open-pit mining of minerals. *Mining Journal of Kryvyi Rih National University*, 59(2), 10-20. doi: 10.31721/2306-5435-2025-2-10-20.

*Corresponding author

influences the propagation of deformations from underground operations and leads to the development of specific failure mechanisms.

M. Kimour *et al.* (2023) indicated that the occurrence of ground surface displacements and deformations during underground mining differs significantly, even within a single deposit. This is particularly noticeable at mines extracting the upper horizons of steeply dipping ore bodies. The behaviour of the rock mass is non-linear and time-dependent, which, when combined with natural factors such as fracturing, rock inhomogeneity, and others, introduces elements of randomness into deformation prediction. The nature of ground surface deformations during ore body extraction depends on the dimensions of the worked-out space, specifically its extent and depth. If the dimensions of the extraction beneath the open-pit floor are sub-critical relative to the depth of the ore body, the overlying barren rock forms a stress arch, which redistributes the load to the undisturbed rock mass. In this scenario, deformations do not reach the ground surface or the pit surface at all, causing only minor, localised displacements. When the dimensions of the worked-out area, particularly the strike length or total length, reach super-critical values relative to depth, the overlying rock mass no longer creates a stable arch; it collapses, and deformations propagate to the ground or pit surface. According to research by O. Ivasivka *et al.* (2023), this leads to the formation of a subsidence basin, gradual ground subsidence, surface collapses, or slope and bench failures of the open pit.

M.N. Bagde (2021) noted that the ratio of critical dimensions to depth depends on multiple factors. These include the physico-mechanical properties of the rocks, their fracturing, the dip angle of the ore body, and the selected mining method. An example of such a method is the use of cemented backfill to fill the worked-out space. Subsequently, in the hanging wall, zones of collapse or funnel formation, terraces, followed by cracks, and finally gradual subsidence are formed. This sequence reflects the progressive dampening and change in the nature of deformations as one moves away from the epicentre of the underground extraction influence towards the hanging wall. This is a result of the hanging wall being prone to more active displacement and subsidence towards the worked-out space due to gravity and mining-induced stresses. Thus, the mechanism described by O. Kulikovska *et al.* (2024) leads to the deformation and failure of the hanging wall, from the most intense manifestations near the underground stoping area to more gradual ones at the periphery of the zone of influence. With further extraction, the zone of gradual subsidence moves into the hanging wall of the ore body. In its place, cracks and terraces appear, and collapses in the form of funnels are formed on the ground surface. The former funnels merge into several groups, creating larger collapses that extend towards the hanging wall of the rock mass.

Determination of stable slope angles for the open-pit-to-underground mining level is performed by a calculation method. For instance, to determine the limit stability of slopes during the transition from open-pit to open-pit-to-underground mining, Y. Shen *et al.* (2024) propose a methodology based on using a rock mass displacement indicator. In this methodology, the displacement indicator is used as a criterion because excessive displacements or their rate of development are a direct indication that the rock mass is losing its integrity, significant deformations are occurring, and it is approaching a state of failure or is beyond the limits of acceptable deformation for the safe preservation of the pit slope. An algorithm also exists for determining the limit stability of slopes during the transition from open-pit to open-pit-to-underground mining, according to the methodologies concerning the Hannivske quartzite deposit in Kryvbas. According to this methodology, the calculation of stable slope angles is carried out with a safety factor of 1.3. This value is a design criterion for stability, considered sufficient to ensure the safety and reliability of the slopes under the conditions of the Hannivske deposit. As noted by N. Zuievska *et al.* (2023), this takes into account the properties of the quartzites, depth, hydrogeology, etc. The development of ground surface displacements with physical destruction and collapse during the transition from open-pit to open-pit-to-underground mining is dangerous and requires the implementation of safe transitional technologies. Such technologies prevent the development of any disturbances to the pit slopes during the transition to integrated mining of minerals within the existing open-pit area. Therefore, ensuring the stability and load-bearing capacity of pit slopes are important conditions for mining deposits using the open-pit-to-underground method.

The aim of the work was to study the stress-strain state of the rock mass to justify its load-bearing capacity and the stability of the pit slopes and underground workings during their combined extraction. For this purpose, using a developed model, the influence of open-pit mining on the stress-strain state of the rock mass during the transition to underground operations was determined.

Materials and Methods

Mathematical modelling was used as a tool for finding optimal solutions. Its essence lies in the iterative or analytical modification of input parameters. At each stage, the influence of these changes on associated technological characteristics was assessed to ultimately find the extreme maximum or minimum value of the objective function. Regarding the specific task of mathematical modelling, a phased change in parameters was carried out. These parameters characterise the direction of development of the open-pit and open-pit-to-underground mining operations, the change in the structure of comprehensive mechanisation at the quarry, and their influence on the intensity of ore production (the production capacity of the open-pit and open-pit-to-underground operations) in the combination zone. The developed mathematical model represents a set of numerical parameters that describe the geological and technological features of both the open pit and the mine field. This model links these parameters with one another, and its main goal is to maximise mineral extraction.

The research was conducted using the quarries of the Kryvyi Rih mining and processing plants as an example. The selection of these quarries was relevant, as it is here that the problems of deep open pits during the transition to underground mining, complex mining and geological conditions (strong but fractured quartzites), and the presence of large volumes of worked-out spaces make the issues of ensuring the stability and load-bearing capacity of the pit slopes urgent and complex. A model was presented for the research that corresponded to the average statistical dimensions of the Kryvbas quarries (Razumova *et al.*, 2021). The model was based on averaged data from the Kryvyi Rih mining and processing plants, such as Nothern, Inhulets, and Central. It also corresponded to the optimal dimensions of open pits in developed mining countries that have transitioned from open-pit to underground or integrated methods of mineral deposit extraction.

Initial geometric data for the open-pit model included a final depth of 300 m. The average height and width of the bench were 15 m. The total width of the open pit at the top, at ground level, was approximately 2,000 m, while its bottom width, corresponding to the thickness of the ore body, averaged 80 m. Mathematical methods were used in the work to create models that predicted how open-pit mining influenced subsequent underground mining. Specifically, numerical modelling methods and finite element analysis were used. To increase the accuracy of the modelling, the physico-mechanical properties of heterogeneous rocks and the technological features of the stoping operations were taken into account. The data obtained from the model were analysed using statistical and factor analysis methods, which allowed for the assessment and minimisation of risks.

To investigate the stress-strain state of the rock mass surrounding the depleted open pit, the software "Ansys, Inc. Products 2019 R3" was applied. This powerful tool, which is based on the finite element method, made it possible to model the behaviour of the rock mass under the load of the overlying barren rock. To investigate the stress-strain state of the rock mass surrounding the open pit using the "Ansys, Inc. Products 2019 R3" software, the following stages had to be performed. First of all, a three-dimensional geometric model had to be created. The model included the open pit and the adjacent rock mass. After the model was created, it had to be divided into smaller elements, specifically, meshed. The process of building a mesh for the deposit model consisted of discretisation; that is, the complex three-dimensional volume of the rock mass, the ore body, and the rocks in the pit slopes was divided into a large number of small finite elements.

During the modelling of the rock mass deposit between the existing and the designed open-pit mine, the model's mesh division was a key element for conducting a numerical analysis of the stress-strain state. Effective modelling required a substantiated choice of mesh element type, which corresponded to the physics and geometry of the problem, as well as the selection of element size, which ensured the necessary accuracy, especially in critical zones, with acceptable computational power. As part of the modelling methodology, mesh densification was applied in critical areas. This allowed for more detailed results in locations of greatest interest, such as in the corners formed at the bottom of the open-pit.

Unstructured meshing has been an indispensable tool for modelling complex geology, with its quality and accuracy achieved through appropriate refinement in specific zones and the use of higher-order elements. While it was necessary to refine the mesh in areas of concentration, it was critically important to ensure a smooth transition from a fine mesh to a coarser one at a certain distance from the concentrator itself. The software suite "Ansys, Inc. Products 2019 R3" had special tools and settings to control the rate of change in element size between adjacent regions, for instance, the element size growth rate. According to research by M. Tomova & A. Kisyov (2024), adherence to the rule of a smooth mesh transition is one of the factors that ensures its high quality and, consequently, the reliability of the stress and strain field modelling results.

If the mesh size was significantly reduced, for example, to 2 m, the process of meshing the model and the calculation itself took an excessive amount of time on a personal computer with 16.0 GB of RAM. For efficient modelling, a minimum of 32 GB of RAM or more is recommended. The quality of the mesh directly affected the accuracy of the results. Next, it was necessary to define material properties, loads, and boundary conditions. For the research, average mining conditions were adopted, with corresponding geo-mining and technical parameters for integrated open-pit-to-underground mining. Specifically, magnetitic quartzites are characterised by a high Young's modulus value (35,000 MPa) and a significant bulk density (3,400 kg/m^3). Their compressive strength (120 MPa) significantly exceeds their tensile strength (12 MPa), and the Poisson's ratio is 0.25.

Based on L. Jiangnan & X. Kuangdi (2023), for the calculation of the rock mass stress-strain state, variants of the classic open-pit-to-underground mining scheme for magnetitic quartzites were adopted, representing average conditions for the transition from open-pit to underground mining. After configuring all parameters, the calculation was initiated. The calculation program solved the system of equations to determine the distribution of stresses and strains throughout the entire rock mass. Typically, this analysis was conducted in stages, simulating the sequence of rock extraction. A three-dimensional model covering 60 m along the Z-axis was chosen for the simulation to most accurately reproduce the interaction conditions of the open-pit and underground complexes. Although the model was three-dimensional, two-dimensional cross-sections were used for analysing and visualising key patterns of the stress-strain state. This made it possible to present the main research results more clearly, without excessive detail.

Elements along the bottom and side boundaries of the model were fully fixed to prevent their movement. Gravitational loading and the pressure from the rock mass were taken into account in the model. These loads were applied to all elements to simulate realistic physical conditions. The calculation results were provided in the form of visualised maps of stress, deformation, and safety factor distributions. By analysing this data, it was possible to identify the most hazardous zones where the probability of failure is highest. The relationship between the maximum magnitude of vertical displacements and the depth of pit excavation was established by means of regression analysis, performed on the basis of the obtained modelling data.

Results

The application of mathematical methods is the most widespread. The availability of personal computers allows for the modelling and calculation of a large number of variant models in a relatively short period (Mehnert *et al.*, 2022). Based on a numerical analysis of the model, performed using the finite element method, it was established that any medium in which the natural balance has been altered strives to gradually restore it, transitioning to a new stable state. According to research by M. Karlsmo *et al.* (2024), this process is determined by Le Chatelier-Braun's principle. The time during which the medium returns to a new stable state is referred to as the relaxation period of the disturbed rock mass. Typically, at the bottom of an open-pit mine, the occurrence of deformations, subsidence, and cracks can be observed, and with significant extraction scales at a shallow distance to the bottom, even localised collapses or cave-ins directly within the bottom contours. The pit bottom is a free surface, making it sensitive to additional stresses and deformations (Kalinichenko, 2020).

Changes in the stress state were expected on the pit's contours and slopes, leading to a reduction in their stability. The underground workings activated existing tectonic disturbances (faults, cracks) within the slopes and initiated the development of new failure mechanisms (displacements of individual blocks, bench collapses, general slope failures), particularly in the hanging wall where mass movement was more intense. As shown in Figure 1, the entire hanging wall slope of the pit is failing under the influence of underground mining. It is in this zone that terraces, cracks, and zones of gradual subsidence are apparent. These are the visible signs of the influence of underground operations on the pit slope's surface.

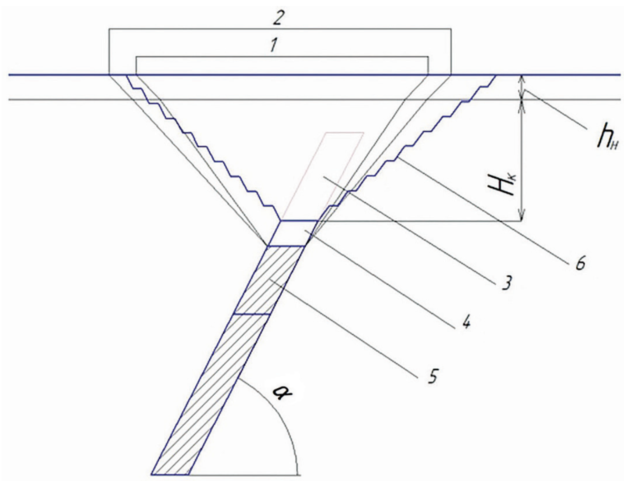

Figure 1. *Plan of rock mass caving and displacement zones in the hanging wall and footwall above the worked-out space of a deposit mined using an integrated method*

Notes: *1, 2 – accordingly, zone of ground collapse and ground subsidence above the worked-out underground space; 3 – contour of the deposit being mined by open-pit method; 4 – worked-out part of the deposit by underground method; 5 – part of the deposit subject to underground mining only; 6 – contour of the open pit in the form of benches;* $H_к$ *– final depth of the open pit; α – dip angle of the deposit; hн – thickness of the overburden*

Source: *developed by the author*

The zone of subsidence in the hanging wall extends beyond the pit contours, forming a subsidence basin on the ground surface with characteristic settlements and cracks, the scale of which depends on the dimensions of the excavation at depth and the distance to the surface. As underground mining operations deepen, the zones of collapse and subsidence move completely beyond the pit contours, leading to its physical destruction and collapse. Figure 1 illustrates the scale of the rock collapse and subsidence zones in the hanging wall and footwall of the deposit during combined open-pit-to-underground mining. Accordingly, the degree of their influence on the pit and the ground surface can be observed, which depends on a multitude of factors: the depth, dimensions, and shape of the stope, the physico-mechanical properties of the rocks, the presence and effectiveness of backfilling the worked-out space, as well as the sequence of block excavation (Ivadilinova *et al.*, 2023).

Even in more complex numerical methods, such as the finite element method in "Ansys, Inc. Products 2019 R3", where the stress-strain state was analysed and material strength criteria were applied at each point, the final stability assessment was also based on comparing the acting stresses (especially shear stresses) with the shear strength of the rocks at various points in the rock mass. The safety factor was calculated, or a stability analysis was performed by progressively reducing the rock strength parameters until a state of failure was reached, which was also essentially a determination of the safety factor. During the transition from open-pit to open-pit-to-underground mining operations, the necessity to consider the potential influence of underground mining was added to determine the magnitude of possible deformations of the pit slopes and surface. Induced deformations and altered stresses were superimposed on and interacted with the pre-existing stress-strain state caused by open-pit excavation, namely the open pit itself. This was not simply a linear sum of influences but a complex non-linear interaction that intensified negative phenomena.

Based on the properties of the magnetite quartzites, the geometry of the underground stopes was modelled with a stope inclination angle of 45 degrees and a bench height of 90 m. Figure 2 presents the overall initial calculation scheme for the option with mineral extraction conducted exclusively by the classical open-pit method. The figure is a visualisation of the finite element mesh used to model the stress-strain state of the rock mass around the open pit. The image demonstrates how the model space, which included the open pit and the adjacent rock mass, was divided into small elements (a mesh). This is a key stage of preparation for numerical calculations.

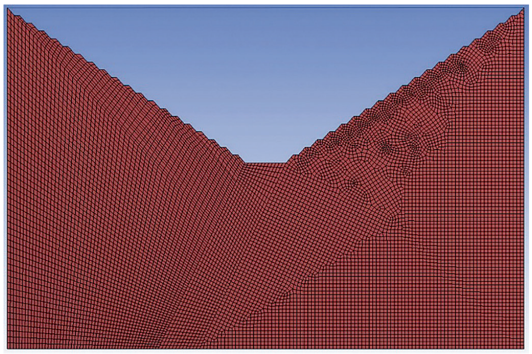

Figure 2. *Initial calculation model for the classical open-pit mining of minerals*

Source: *developed by the author*

Such a calculation scheme was applied to research different types of mineral deposits. For this purpose, the corresponding physico-mechanical properties of the minerals and host rocks were used in the calculations. Figure 3 presented the deformation magnitudes on the contour of the worked-out open pit depending on the depth of the working horizon, and in the undisturbed rock mass on the calculated contours of the future stopes during the transition to a combined open-pit-to-underground mining technology. The figure visualised the distribution of deformations (isolines) in the rock mass after the pit had been mined. This is a direct result of modelling and analysing the stress-strain state. The coloured lines in the figure were deformation isolines. They show how the intensity of deformations changed at different depths and locations within the rock mass. The figure clearly shows that the largest changes in deformation occurred specifically in the zone of the upper pit slopes and at its bottom. These areas were the most critical in terms of potential deformations and failures.

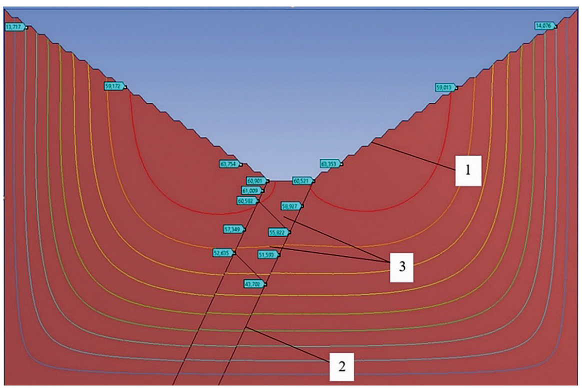

Figure 3. *Results of calculations of rock mass deformation during open-pit mining of minerals*

Notes: *1 – open pit contour; 2 – ore body; 3 – contours of the future first and second stage stopes, respectively*

Source: *developed by the author*

The results of calculations for the magnitude of maximum vertical displacements in the rock mass showed that the maximum vertical displacements of the pit slope's benches increased with increasing pit depth, from 13-14 mm on the upper benches at depths of 30-45 m from the ground surface to 60-63 mm on the lower benches at depths of 270-300 m at the bottom of the depleted pit. The results of the studies, presented in figures, were key to understanding the baseline stress-strain state of the open-pit area before or without the influence of underground mining. They allowed for the identification of red isolines in the upper parts of the slopes and at the pit bottom, which corresponded to larger deformation values. In these same areas, it was also visually confirmed that the rock mass was experiencing the greatest compression or tension, which were the zones of deformation concentration. Additionally, the figure enabled a clear assessment of how the pit influenced the entire volume of the rock mass, not just its immediate sections.

Such figures provided a clear understanding of the rock mass's reaction to open-pit excavation and served as a starting point for further analysis during the transition to the open-pit-to-underground method, as the influence of underground mining was superimposed on this baseline stress-strain state. The dependence of the magnitude of the maximum vertical displacements of the pit slope elements (benches) on the depth of the examined area from the ground surface is presented in Figure 4. This figure demonstrates the dependence of the maximum vertical displacements of the pit slope on the depth of its excavation.

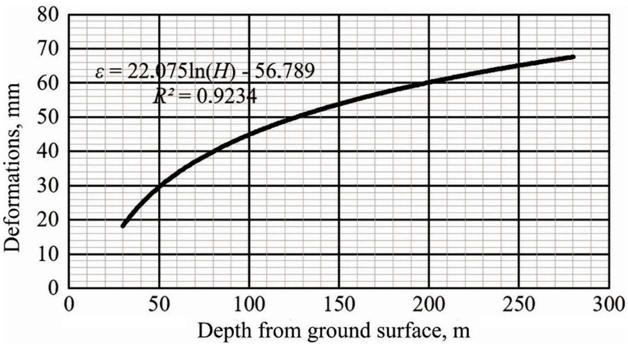

Figure 4. *Dependence of the magnitude of maximum vertical displacements of pit slope elements on the depth of excavation*

Source: *developed by the author*

The graph shows that as the excavation depth increases, so does the magnitude of vertical displacements on the pit slope. However, this increase is not linear; it follows a logarithmic pattern, which is confirmed by the regression equation on the graph. This indicates that the largest deformations occur during the initial stages of deepening, while at significant depths, the rate of deformation increase slows down. This logarithmic relationship is typical for mining operations and is explained by Le Chatelier-Braun's principle. According to this principle, disturbances are significant at initial depths, and the rock mass reacts sharply, causing a rapid increase in deformations. The data analysis carried out made it possible to establish a relationship with a high coefficient of determination, which is described by the following logarithmic equation:

$$\varepsilon = 22.075 \ln(H) - 56.789; \quad R^2 = 0.9234, \tag{1}$$

where ε – magnitude of the maximum vertical displacements of the pit slope, in mm; H – depth of the horizon (bench) from the ground surface, in m; R – magnitude of the coefficient of determination.

Figure 5 presents the results of calculations for stress magnitude in the rock mass during mineral extraction exclusively by open-pit mining. The location of the isolines with cold colours (blue) at the pit bottom and near its slopes indicates a low magnitude of stresses in these specific areas. The figure visually illustrates how the gravitational load was redistributed from the pit slopes to the internal sections of the rock mass. An analysis of the stress distribution at depth also allowed the influence of the open pit on future underground stopes, which were planned for extraction beneath its floor, to be assessed.

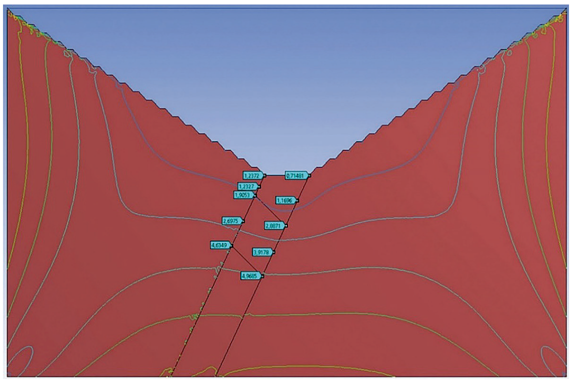

Figure 5. *Results of stress magnitude calculations in the rock mass during open-pit mining of minerals*

Source: *developed by the author*

Based on the research conducted, the magnitude of stresses in the rock mass beneath the open-pit floor increases from the ground surface at the bottom of the pit into the depth of the rock mass. In a natural, undisturbed rock mass, geostatic vertical stresses from the self-weight of the overlying rocks increase with depth. When the pit was created, a significant volume of rock was excavated. This led to a redistribution of the natural stress field. Directly on the pit floor and in the near-surface part beneath it, stresses are significantly reduced (unloaded) compared to the initial geostatic stresses, as the overlying rock mass has been removed. However, deeper into the rock mass from the pit floor, the influence of the unloading zone diminishes. Stresses gradually begin to recover and approach the values of natural geostatic stresses. Thus, at a certain depth beneath the pit floor, stresses become greater again and continue to increase with the depth of the deposit. The magnitude of stresses ranged from 0.7-1.2 MPa at the pit floor to 4.6-4.9 MPa beneath the pit floor at the depth of the future underground stopes for the second stage of mining. Figure 6 presents the dependence of the magnitude of stresses in the rock mass beneath the pit floor at the depth of the future underground stopes for the first and second stages of mining.

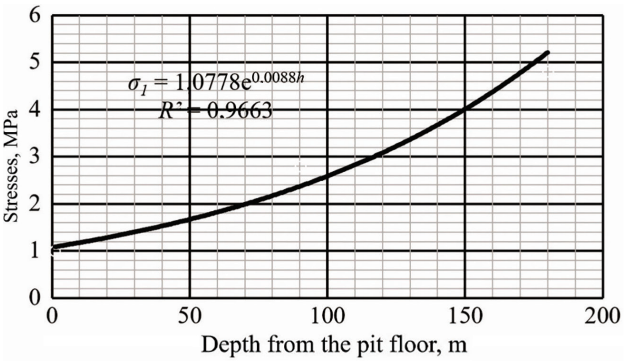

Figure 6. *Dependence of the maximum stresses in the rock mass beneath the pit floor on the depth of the future underground stopes*
Source: *developed by the author*

The graph shows a key finding of the modelling: stresses increase with depth, but this increase is not linear. Stresses grow following an exponential law, which is confirmed by the equation obtained from the regression analysis. This indicates that the influence of stresses becomes increasingly pronounced as depth increases. This relationship allows for the prediction of the rock mass's stress state at various depths. This is critical for planning underground stopes and selecting an appropriate mining technology to ensure safe operations. The relationship identified by the research is described by the exponential function of the form:

$$\sigma_1 = 1.0778e^{0,0088h}; \quad R^2 = 0.9663, \qquad (2)$$

where σ_1 – magnitude of the maximum stresses in the rock mass, MPa; h – depth of the future underground stopes from the pit floor, m; R – magnitude of the coefficient of determination.

The obtained dependence is confirmed by studies conducted for similar conditions, for example, in the work of H. Luo *et al.* (2024). The reliability of the results is confirmed by the fact that the error margin does not exceed 12-15%, which is an acceptable value for geomechanical research. The obtained results make it possible to visualise the distribution of stresses, stress concentration zones, and deformations in the rock mass. This allows for the analysis of the influence of various mining technologies on rock mass stability, leading to the selection of the most effective solutions. Therefore, the calculations make it possible to obtain quantitative data on the change in the stress state depending on depth. This underscores the critical importance of these indicators for ensuring a safe and effective transition to underground mining technology.

Discussion

M. Zhe & M. Zhuoqian (2024) conducted analytical and field studies on the stability of rock slopes along a high-speed motorway that were prone to landslides. The authors used "Rocscience" software to evaluate these slopes. The results of the numerical modelling were in full agreement with the field observations, confirming the high risk of slope failure, especially during rainfall and earthquakes. The paper made an important contribution to mining geomechanics as it confirmed that the geometric parameters of slopes and external factors (water saturation, seismicity) are critical for their stability. It demonstrated the effectiveness of the software for predicting rock mass behaviour and preventing dangerous situations, which fully aligns with the demands regarding stresses and deformations. The presence of water in rock cracks and pores reduces their strength and increases pore pressure, which leads to a weakening of the rock mass. An increase in the groundwater level or heavy rainfall causes landslides and collapses, which directly affects the stability of the pit slopes and underground stopes. Earthquakes or even microseismic activity, for example from explosions, create dynamic loads that sharply increase stresses in the rock mass. This destroys existing stress arches or causes rock bursts and collapses, especially in weakened areas between open-pit and underground mining. Ignoring these factors leads to an underestimation of risks and, as a result, to catastrophic failures that threaten human life and infrastructure. Therefore, in geomechanical research, an analysis is obligatorily conducted with consideration of the hydrogeological and seismodynamic conditions of the working area. Studies concerning the transition from open-pit to underground mining are particularly sensitive to these factors, as it is precisely here that new zones of stress concentration are created, and the old rock mass of the open pit receives additional load. The commonality in the obtained results is the confirmation of the critical influence of external factors on the stability of the rock mass and the effectiveness of numerical modelling methods, whereas the difference lies in the fact that M. Zhe & M. Zhuoqian (2024) focused on slopes along a motorway, while this study focused on the specific issues of open-pit-to-underground mining of deposits.

Stress analysis using "SolidWorks Simulation" is a study that demonstrates the effectiveness of using software to analyse the behaviour of components under various loads, as presented by M. Yazeed *et al*. (2023). The paper highlights the power and importance of using modern software for engineering analysis. It shows that such tools are an effective alternative to complex manual calculations and allow for the visualisation and analysis of results with high accuracy. This work demonstrates that effective and precise tools exist for modelling the stress-strain state of a rock mass, which are key for this type of research. However, this published work demonstrates the effectiveness of mathematical modelling using various types of software on personal computers. Common to both studies is the confirmation of the effectiveness and key role of modern software for modelling the stress-strain state, but the difference lies in one case focusing on stress analysis in engineering components, while this study applied the approach to the specific problem of mining geomechanics.

B.O. Taiwo *et al*. (2023) noted that the state of pit slopes was influenced by explosive works used during extraction, as blasts were one source of localised seismicity affecting the rock mass's stress-strain state. The authors used a combination of geotechnical methods, monitoring, and data analysis to assess how blasts caused microcracks, which weakened the rock and increased the risk of collapses. This work highlighted the importance of considering not only static but also dynamic stresses when analysing rock mass stability. It confirmed the need to account for seismic factors in the pit during the transition from open-pit to underground mining. The results obtained in the current work align with the finding that dynamic loads from drilling and blasting are a key factor influencing the stress-strain state of the rock mass. The difference, however, lies in the fact that the original study focused on analysing the stability of pit slopes, whereas this research applied these findings to geomechanical processes under conditions of combined mining.

O.V. Kalinichenko (2020) noted that to determine changes in the stress-strain state of a rock mass when creating underground voids, analytical modelling with effective computer software is necessary. Particular attention is paid to methods for controlling the stress-strain state, which ensure stability and safety. The research findings contain recommendations and methodologies that prevent collapses, the formation of subsidence basins, and other negative geomechanical phenomena. This is directly related to the influence of worked-out space dimensions on surface deformations, as this dissertation developed a scientific basis for understanding and controlling geomechanical processes. The results of that study had an approximately similar error to the results of this research. What both works have in common is the application of software for modelling and analysing the stress-strain state to enhance mining safety. The difference is that the author focused on the creation of underground voids and workings, whereas this study focused on the interaction between open-pit and underground mining.

In the published work, Y. Lu *et al*. (2024) proposed an analysis of open-pit slope deformations and failures resulting from the combined influence of blasting operations and rainfall. The authors emphasised that although these factors are common, their combined effect has rarely been studied. An integrated approach, which included using finite difference method modelling to investigate slope response mechanisms, was used to study a large-scale landslide that occurred at a mine in China. The paper is relevant as it confirmed that to fully understand the behaviour of the rock mass, it is not enough to study only internal factors, such as stresses from mining. It is necessary to consider external factors, such as hydrogeology and dynamic loads, which made it an ideal complement to the results of this study on the open-pit-to-underground transition. The two studies similarly confirm the need to consider factors of natural and man-made origin for a comprehensive stability analysis, while the difference lies in the fact that one focused on open-pit slopes and this study focused on the interaction of the depleted open-pit with the surrounding rock mass.

The research results in the paper by M. Marchelli *et al*. (2023) are practical, as they provided specific tools for the preliminary design of open-pit geometry and risk assessment. This study confirmed that proper planning and consideration of the geomechanical properties of the rock mass significantly increased work safety. It also emphasised that every element of the open pit, from the bench to the overall geometry, was crucial for preventing dangerous situations. Both works used a single approach of applying geomechanical calculations for improving the safety of mining operations, but the difference lies in the fact that one focused on specific tools for designing open-pit geometry, while this research focused on the problem of subsequent combined mining.

In the paper by A. Driouch *et al.* (2023), it was proven that numerical modelling is an extremely important tool for selecting the safest and most effective mining sequence. It was also emphasised that the correct choice of mining methods is crucial for managing the stress-strain state of the rock mass, especially in conditions with weak rocks. The results obtained from both studies converge on the key factor being the necessity of applying numerical modelling to select effective mining methods. However, the difference lies in the fact that one study focused on choosing a mining sequence in weak rock conditions, whereas this research concentrated on geomechanical processes in a combined mining operation.

In mining science, a number of calculation schemes and methodologies are applied to determine the stability of open-pit slope elements. As stated by E.B. Gridina *et al.* (2020), a common feature of all existing calculation schemes is the comparison of shear and retaining forces acting along the weakest surface. This principle is used to calculate the factor of safety, which is the most common indicator of slope stability. The factor of safety is defined as the ratio of the total sum of retaining forces or moments, depending on the methodology, resisting movement along the surface, to the total sum of shearing forces or moments that tend to cause movement along this surface. A common feature of all existing calculation schemes is the comparison of shearing and retaining forces to determine the factor of safety, which is considered a classic approach, whereas this study considers the application of this principle in the context of open-pit mining, which is its distinctive feature.

A.G. Irwan & I.T. Wiati (2023) noted that the stability parameters of pit slopes obtained by calculation require adjustment as they do not reflect all factors that occur in the rock mass at each specific deposit during its development. The main parameters of the pit slope, such as its inclination angle and height, are determined by taking into account the main influencing factors, which include: the physico-mechanical properties of the rocks; the structural features of the rock mass and the deposit's structure; the dimensions and shape of the open pit; hydrogeological conditions; technological influence (the effect of drilling and blasting operations, external loads on the slope, particularly the close proximity of waste dumps, and so on); and the duration of the open pit's operation. A key shared conclusion is the confirmation that the calculated stability parameters require adjustment to account for a multitude of factors, whereas the difference lies in the fact that attention was focused on general parameters, while this study analyses the influence of the open pit on the rock mass.

Thus, the analysis of scientific sources and the results of the modelling confirm that assessing the stability of the rock mass around a depleted open pit requires a comprehensive approach. It has been established that stability parameters calculated by standard methods are insufficient, as they do not account for the combined influence of hydrogeological, seismodynamic, and technological factors. Therefore, to ensure the stability of the pit slopes and underground workings during their combined extraction, it is necessary to apply numerical modelling methods that allow all these factors to be taken into account for an accurate prediction of the stress-strain state.

Conclusions

The conducted research made it possible to perform a geomechanical justification for the stability of the elements of the open-pit mining complex. The obtained results confirmed the fundamental regularities of the rock mass's stress-strain state and provided a quantitative assessment of its behaviour. The research established that the magnitude of the maximum vertical displacements of the pit slope on its benches increased with increasing pit depth, from 13-14 mm on the upper benches at depths of 30-45 m from the ground surface to 60-63 mm on the lower benches at depths of 270-300 m at the bottom of the depleted pit. It was established that the dependence of the magnitude of the maximum vertical displacements of the pit slope elements on the depth of excavation was described by a logarithmic function with a high coefficient of determination. The results of the calculations made it possible to establish that the magnitude of stresses in the rock mass beneath the pit floor increased from the ground surface at the bottom of the pit into the rock mass according to an exponential law. It was established that the stress magnitude ranged from 0.7-1.2 MPa at the pit bottom to 4.6-4.9 MPa beneath the pit floor at the depth of the future underground stopes. During the research, it was established that stresses in the rock mass beneath the pit floor increased with depth. The results obtained confirmed that vertical geostatic stresses increased with depth, which was caused by the weight of the overlying rocks. However, upon the creation of the pit, a significant portion of these rocks was removed, leading to a redistribution of the initial stress field. The conducted studies showed that the stresses directly at the pit bottom and in the near-surface zone beneath it significantly decreased, which indicated the unloading of the rock mass. Nevertheless, with an increase in depth, the influence of this zone decreased. The stresses began to gradually recover and approached the initial geostatic values, continuing to increase further down the dip of the deposit. The performed analysis demonstrated zones of stress concentration on the pit slopes, as well as zones of unloading in the near-surface rock mass beneath its bottom. The obtained dependencies were confirmed by research performed for analogous conditions. The reliability of the results was confirmed by the fact that the error magnitude did not exceed 12-15%, which was an acceptable value for geomechanical studies. The obtained results were the basis for further work planning for the transition to underground mining. In further research, a focus is planned on studying key parameters to ensure the stability of the rock mass during the excavation of Chambers I, II, and III. The main objects of analysis will be changes in the distribution of stresses and deformations in the rock mass, as well as the mutual influence of the chambers on the overall stability of the rock mass around the pit.

Acknowledgements

None.

Funding

None.

Conflict of Interest

None.

References

[1] Bagde, M.N. (2021). Ore and backfill dilution in underground hard rock mining. *Journal of Mining Science*, 57(6), 995-1005. doi: 10.1134/s1062739121060120.

[2] Driouch, A., Ouadif, L., Lahmili, A., Belmi, M.A., & Benjmel, K. (2023). Geotechnical modeling of the method for mining cobalt deposits at the Bou Azzer Mine, Morocco. *Mining of Mineral Deposits*, 17(1), 51-58. doi: 10.33271/mining17.01.051.

[3] Gridina, E.B., Rudakov, M.L., & Rumiantseva, A.M. (2020). Evaluation of stability of sides of quarries and dumps on the basis of a risk-oriented approach. *Naukovyi Visnyk Natsionalnoho Hirnychoho Universytetu*, 4, 47-52. doi: 10.33271/nvngu/2020-4/047.

[4] Irwan, A.G., & Wiati, I.T. (2023). Reconstruction of natural slope stability by limit equilibrium methods and finite element methods. *Dinamika Teknik Sipil: Majalah Ilmiah Teknik Sipil*, 16(2), 43-49. doi: 10.23917/dts.v16i2.23276.

[5] Ivadilinova, D.T., Issabek, T.K., Takhanov, D.K., & Yeskenova, G.B. (2023). Predicting underground mining impact on the earth's surface. *Naukovyi Visnyk Natsionalnoho Hirnychoho Universytetu*, 1, 32-37. doi: 10.33271/nvngu/2023-1/032.

[6] Ivasivka, O., Hevpa, Z., & Dyakiv, V. (2023). Activation of karst-fall phenomena within the mining district of Mine No. 2 and its impact on the state of infrastructure facilities and living conditions of residents. *Visnyk of the Lviv University. Series Geology*, 37, 42-55. doi: 10.30970/vgl.37.04.

[7] Jiangnan, L., & Kuangdi, X. (2023). Open-pit and underground combined mining. In K. Xu, (Ed.), *The ECPH encyclopedia of mining and metallurgy*. Singapore: Springer. doi: 10.1007/978-981-19-0740-1_348-1.

[8] Kalinichenko, O.V. (2020). *Development of scientific principles for controlling the stress-strain state of rock mass during underground excavation*. (Doctoral dissertation, M.S. Polyakov Institute of Geotechnical Mechanics of the National Academy of Sciences of Ukraine, Dnipro, Ukraine).

[9] Karlsmo, M., Hosaka, T., & Johansson, P. (2024). Le Chatelier's principle enables stable and sustainable aqueous sodium/magnesium-ion batteries. *Journal of Materials Chemistry A*, 12(7), 4029-4036. doi: 10.1039/d3ta06826a.

[10] Kimour, M., Boukelloul, M.L., Hafsaoui, A., Narsis, S., Benghadab, K.M., & Benselhoub, A. (2023). Geomechanical characterization of rock mass rating and numerical modeling for underground mining excavation design. *Journal of Geology, Geography and Geoecology*, 32(1), 67-78. doi: 10.15421/112308.

[11] Kulikovska, O., Stupen, R., & Kolodiy, P. (2024). Cartographic and analytical model of the formation of the failed relief in a large mining region. *Spatial Development*, 10, 482-497. doi: 10.32347/2786-7269.2024.10.482-497.

[12] Lu, Y., Jin, C., Wang, Q., Li, G., & Han, T. (2024). Deformation and failure characteristic of open-pit slope subjected to combined effects of mining blasting and rainfall infiltration. *Engineering Geology*, 331, article number 107437. doi: 10.1016/j.enggeo.2024.107437.

[13] Luo, H., Wang, Z., Liu, K., Qiao, L., & Qing, L. (2024). Stress-strain state zoning model and novel large deformation classification method for squeezing tunnels. *Engineering Failure Analysis*, 164, article number 108711. doi: 10.1016/j.engfailanal.2024.108711.

[14] Marchelli, M., Peila, D., & Giacomini, A. (2023). Rockfall in open pit mines: Management of the pit geometry and protection measures design. *International Journal of Rock Mechanics and Mining Sciences*, 170, article number 105551. doi: 10.1016/j.ijrmms.2023.105551.
[15] Mehnert, M., Oates, W., & Steinmann, P. (2022). Numerical modeling of nonlinear photoelasticity. *International Journal for Numerical Methods in Engineering*, 24(7), 1602-1619. doi: 10.1002/nme.7177.
[16] Razumova, K.M., Temchenko, O.A., Maksymov, S.V., & Maksymova, O.S. (2021). Research of duration influence of loading and unloading operations on the use efficiency of technological motor transport on open pit iron mines. *Science and Transport Progress*, 6(96), 24-38. doi: 10.15802/stp2021/256794.
[17] Shen, Y., Feng, Z., Zhou, D., & Zhang, B. (2024). Different rock failure precursors using displacement coordination coefficient. *Environmental Earth Sciences*, 83, article number 490. doi: 10.1007/s12665-024-11814-9.
[18] Taiwo, B.O., Yewuhalashet, F., Ogunyemi, O.B., Babatuyi, V.A., Okobe, E.I., & Orhu, E.A. (2023). Quarry slope stability assessment methods with blast induced effect monitoring in Akoko Edo, Nigeria. *Geotechnical and Geological Engineering*, 41, 2553-2571. doi: 10.1007/s10706-023-02414-8.
[19] Tomova, M., & Kisyov, A. (2024). Applications and advantages of geophysical methods in underground mining. *Annual of the University of Mining and Geology "St. Ivan Rilski"*, 67, 184-188. doi: 10.5281/zenodo.13762777.
[20] Yazeed, M.A.A., Abdullah, A.A., Muhab M.F.A.-G., & Mithun, V.K. (2023). Stress analysis using solidworks simulation. *EPRA International Journal of Multidisciplinary Research (IJMR)*, 9, 28-35. doi: 10.36713/epra14295.
[21] Zhe, M., & Zhuoqian, M. (2024). Stability analysis of rock slope based on rocscience software. *Civil Engineering*, 13(7), 1152-1157. doi: 10.12677/hjce.2024.137124.
[22] Zuievska, N., Shaidetska, L., Kosenko, T., & Hutsuliak, Z. (2023). Application of engineering measures for the stabilization of the soil slope. *Collection of Research Papers of the National Mining University*, 73, 187-196. doi: 10.33271/crpnmu/73.187.

Олександр Шепель
Кандидат технічних наук, доцент
Криворізький національний університет
50027, вул. Віталія Матусевича, 11, м. Кривий Ріг, Україна
https://orcid.org/0000-0003-4581-5441

Дослідження напружено-деформованого стану гірського масиву при видобутку корисних копалин відкритим способом

Анотація. Забезпечення стійкості та несучої здатності бортів кар'єрів це актуальна та складна умова для відпрацювання родовищ відкрито-підземним способом. У зв'язку з цим метою досліджень в роботі було геомеханічне обґрунтування стійкості технологічних елементів відкрито-підземного комплексу гірничих робіт. Це обґрунтування, проведено за допомогою розробленої моделі, мало на меті визначення впливу на формування напружено-деформованого стану масиву на прикладі кар'єрів Криворізьких гірничо-збагачувальних комбінатів. У даній роботі для прогнозування впливу кар'єру на подальший підземний видобуток були застосовані математичні та чисельні методи, зокрема метод скінченних елементів, а також статистичний та факторний аналіз. Крім того, для дослідження напружено-деформованого стану гірського масиву навколо відпрацьованого кар'єру було використано програмне забезпечення «Ansys, Inc. Products 2019 R3». Встановлено, що величина максимальних вертикальних зсувів борта кар'єру збільшується з 13-14 мм на верхніх горизонтах (уступах) на глибинах 30-45 м від денної поверхні до 60-63 мм на нижніх уступах на глибинах 270-300 м на дні відпрацьованого кар'єру. Залежність величини максимальних вертикальних зсувів елементів борта кар'єру від глибини розробки описується логарифмічною функцією. Було встановлено, що величина напружень коливається від 0,7-1,2 МПа на дні кар'єру до 4,6-4,9 МПа під дном кар'єру на глибині розташування майбутніх підземних очисних камер. Залежність величини максимальних напружень у гірському масиві під дном кар'єру від глибини описується експоненціальною функцією. Розрахунки дозволили отримати кількісні дані про зміну напруженого стану гірського масиву в залежності від глибини. Практична значимість роботи полягає у використанні цих показників для забезпечення безпечного та ефективного переходу до підземної технології розробки

Ключові слова: кар'єр; геомеханічне обґрунтування; комплексна розробка; залежність; моделювання

Journal homepage: https://mining-journal.com.ua/en
ISSN 2306-5435
MINING JOURNAL of Kryvyi Rih National University
Vol. 59, No. 2, 2025
Received: 17.07.2025; Revised: 27.11.2025; Accepted: 24.12.2025; Published: 05.01.2026

UDC 622.274.53
DOI: 10.31721/2306-5435-2025-2-21-31

Mykola Stupnik*
Doctor of Technical Sciences, Professor
Kryvyi Rih National University
50027, 11 Vitalii Matusevich Str., Kryvyi Rih, Ukraine
https://orcid.org/0000-0003-3318-3889

Vsevolod Kalinichenko
Doctor of Technical Sciences, Professor
Kryvyi Rih National University
50027, 11 Vitalii Matusevich Str., Kryvyi Rih, Ukraine
https://orcid.org/0000-0002-1938-2286

Mykhailo Fedko
PhD in Technical Sciences, Associate Professor
Kryvyi Rih National University
50027, 11 Vitalii Matusevich Str., Kryvyi Rih, Ukraine
https://orcid.org/0000-0002-8437-3175

Serhii Pysmennyi
PhD in Technical Sciences, Associate Professor
Kryvyi Rih National University
50027, 11 Vitalii Matusevich Str., Kryvyi Rih, Ukraine
https://orcid.org/0000-0001-5384-6972

Mykhailo Hryshchenko
Senior Lecturer
Kryvyi Rih National University
50027, 11 Vitalii Matusevich Str., Kryvyi Rih, Ukraine
https://orcid.org/0000-0002-9365-1886

Development of highly efficient technologies for extracting rich iron ores at deep levels of Kryvbas mines

Abstract. About half of the rich iron ore mined in the Kryvbas mines is extracted applying various types of sublevel caving systems. At the same time, ore haulage in the mining panels is carried out exclusively by scraper equipment, which does not meet modern requirements in terms of miners' working conditions, productivity and safety. The aim of the work was to develop more efficient flowsheets for the extraction of rich iron ores applying the sublevel caving system. This was achieved primarily through the employment of self-propelled underground loaders, haulers and dumpers (LHDs) and other technical solutions for ore. The new flowsheets for the development of iron ore deposits applying the sublevel caving system based on the use of the mentioned self-propelled machinery for haulage are proposed. This is achieved by using, in addition to the main draw level,

Suggested Citation:
Stupnik, M., Kalinichenko, V., Fedko, M., Pysmennyi. S., & Hryshchenko, M. (2025). Development of highly efficient technologies for extracting rich iron ores at deep levels of Kryvbas mines. *Mining Journal of Kryvyi Rih National University*, 59(2), 21-31. doi: 10.31721/2306-5435-2025-2-21-31.

*Corresponding author

where only this self-propelled machinery operates, an additional draw level with the use of scraper equipment, for which the drill drift is reused. This ensures more intensive mining of panels, thereby reducing the cost of maintaining workings and improving ore extraction rates. Another option, designed for mining deposits with a thickness of up to 30-35 m, involves application of inclined compensation rooms, which makes it possible to create rooms of sufficient volume even in low-strength ores, as well as combined ore haulage by self-propelled LHDs and scraper equipment. To increase the efficiency of the self-propelled LHDs, productivity of which is significantly higher than that of scraper equipment, it is possible to employ one self-propelled machine for the simultaneous haulage of ore from two adjacent panels. Thus, the main advantages of the proposed mining system options are an increase in the intensity of panel mining, a significant reduction in the loss of ore on the footwall of the deposit, and the possibility of employing self-propelled machinery in the conditions of Kryvyi Rih iron ore basin mines

Keywords: iron ore raw materials; underground mining; mining technology; sublevel caving; ore haulage; self-propelled equipment

Introduction

Naturally rich iron ores in Kryvbas – which was, is, and will remain Ukraine's primary iron ore base – are extracted exclusively underground (Bazaluk *et al.*, 2024). Mining is conducted at depths of 1,100-1,400 m. To extract these ores, a variety of systems are employed, including sublevel-room and sublevel caving systems. The current proportion of these systems is approximately equal, but as mining depths increase and conditions deteriorate, the share of the sublevel caving system is expected to gradually increase.

The optimisation of sublevel caving technology for mining deposits is the focus of numerous publications. These works provide a detailed history of the system's evolution, present various operational variants, and outline paths for their improvement. It should be noted that while existing technologies offer a number of benefits, including simple design and limited development work, they do not provide the use of imported self-propelled loaders, haulers and dumpers (LHDs). O. Bazaluk *et al.* (2022) proposed a block mining technology that employs high-performance self-propelled equipment. This method eliminates the need for drawpoints, drawbells, and draw niches, which are rather dangerous and labour-intensive to create. Conversely, M. Stupnik *et al.* (2021) observed that the use of such equipment necessitates larger-cross-section workings. The stability of these workings is expected to deteriorate as mining depths increase, and their maintenance will be associated with a rise in both labour and material costs. Based on an analysis of development trends and existing problems at Kryvbas mining enterprises, M. Stupnik *et al.* (2023) concluded that traditional means of ore haulage from stopes using scraper equipment are currently inefficient. Nevertheless, through technical re-equipment, the implementation of self-propelled LHDs would allow for an increase in ore extraction indicators. This can be achieved by the simplification of mining panel bottom designs, a reduction in the volume of preparatory-development work, and the mechanisation of the most labour-intensive operations.

Addressing the issue of mitigating broken ore losses on the footwalls of deposits during sublevel caving, I. Lutsenko *et al.* (2017) proposed replacing the broken ore that enters the "dead" zone on the footwall with waste rock. This is achieved by drilling and caving the waste rock during bulk blasting. A separate study by A. Kosenko *et al.* (2024) examined different bottom designs for ore extraction and haulage employing self-propelled LHDs. These designs can be trench-, drawbell-, pocket-like, and integrated haulage and transportation workings. In their research, S. Pysmennyi *et al.* (2020) demonstrated that the application of a trench-like bottom is the most suitable method for the complex geomechanical conditions encountered in the Kryvbas mines. The primary justification for this is its enhanced stability and the reduced costs required for its creation. A. Mazhitov *et al.* (2020) and M. Stupnik *et al*. (2023) conducted comprehensive research using mathematical modeling to compare the stability of various compensation room shapes. Based on these studies, the authors concluded that the compensation rooms of the vaulted (arched) and parabolic shapes offer the best stability. A critical review of scientific literature enabled an evaluation of existing sublevel caving system variants to develop solutions for their application in the challenging mining-geological conditions of the Kryvbas mines.

An analysis of the literature indicated that the implementation of classical mining systems employing self-propelled equipment is not viable under the conditions prevalent in Kryvbas. Nevertheless, given the complex mining and geological conditions of the Kryvbas deposits (i.e. low ore strength and stability, as well as inconsistent thickness and dip angles of ore bodies), it is advisable to apply specific concepts previously proposed by researchers. A significant limitation of these earlier studies, however, is that their authors failed to consider the significant depth of the underground mining operations. The depth of mining is a crucial factor in the mining of ore deposits, as it substantially modifies the stress field around underground workings. This not only complicates operations but also imposes specific constraints, particularly on the cross-sectional area of the workings. These constraints, in turn, directly dictate the type and size of the self-propelled equipment that can be used and the service life over which the workings can be maintained without incurring significant costs.

Given rather challenging conditions associated with extracting these ores – resulting primarily from the inadequate strength and stability of the ore and host rock, as well as the significant manifestation of rock pressure – a common constraint in these systems is the exclusive use of an inefficient means for ore drawing and haulage (i.e. scraper equipment). This equipment fails to provide sufficient productivity or safe working conditions for miners. A prominent issue at these depths is the heightened stress-strain state of the rock massif, which demands a deliberate approach to the selection of compensation room shapes. The chosen shape is crucial, as it is a major determinant of both operational safety and overall ore extraction indicators. Consequently, the improvement of systems employing sublevel bulk caving for rich iron ore mining at depths exceeding 1,200 m represents a highly relevant research problem that this work seeks to resolve.

Materials and Methods

The research employed a comprehensive approach, combining a literature review, a graphical-analytical method, and mathematical modelling. The graphical-analytical method served to calculate the primary parameters of underground workings considering the stress-strain state of the rock massif. This approach also facilitated the determination of their optimal spatial arrangement within the mining block, the feasibility of their construction, and their potential negative influence on adjacent mining panels and workings. The primary results of these calculations were subsequently presented in research papers supported by the Ministry of Education and Science of Ukraine. For the analytical component of the research, the authors employed the finite element method. This method enabled them to ascertain the normal, tangential, and equivalent stresses around the workings as a function of the deposit's mining-geological conditions and the cross-sectional area of the underground working.

To study the stress-strain state, the equivalent stress coefficient was employed. It allowed the arbitrary three-dimensional stress state of a rock massif area to be represented as a single, positive equivalent stress value, as noted in the works of B.M. Andreev *et al.* (2015), M.R.S. Seyed *et al.* (2025), and A.R. Abdiev *et al.* (2025). Additionally, this approach enabled the calculation and determination of stress in a heterogeneous rock massif under complex mining-geological conditions, consistent with the research of S. Pysmennyi *et al.* (2018). By applying the generalised Hooke's law, equivalent stresses were determined based on the physical and mechanical properties of the rocks and the depth of development using the formula (Tayebi *et al.*, 2019):

$$\sigma = \sqrt{\frac{(\sigma_z-\sigma_x)^2+(\sigma_x-\sigma_y)^2+(\sigma_y-\sigma_z)^2}{2}}, \text{ MPa} \quad (1)$$

where σ – the equivalent stresses that occur in the rock massif around the working, MPa; σ_z – the principal vertical stresses, MPa; σ_x, σ_y – the principal horizontal stresses, MPa.

Equivalent strains of the rock massif around the working were determined by the expression:

$$\varepsilon = \frac{1}{1+\mu}\sqrt{\frac{(\varepsilon_z-\varepsilon_x)^2+(\varepsilon_x-\varepsilon_y)^2+(\varepsilon_y-\varepsilon_z)^2}{2}}, \quad (2)$$

where ε – the equivalent strains that occur in the rock massif around the working; μ – the Poisson's ratio; ε_z – the vertical linear strains; ε_x, ε_y – the horizontal linear strains along and across the strike of the deposit, respectively.

The following input parameters were adopted to study the principal and equivalent stresses: model dimensions – 25×25 m; grid size – 0.25×0.25 m; nodal connection type – triangular; nodal load: vertical – 18,000 Pa, horizontal – 8,000 Pa, Poisson's ratio – 0.22; modulus of elasticity – 2×10^3 Pa; volume weight of rocks – 34,000 N; arched working width – 3.5 m.

Mathematical modeling was used to solve the problem of rock massif stability around the underground working, applying the theory of elasticity for a body in equilibrium under given external forces. At each point, a component of the stress tensor was calculated to simultaneously satisfy equilibrium within the body and on the contour of the working. The shear stress tensor, relative to the equivalent stress, is described by the following matrix:

$$D = \begin{vmatrix} \sigma_x-\sigma & \tau_{xy} & \tau_{xz} \\ \tau_{xy} & \sigma_y-\sigma & \tau_{yz} \\ \tau_{xz} & \tau_{yz} & \sigma_z-\sigma \end{vmatrix}, \quad (3)$$

where D – the stress tensor at the point under study; σ_i – the stresses of the internal forces arising in the massif, N/m^2; τ_i – the tangential stresses arising in the massif, N/m^2. The stress tensor thus describes the strain state at a given point in a solid body. When the equilibrium of the stress tensor is disrupted, linear and angular strains occur in the rock massif on the contour of the working. The results of the calculations are shown in Figure 1.

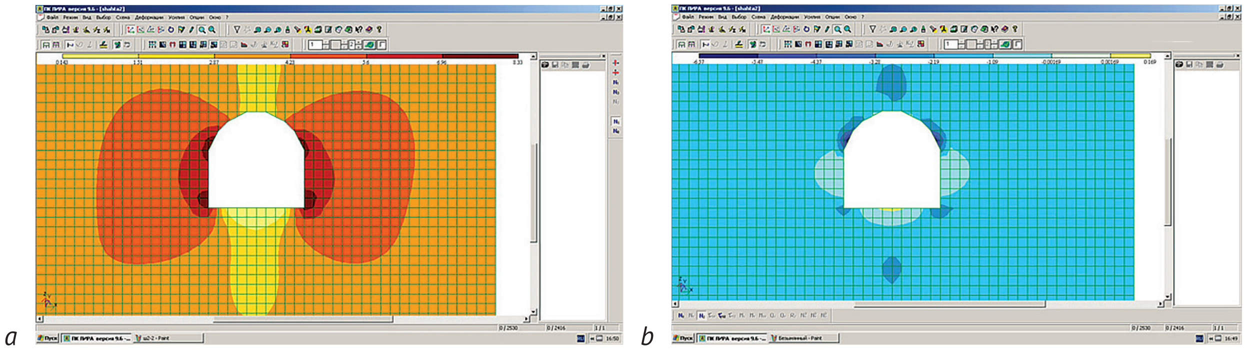

Figure 1. *Stress distribution around the underground working with a cross-sectional area of 10 m^2 at a depth of 1,350 m*
Notes: *a – equivalent; b – vertical*
Source: *developed by the authors*

The conducted research established the optimal parameters and rational placement of underground workings, confirming their adherence to the primary requirements for mining rich iron ore deposits. The crucial requirement considered was the safety of the miners. Furthermore, the completed studies on parameters of workings integrated the risks of technological seismicity, a factor which, as recommended by A. Matayev *et al.* (2024), warrants careful consideration. Following the findings of A. Salkynov *et al.* (2023), strain processes within the rock massif were also taken into account, as they can compromise the stability of workings in weak ores, especially under conditions of high rock pressure at deep levels. The model was constructed by incorporating the stress and strain relationships for fractured rocks, as proposed by Chong *et al.* (2021). This involved adapting the model's parameters to reflect changes in the actual stress-strain state of the workings, thereby enhancing the reliability of the calculation results for the complex structure of the ore massif. In the design of stoping flowsheets, particular emphasis was placed on maximising ore extraction indicators and increasing labour productivity. The unique aspect of the research presented here is that individual technological processes were examined within a comprehensive framework using the graphical-analytical method. Consequently, this allowed for the development of improved sublevel caving system variants, which employ self-propelled equipment and are tailored to the specific conditions of rich iron ore extraction in the Kryvbas mines.

Results

Experience of leading mining companies that extract minerals underground shows that improving their extraction technology is practically impossible without the employment of modern equipment, particularly self-propelled LHDs, the use of which at the Kryvbas mines, as already noted, is hindered by the rather complex geological and technical conditions of ore deposit mining. Taking into account the specific application of this technology in both leading global mining companies and the Kryvbas mines, and building on the results of prior research, the authors of this work developed two new variants of the sublevel caving system. These variants, employing self-propelled LHDs for ore extraction and haulage, are designed to extend their applicability in challenging conditions when working with iron ore deposits of different thicknesses. Furthermore, variations in the elemental composition of the rocks were incorporated to improve the accuracy of ore body boundaries, as recommended by D. Shihov *et al.* (2024). A specific variant of the sublevel caving system developed in this work, intended for mining thick ore deposits, is presented in Figure 2.

A distinguishing feature of this system is the use of parabolic or vaulted compensation rooms within the mining panels, which are oriented with their long side across the strike of the deposit. This design enhances the stability of the rooms. To substantially mitigate broken ore losses on the footwall, the system also incorporates an additional draw level with scraper haulage, which supplements the main draw level that operates exclusively with self-propelled LHDs. To minimise the volume of development work, this additional level is proposed to be a repurposed drill drift that was previously driven through the footwall rocks. Based on this technology, the deposit is developed in mining blocks 60 m long along the strike. These blocks are vertically divided into two sublevels of approximately equal height within a single level (75-80 m). Block preparation involves the following: from a footwall haulage drift *1*, access crosscuts *2* are driven at 60-meter intervals; from these crosscuts, block ventilation-and-manway raises *3* are created to connect to the upper ventilation level; an inclined runaway *4* is driven in the footwall rock to provide access for self-propelled equipment to the intermediate sublevels (one runaway per mine wing).

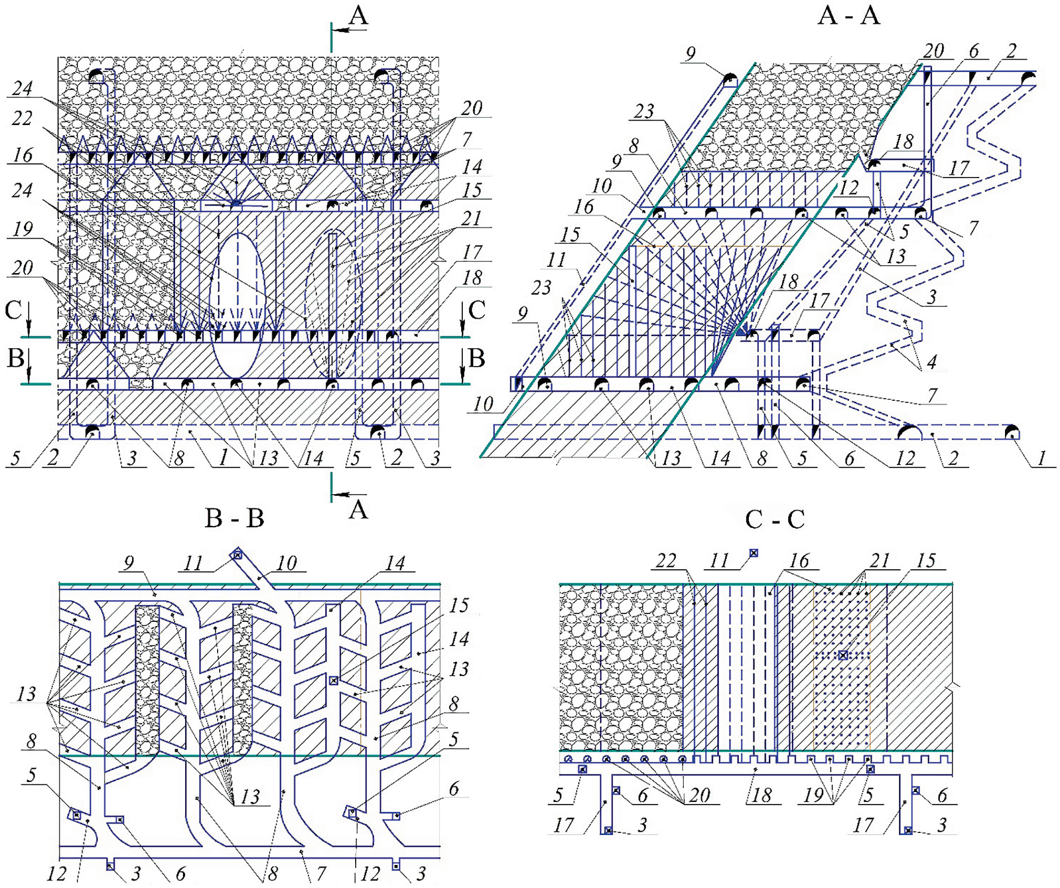

Figure 2. *The developed variant of the sublevel caving system for mining thick steep iron ore deposits with combined ore haulage by self-propelled LHDs and scraper equipment*

Source: *developed by the authors*

Development work begins with the creation of orepasses *5* and service raises *6* to facilitate the driving of other workings and support activities on the intermediate sublevels. At the ore drawing and haulage level, where self-propelled LHDs will be used, sublevel haulage drifts *7* are driven in the footwall rock 15-20 m from the ore body's contact. From these sublevel haulage drifts drifts, haulage crosscuts *8* are driven every 20 m. In the hanging wall, these crosscuts are connected to each other by a ventilation drift *9*, which is then connected via a ventilation crosscut *10* to a ventilation raise *11*. Depending on the mine's ventilation scheme, this raise can connect to either the upper ventilation level or the sublevel dirty-air collecting drift.

From the haulage crosscuts *8* located above the access crosscut *2*, an unloading niche *12* is created and connected to an orepass *5*. Starting 8-10 m from the ore body contact, diagonal loading workings *13* are developed from these haulage crosscuts *8* at 10 m intervals in a staggered configuration along both directions. From the first such crosscut, located in the footwall rock, cut crosscuts *14* are driven through the panel centers. Subsequently, a cut raise *15* is developed upwards from the central part of these cut croscuts opposite a loading working to form a compensation room *16*. Service crosscuts *17* are 10 m above the main draw and haulage levels in the footwall rock. These crosscuts are connected to the block ventilation-and-manway, service and orepass raises (*3*, *6*, *5*, respectively). Drill drifts *18* are also created and will later be used as scraper drifts. From the drill drifts, drill niches *19* are driven towards the ore body and will subsequently be used as drawpoints

20. To create a compensation room, which is given a parabolic or vaulted (arched) shape for greater stability, rings of boreholes *21* are drilled from a cut crosscut *14*. For breaking the main ore reserve in the panel, rings of long holes *22* are drilled in the panel from the drill niches. Finally, to cave the pillars above the haulage crosscuts, borehole rings *23* are drilled from these crosscuts.

Ore reserves within each sublevel are mined using 20-meter-wide panels. The panels are arranged so that the cut crosscuts on the lower sublevel are driven directly under the haulage crosscuts of the upper sublevel. These haulage crosscuts are developed within temporary pillars, which prevents waste rock from breaking into the compensation rooms. Stoping begins with the creation of a compensation room in each panel. To achieve this, the cut raise is first widened to the full width of the compensation room's contour. Then, rings of long holes *21*, which are drilled from the cut crosscut *14*, are blasted in a series of blasts into this widened cut raise *15*. After each blast, the broken ore is drawn from the loading workings and hauled to the orepass by a self-propelled LHD. In parallel with the formation of the compensation room, the main ore reserve is drilled using rings of long holes *22* from the drill niches of the drill drift *18*. From these same drill niches *19*, blast holes *24* are also drilled to develop the drawbells. The drilling of the main ore reserve and the creation of the compensation room should be completed simultaneously. This ensures the shortest possible duration of the compensation room existence. Bulk caving of the main ore reserve is achieved through multi-row millisecond-delay blasting of long hole rings *22*. The holes are undercharged by 3-5 m from their collar to ensure the preservation of the drill drift. During the bulk blast, the blast holes *24* are also detonated. This develops the drawbells in the drill niches, which will later be used as drawpoints. As previously mentioned, the drill drift *18* will subsequently be used as a scraper drift (the "catching" level) to reduce ore losses on the footwall of the ore body. The drawing and haulage of the broken ore from the loading workings *13* to the orepass *5* are performed by a self-propelled LHD. To intensify ore drawing from the panel and further reduce ore losses on the footwall, ore drawing is also performed simultaneously on the "catching" level, and the ore is hauled to the orepass by a scraper. To mine iron ore deposits up to 30-35 m thick, the authors developed a variant of the sublevel caving system with combined ore haulage by self-propelled LHDs and scraper equipment. This system is illustrated in Figure 3.

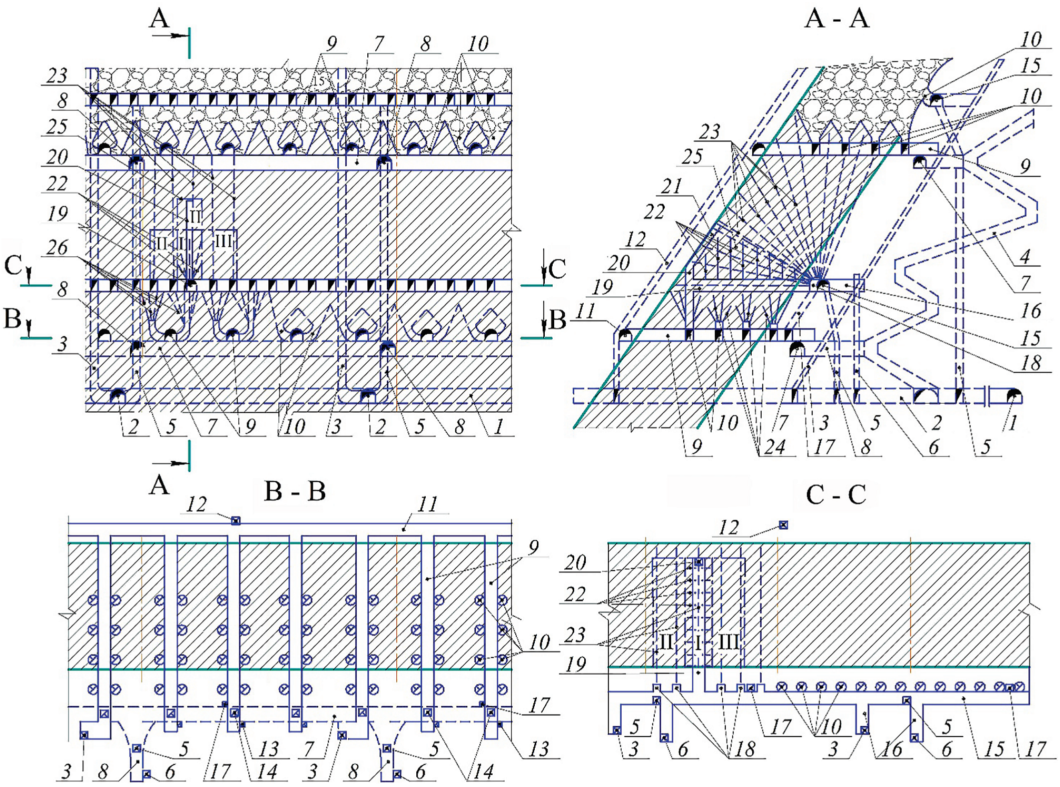

Figure 3. *The developed variant of the sublevel caving system for mining deposits up to 30-35 m thick with combined ore haulage by self-propelled LHDs and scraper equipment*

Source: *developed by the authors*

This variant was developed for use in deposits consisting of low-strength and low-stability ores. The combination of deep-level mining and high rock pressure presents a significant challenge for developing workings with a cross-sectional area of approximately 10 m², which is sufficient for the deployment of minimum-sized self-propelled LHDs (with a bucket capacity of 1.5-2.0 m³), thereby extending the scope of self-propelled equipment in complex mining-geological environments. The proposed technology involves mining the deposit in 50-60 m long blocks along the strike. These blocks are vertically divided into two sublevels of approximately equal height within a single level (75-80 m). The preparation of the block is practically no different from its preparation in the previous version (Fig. 2) and involves the following: from a footwall haulage drift *1* access crosscuts *2* are driven at 50-60-meter intervals; from these crosscuts, block ventilation-and-manway raises *3* are created to break through to the upper ventilation level; an inclined runaway *4* is driven in the footwall rock to provide access for self-propelled equipment to the intermediate sublevels.

Development work begins with the creation of orepasses *5* and service raises *6* to facilitate the driving of other workings and support activities on the intermediate sublevels. Haulage drifts *7* are driven in the footwall rock, the lower of which is located 10 m above the haulage level. These drifts are directly connected to the block ventilation-and-manway raise *3* and via unloading workings *8* – to the orepasses *5* and the service raise *6*. In the roof of the haulage drifts, scraper crosscuts *9* with drawpoints *10* are created. In the hanging wall, these crosscuts are connected to each other by a ventilation drift *11*, which in turn is connected to a ventilation raise *12*. Depending on the mine's ventilation scheme, this raise can connect to either the ventilation level. The scraper crosscuts are connected to the haulage drift via manways *13* and unloading apertures *14* that are covered with grizzly screens.

In the footwall rock, drill drifts *15* are driven 10 m above the floor of the scraper crosscuts *9*. These drifts will also be used as scraper drifts, connecting directly to the orepasses *5* and, via crosscuts *16*, to the service *6* and orepass *5* raises. When positioning these workings, it is also necessary to consider the refined boundaries of the ore bodies in zones of tectonic disturbances. To ventilate this level, air connections *17* are created from the drill drift *15* to the scraper crosscuts *9*. From the drill drifts, drill niches *18* are developed towards the ore body and will later be used as drawpoints *10* on this level. Additionally, cut crosscuts *19* are created, which connect to the cut raise *20* that is developed from one of the end drawpoints. To form the inclined slot *21* at the initial stage, rings of boreholes *22* are drilled from a cut crosscut *19*. To break the main ore reserve in the panel, rings of long holes *23* are drilled from the drill niches 18. Subsequently, blast holes *24* are drilled from the niches to develop the drawpoints into receiving drawbells.

The block within each sub-level is divided into two panels, each with a width of 25-30 m. Each panel is subsequently mined by two scraper crosscuts, with the main ore reserve caved into an inclined compensation room. The stoping process begins by creating an inclined slot *21* in each panel. For this, the cut raise is first expanded to the width of the slot by sequentially blasting paired blast holes drilled on both sides of the raise. Following the broken ore drawing on the expanded cut raise *20*, rings of blast holes *22* of varying heights are blasted in a series of blasts. Simultaneously, one row of drawbells is developed beneath them by detonating blast holes *24* drilled from the drawpoints *10*. Following each blast, the broken ore is drawn via the drawpoints and hauled to the unloading apertures by a scraper. Through the aperture, the ore then falls to the haulage drift, where a self-propelled LHD transports it to the orepass. After the inclined slot is formed, a portion of the long hole rings *23* situated above and on either side of the inclined slot are sequenially detonated in multiple blasts. This creates an inclined compensation room *25* of the necessary volume. Simultaneously, the drawbells are developed beneath the compensation room by blasting the blast holes *24* drilled from the drawpoints. The resulting broken ore is drawn after each blast.

In the vertical projection, Roman numerals denote the stages of the inclined compensation room creation: I – formation of the inclined slot, II and III – the blasting of a portion of the rings of long holes situated above and on either side of the inclined slot, thereby forming the inclined compensation room *25* within its designed contours. In parallel with the development of the inclined compensation room, the main ore reserve is drilled using rings of long holes *23* from the drill niches of the drill drift. From these same drill niches, blast holes *24* are also drilled to deploy the drawbells. It is essential that the drilling of the main ore reserve is completed simultaneously with the creation of the compensation room to ensure a minimal duration of the compensation room existence. Bulk caving of the main ore reserve is achieved through multi-row millisecond-delay blasting of long hole rings *23*. The holes are undercharged by 3-5 m from their collar to ensure the preservation of the drill drift. During the bulk blast, the blast holes *24* are also detonated. The drill drift will subsequently be used as a "catching" level to reduce broken ore losses in the "dead" zone on the footwall.

After the bulk caving of the ore in the panel, it is drawn and hauled according to the developed drawing schedule. The ore is drawn through the drawpoints and hauled by a scraper to an unloading aperture. From there, the ore falls onto the haulage drift, where a self-propelled LHD hauls it to the orepass. The ore drawn from the drawpoints on the "catching" level is hauled directly to the orepass by a scraper. To improve the efficiency of the self-propelled LHDs – whose productivity is significantly higher than that of scrapers for primary haulage in the stopes – one LHD can be used to haul ore simultaneously from two adjacent panels on opposite sides of the orepass. In this case, unloading workings *8* are used for the LHD to make a U-turn. Both proposed variants for the sublevel caving system facilitate the application of high productivity self-propelled LHDs for ore haulage even when mining iron ore deposits in the demanding conditions of the deep Kryvbas mines. The variant for mining thick deposits incorporates a parabolic or vaulted (arch) shaped compensation room, which improves its stability. This design mitigates the formation of critical tensile stresses in the surrounding rock massif, ensuring the room's integrity even in ores with low compressive strength (30-50 MPa) at depths of up to 2,000 m. This finding was supported by the research of W. Elrawy *et al*. (2020). The ability to create compensation rooms of required volume under these demanding conditions ensures effective ore fragmentation during bulk caving. This is achieved by maintaining the required ore loosening coefficient, which minimises the generation of oversize material and mitigates ore congestions during drawing, as highlighted by A. Kosenko *et al*. (2024). This approach also contributes to improved labour productivity and safety for ore drawing and haulage operations, while simultaneously reducing the costs associated with secondary crushing. It should also be noted that the implementation of an additional "catching" level facilitates a higher indicator of extraction within the panels. This, in turn, shortens the overall mining cycle, reduces the volume of re-timbering required for the haulage workings, and decreases broken ore losses on the footwall of the ore body.

Given that the predominant method of iron ore extraction in the Kryvbas mines involves breaking into a compensation space, considerable research was dedicated to identifying a more stable form for this space. For instance, A. Matayev *et al*. (2024) proposed a "reverse trench" shape for the tent-like compensation room. The accuracy of determining the equivalent mechanical properties of the rock massif was further enhanced by incorporating a digital characterisation of the fractured rock massif, based on the structural features of the deposit, as outlined in Huang *et al*. (2024). This approach facilitated a more refined calculation of the stress-strain state of the rock in areas subjected to high rock pressure. W. Elrawy *et al*. (2020) proposed to improve the mining of panels with this system by increasing the intensity of ore drawing with scrapers. To achieve this, the authors suggested almost halving the average haulage distance by driving only two to three pairs of drawpoints in the workings. Furthermore, A. Khorolskyi & A. Kosenko (2022) proposed increasing the efficiency of combined haulage by using more powerful (55 kW) scraper units equipped with multi-bucket scrapers. These units would operate in conjunction with a powerful self-propelled LHD (such as the TORO-400E).

In the variant developed for mining deposits up to 30-35 m thick, a combined ore haulage system using scrapers and self-propelled LHDs was proposed, as suggested by I.B. Bondarchuk *et al*. (2015) and O. Khomenko *et al*. (2015). This approach offers several key advantages. It provides better ore extraction indicators through areal drawing in the panels by scrapers and increases mining intensity by using LHDs for secondary haulage to the orepass. The additional "catching" level also contributes to these benefits. Furthermore, this system helps reduce the cost of maintaining haulage workings by utilising more stable scraper crosscuts instead of drifts, and by locating the larger cross-section workings for the self-propelled LHDs in the stronger and more stable rock of the footwall. To increase the efficiency of self-propelled LHDs – whose productivity for primary haulage in stopes is significantly higher than that of scrapers – it was proposed that a single LHD be used to haul ore simultaneously from two adjacent panels on opposite sides of the orepass. The use of an inclined compensation room in this variant allows for the creation of rooms of required volume, even in low-stability ores under high rock pressure. According to M. Stupnik *et al*. (2023), the roof of the room should have an inclination of at least 35-40 degrees to enhance its stability. This approach is supported by many years of successful practical experience of using compensation rooms of this shape at the deep levels of the Kryvorizka mine, owned by Kryvbaszalizrudkom JSC.

Conclusions

The developed variants of the sublevel caving system allow their application in the challenging conditions of deep Kryvbas mines for mining iron ore deposits of varying thicknesses. The use of self-propelled LHDs for ore haulage during stoping is expected to increase labour productivity in this process by approximately 1.5-2.0 times compared to the existing system employing scrapers. This also improves working conditions and safety. To enable the creation of compensation rooms of sufficient volume even in low-strength and low-stability ores, the system provides a parabolic, vaulted (arch) shape, or an inclined compensation room with an optimal roof inclination angle (no less than 35-40 degrees). This design ensures the necessary ore loosening coefficient for a specific ore type during bulk caving of the main panel reserve, which improves the quality of ore fragmentation and reduces the production of oversize material. Combined ore haulage with scrapers directly in the stopes and then with self-propelled LHDs to the orepass allows for a combination of better ore extraction (due to drawing across the entire panel area) and higher productivity during secondary haulage. At the same time, positioning the scraper workings across the strike of the ore body and locating the LHD workings in more stable footwall rock improves their stability and reduces the cost of maintaining the workings during operation. The use of an additional "catching" level in both variants helps reduce broken ore losses on the footwall and increases the mining intensity of the panels. This, in turn, shortens the overall mining time, which helps reduce the amount of re-timbering needed for the workings at the bottom of the panels, and the associated costs. Future research will focus on optimising the size of mining panels, as this significantly influences the mining time. The duration of mining is a key factor affecting the stability of workings, as well as the overall efficiency and safety of the operations.

Acknowledgements

The authors wish to extend their sincere gratitude to the engineering and technical personnel of Kryvbaszalizrudkom JSC for their invaluable assistance in providing data on the operation of self-propelled equipment within the company's mining operations.

Funding

The authors gratefully acknowledge the financial support of the Ministry of Education and Science of Ukraine. This research was conducted as part of the state scientific project "Investigation and scientific-practical substantiation of technological methods for raw material control during ore mining at deep levels" (state registration 0122U000843).

Conflict of Interest

None.

References

[1] Abdiev, A.R., Wang, J., Mambetova, R.Sh., Abdiev, A.A., & Abdiev, A.Sh. (2025). Geomechanical assessment of stress-strain conditions in structurally heterogeneous rock masses of Kyrgyzstan. *Engineering Journal of Satbayev University*, 147(2), 31-39. doi: 10.51301/ejsu.2025.i2.05.

[2] Andreev, B.M., Brovko, D.V., & Khvorost, V.V. (2015). Determination of reliability and justification of object parameters on the surface of mines taking into account change-over to the lighter enclosing structures. *Metallurgical and Mining industry*, 12, 378-382. doi: 10.13140/RG.2.2.30779.31529.

[3] Bazaluk, O., Ashcheulova, O., Mamaikin, O., Khorolskyi, A., Lozynskyi, V., & Saik, P. (2022). Innovative activities in the sphere of mining process management. *Frontiers in Environmental Science*, 10, article number 878977. doi: 10.3389/fenvs.2022.878977.

[4] Bazaluk, O., Petlovanyi, M., Sai, K., Chebanov, M., & Lozynskyi, V. (2024). Comprehensive assessment of the earth's surface state disturbed by mining and ways to improve the situation: Case study of Kryvyi Rih Iron-ore Basin, Ukraine. *Frontiers in Environmental Science*, 12, article number 1480344. doi: 10.3389/fenvs.2024.1480344.

[5] Bondarchuk, I.B., & Shenderova, I.V. (2015). Classification of hydraulic borehole mining technological processes during pay zone development. *IOP Conference Series: Earth and Environmental Science*, 24, article number 012004. doi: 10.1088/1755-1315/24/1/012004.

[6] Chong, S.-H., Song, K.-I., & Cho, G.-C. (2021). Development of equivalent stress- and strain-dependent model for jointed rock mass and its application to underground structure. *KSCE Journal of Civil Engineering*, 25, 4887-4896. doi: 10.1007/s12205-021-0616-6.

[7] Elrawy, W.R., Abdelhaffez, G., & Saleem, H. (2020). Stability assessment of underground openings using different rock support systems. *Rudarsko-Geološko-Naftni Zbornik*, 35(1), 49-63. doi: 10.17794/rgn.2020.1.5.

[8] Huang, X., Mei, G., Wang, J., & Shi, C. (2024) Digital characterization and equivalent mechanical parameters of broken rock mass based on structural characteristics of rock mass. *Bulletin of Engineering Geology and the Environment*, 83, article number 508. doi: 10.1007/s10064-024-04020-1.

[9] Khomenko, O., Kononenko, M., & Petlovanyi, M. (2015). Analytical modeling of the backfill massif deformations around the chamber with mining depth increase. In G. Pivnyak, V. Bondarenko & I. Kovalevska (Eds.). *New developments in mining engineering 2015: Theoretical and practical solutions of mineral resources mining* (pp. 265-269). London: Taylor & Francis Group.

[10] Khorolskyi, A., & Kosenko, A. (2022). Results of simulation modeling of the influence of technological parameters on the outburst hazard of coal seams. In *5th international scientific and technical internet conference "Innovative development of resource-saving technologies and sustainable use of natural resources"* (pp. 157-160). Petroșani: Universitas Publishing.

[11] Kosenko, A., Khomenko, O., Kononenko, M., Yegorchenko, R., Starikov, G., & Dychkovskyi, R. (2024). Management of scraper-self-propelled ore delivery parameters in caving operations. *Mining Machines*, 42(4), 277-287. doi: 10.32056/KOMAG2024.4.4.

[12] Lutsenko, I., Tytiuk, V., Oksanych, I., & Rozhnenko, Z. (2017). Development of the method for determining optimal parameters of the process of displacement of technological objects. *Eastern-European Journal of Enterprise Technologies*, 6(3(90)), 41-48. doi: 10.15587/1729-4061.2017.116788.

[13] Matayev, A., Uakhitova, B., Kaumetova, D., Imangazin, M., Sarkulova, Z., Issengaliyeva, G., & Orazbekova, R. (2024). Substantiation and selection of parameters for supporting mine workings at deep levels. *Mining of Mineral Deposits*, 18(4), 125-138. doi: 10.33271/mining18.04.125.

[14] Mazhitov, A.M., & Volkov, P.V. (2020). Substantiation of parameters of underground geotechnology in the development of complex structural deposit of various grades of ores. *IOP Conference Series: Materials Science and Engineering*, 966, article number 012003. doi: 10.1088/1757-899X/966/1/012003.

[15] Pysmennyi, S., Brovko, D., Shwager, N., Kasatkina, I., Paraniuk, D., & Serdiuk, O. (2018). Development of complex-structure ore deposits by means of chamber systems under conditions of the Kryvyi Rih iron ore field. *Eastern-European Journal of Enterprise Technologies*, 5(1(95)), 33-45. doi: 10.15587/1729-4061.2018.142483.

[16] Pysmennyi, S., Fedko, M., Shvaher, N., & Chukharev, S. (2020). Mining of rich iron ore deposits of complex structure under the conditions of rock pressure development. *E3S Web of Conferences*, 201, article number 01022. doi: 10.1051/e3sconf/202020101022.

[17] Salkynov, A., Rymkulova, A., Suimbayeva, A., & Zeitinova, S. (2023). Research into deformation processes in the rock mass surrounding the stoping face when mining sloping ore deposits. *Mining of Mineral Deposits*, 17(2), 82-90. doi: 10.33271/mining17.02.082.

[18] Seyed, M.R.S., Kaveh, A., & Mosleh, E. (2025). Analysis of the impact of different blast energies on rock crushing using numerical modelling. *Rudarsko-Geološko-Naftni Zbornik*, 40(2), 87-105. doi: 10.17794/rgn.2025.2.7.

[19] Shihov, D., & Bekbotayeva, A. (2024). Correlation of ore bodies in a molybdenum-tungsten deposit using the distribution of rock-forming and trace elements. *Engineering Journal of Satbayev University*, 146(2), 29-36. doi: 10.51301/ejsu.2024.i2.04.

[20] Stupnik, M., Fedko, M., Hryshchenko, M., Kalinichenko, O., & Kalinichenko, V. (2023). Study of compensation room impacts on the massif stability and mined ore mass quality. *Inżynieria Mineralna – Journal of the Polish Mineral Engineering Society*, 1(51), 137-144. doi: 10.29227/IM-2023-01-16.

[21] Stupnik, M., Kalinichenko, V., Kalinichenko, O., & Pochtarev, A. (2021). Technological measures to enhance efficiency of mining ore from stopes applying self-propelled equipment. *E3S Web of Conferences*, 280, article number 08010. doi: 10.1051/e3sconf/202128008010.

[22] Tayebi, A., El Maghraoui, M., Bezzout, H., & El Faylali, H. (2019). Numerical simulation of rock massif stress state at normal fault at underground longwall coal mining. *International Journal of Civil Engineering and Technology (IJCIET)*, 10(10), 197-204.

Микола Ступнік
Доктор технічних наук, професор
Криворізький національний університет
50027, вул. Віталія Матусевича, 11, м. Кривий Ріг, Україна
https://orcid.org/0000-0003-3318-3889

Всеволод Калініченко
Доктор технічних наук, професор
Криворізький національний університет
50027, вул. Віталія Матусевича, 11, м. Кривий Ріг, Україна
https://orcid.org/0000-0002-1938-2286

Михайло Федько
Кандидат технічних наук, доцент
Криворізький національний університет
50027, вул. Віталія Матусевича, 11, м. Кривий Ріг, Україна
https://orcid.org/0000-0002-8437-3175

Сергій Письменний
Кандидат технічних наук, доцент
Криворізький національний університет
50027, вул. Віталія Матусевича, 11, м. Кривий Ріг, Україна
https://orcid.org/0000-0001-5384-6972

Михайло Грищенко
Старший викладач
Криворізький національний університет
50027, вул. Віталія Матусевича, 11, м. Кривий Ріг, Україна
https://orcid.org/0000-0002-9365-1886

Розробка високоефективних технологій видобутку багатих залізних руд на глибоких горизонтах шахт Кривбасу

Анотація. Близько половини обсягів багатих залізних руд, які видобувають на шахтах Кривбасу, здійснюють із використанням різних варіантів системи підповерхового обвалення. При цьому доставку руди у виймальних панелях виконують виключно скреперними установками, які не відповідають сучасним вимогам з точки зору умов праці гірників, її продуктивності та безпеки робіт. Метою роботи була розробка більш ефективних технологічних схем видобування багатих залізних руд системою підповерхового обвалення, що було здійснено, в першу чергу, за рахунок застосування на доставці руди самохідних навантажувально-доставочних машин (НДМ) та інших технічних рішень. Запропоновані нові технологічні схеми відпрацювання покладів залізорудної сировини системою підповерхового обвалення, які ґрунтуються на застосуванні на доставці самохідних НДМ. Це досягається застосуванням окрім основного горизонту випуску, де працюють виключно самохідні НДМ, додаткового горизонту випуску із використанням на ньому скреперних установок, для чого повторно використовують буровий штрек. Це забезпечує більш інтенсивне відпрацювання панелей, завдяки чому зменшуються витрати на підтримання виробок та покращуються показники вилучення руди. Інший варіант розроблений для відпрацювання покладів потужністю до 30-35 м, передбачає застосування похилих компенсаційних камер, що дає можливість утворювати камери достатнього об'єму навіть у рудах низької стійкості, а також комбіновану доставку руди самохідними НДМ та скреперними установками. Для підвищення ефективності використання самохідних НДМ, продуктивність яких є значно більшою ніж скреперних установок, передбачена можливість застосування одної НДМ для одночасної доставки руди з двох суміжних панелей. Таким чином, головними перевагами запропонованих варіантів систем розробки є підвищення інтенсивності відпрацювання панелей, суттєве зменшення втрат відбитої руди на лежачому боці покладу, а також можливість застосування самохідних НДМ в умовах шахт Криворізького залізорудного басейну

Ключові слова: залізорудна сировина; підземний видобуток; технологія розробки; підповерхове обвалення; доставка руди; самохідна техніка

Journal homepage: https://mining-journal.com.ua/en
ISSN 2306-5435

MINING JOURNAL of Kryvyi Rih National University

Vol. 59, No. 2, 2025

Received: 20.07.2025; Revised: 02.12.2025; Accepted: 24.12.2025; Published: 05.01.2026

UDC 622.276.5:658.14
DOI: 10.31721/2306-5435-2025-2-32-45

Shahin Ismayilov
PhD in Technical Sciences, Associate Professor
Azerbaijan State Oil and Industry University
AZ1010, 20 Azadliq Ave., Baku, Azerbaijan
https://orcid.org/0000-0002-9558-4701

Zaur Mirzayev*
Graduate Student
Azerbaijan State Oil and Industry University
AZ1010, 20 Azadliq Ave., Baku, Azerbaijan
https://orcid.org/0009-0003-9066-3114

Innovative methods for improvement of production efficiency at wells with sand production: Technological metrics and their role

Abstract. Sand production in production and injection wells is a critical factor that reduces productivity and operational reliability, necessitating innovative control methods. The study aimed to develop a scientific basis for improving the production efficiency of wells prone to sand production using innovative sand control techniques and a system of key performance indicators for their implementation, using typical offshore production conditions as an example. The work uses numerical modelling, scenario analysis using long-short-term memory algorithms and recurrent blocks with controlled updating, simulation of processes in a digital twin of the well, and verification of the results according to American Petroleum Institute Recommended Practice 14E and ISO 17824:2009 standards. The study determined that the implementation of intelligent monitoring systems increases the accuracy of sand detection from 65% to 85% and reduces the number of missed events by 40% compared to threshold schemes. The average operating time of a well without particle removal increased by almost 1.5 times, and specific operating costs decreased by 20%. Practical "before/after" cases have shown that limiting depression in combination with modernising the filtration system increases operational stability (increasing sand-free time from ~45% to ~70%), while controlled pumping with chemical stabilisation reduces the skin factor from ~6 to ~2.5 with a 12-15% increase in productivity. The results demonstrate that the integration of digital twins, predictive analytics algorithms, and combined physical and chemical methods forms a new paradigm for sand control. This ensures coordinated growth in productivity, reliability and environmental sustainability, confirming the strategic potential of digital transformation in the oil and gas industry

Keywords: digital twin; silting; skin factor; productivity coefficient; oil and gas industry; artificial intelligence models

Suggested Citation:
Ismayilov, Sh., & Mirzayev, Z. (2025). Innovative methods for improvement of production efficiency at wells with sand production: Technological metrics and their role. *Mining Journal of Kryvyi Rih National University*, 59(2), 32-45. doi: 10.31721/2306-5435-2025-2-32-45.

*Corresponding author

Introduction

Sand production in production and injection wells remains one of the key causes of production efficiency losses: solid phase removal accelerates abrasive wear of equipment, increases hydraulic losses, causes flow instability and unplanned downtime. In response, the industry is shifting from a "catalogue" of disparate solutions to management based on pre-agreed key performance indicators (KPIs), where the choice of technologies is strictly linked to the sand-free rate, permissible formation depression, productivity coefficient, additional filtration resistance (skin factor), particle retention coefficient and filter erosion indicators, as well as the total sand-free operating time.

Summarising mechanical approaches, B.A. Suleimanov *et al.* (2024) demonstrated that the effectiveness of screens and gravel packs is determined not only by their design, but also by verified criteria for sand retention and throughput capacity in specified extraction modes. At the same time, a gentler "chemical" approach is being developed: a study by M. Soroush *et al.* (2020) analysed the challenges and prospects of designing sand control systems in weakly cemented reservoirs in Kazakhstan, emphasising the importance of chemical consolidation technologies that can maintain permeability with minimal skin factor growth. Early diagnosis and prompt adjustment of sampling modes enhance the effect of control technologies. On large assets in the Caspian region, Z. Hasanov *et al.* (2021) showed that distributed acoustic surveying (DAS) identifies sand signatures in horizontal wells and can be used for calibration of maximum depressions without excessive flow rate restrictions. To predict sand occurrence zones, A. Kukshal *et al.* (2024) integrated rock strength parameters with core microanalysis, improving the accuracy of risk mapping and the quality of candidate selection for mechanical or chemical control. In mature offshore clusters, D. Kazidenov *et al.* (2025) described the transition to comprehensive sand management strategies, where monitoring, properly designed filtration systems, and operating regulations are combined into a single control loop with KPI assessment of sand retention, intervention frequency, and specific operating costs (OPEX).

With high solid phase removal, coupled flow and transport models come to the fore: S. Murillo *et al.* (2025) used dynamic modelling to remove flow assurance uncertainties and optimise pumping modes, reducing the risks of blockages and erosion failures. The results of laboratory and field cycles on the durability of "chemical" solutions were supported by data from J.Z. Kueh *et al.* (2022), which evaluated the durability of consolidation as an alternative to primary mechanical control in marginal reservoirs. At the industry review level, Y. Li *et al.* (2024) noted a trend towards the integration of mechanical and chemical means with online monitoring and analytics, emphasising the need for a unified set of technological indicators to compare options in terms of their contribution to stable flow rates and equipment resources.

The design and technology circuit is reinforced by experimental and numerical filter selection: N.C. Su *et al.* (2025) demonstrated that combining laboratory slurry tests with coupled numerical modelling based on computational fluid dynamics and discrete particle modelling improves the predictability of screen performance and can be used for optimisation of particle retention at a given pressure loss and required erosion resistance. Lastly, the related field of offshore gas hydrate extraction enriches the methodological toolkit for sand control: N. Wu *et al.* (2021) proposed approaches to solid phase management under unstable thermobaric conditions, which can be applied to traditional sand-prone reservoirs. In the context of typical offshore oil and gas fields, the use of programming tools and artificial intelligence methods for real-time interpretation of telemetry data on pressure and temperature at various well circuits, hydrodynamic gradients and monitoring system signals, with automatic comparison of any deviations in these parameters with pre-agreed key performance indicators for sand-free operation and permissible values of formation depression.

The study aimed to substantiate scientific approaches to improving the production efficiency of wells prone to sand production, with a focus on introducing innovative sand control technologies and developing a system of key performance indicators based on typical offshore field conditions. To achieve the research objective, the following tasks were set: perform a comparative analysis of modern mechanical, chemical, and organisational and technological solutions for sand control and establish a consistent set of key performance indicators with target values; develop and theoretically test a real-time telemetry processing circuit based on programming tools and artificial intelligence methods with automatic comparison of deviations in pressure, temperature and acoustic signals with target indicators; perform theoretical modelling and scenario analysis under synthetic conditions, quantitatively assessing the impact of selected techniques on flow stability, productivity coefficient, additional filtration resistance, sand removal rate and specific operating costs, with the formulation of practical recommendations.

Materials and Methods

The basis was a theoretical model of a "digital twin" of a typical sand-hazardous well, built on synthetic data reflecting typical operating conditions, in which the following were specified in advance: wellbore type (horizontal and directional), completion options (open-hole and screened configurations with filters and/or gravel packs), reservoir condition ranges (reservoir pressure and temperature, viscosity and gas content of fluids), as well as representative particle size classes of transported particles. The composition of telemetry streams was determined conceptually and included bottomhole/wellhead pressures and temperatures, phase flow rates, tubing position, hydrostatic gradient in pump-compressor pipes, and surface sand detector signals; these series were used as feature carriers rather than actual field measurements. A set of key performance indicators was recorded as a dictionary with definitions, units of measurement, and target ranges: proportion of time without sand removal, permissible depression on the formation, productivity coefficient, additional filtration resistance (skin factor), pressure drop and retention coefficient on filter elements, frequency of technological interventions, and specific operating costs. To substantiate the research model, a systematic review of scientific and technical sources was conducted using Scopus, Web of Science, SpringerLink, and OnePetro databases. The relationship between the indicators and industrial safety and equipment resources was determined by reference benchmarks: maximum erosion flow rates according to American Petroleum Institute (API) (1991), the recommended practice is 14E, and the level of requirements for sand control screens according to ISO 17824:2009 (2009). Two software environments were used for the calculation implementation: Python in Jupyter Notebook (as a basic tool for analytics and prototyping of interpretation rules) and PIPESIM (as a node simulator of inflow and transport in the wellbore for scenario building).

The study was conducted in three stages. In the first stage, the phenomenology of silting/sand boils and their impact on productivity and safety was formalised: in a "digital twin", the mechanisms of particle mobilisation during depression growth were simulated, libraries of erosion and blockage scenarios were formed, and key indicators were recalculated (changes in flow rate, pressure drops, skin factor, and the proportion of time without sand carryover). The second stage involved a comparative analysis of technologies for controlling and combating particle carryover. For mechanical screens and gravel packs, the particle retention coefficient and expected pressure losses were compared; for physical cleaning, the reduction in clogging with increasing frequency of interventions; for chemical consolidation, the preservation of permeability and durability within acceptable thermobaric windows. The analysis method was based on numerical modelling of scenarios in Python/Jupyter and PIPESIM environments, where the particle retention coefficient, pressure drop across the filter, skin factor, frequency of interventions and operational stability of filtration systems were calculated. The comparison results were summarised in tables and graphs, acceptable depression windows were recorded, and the operational compromises of each approach were determined. In the third stage, a management framework was formed, where the key role was assigned to software tools and artificial intelligence methods. In the Python/Jupyter environment, a modular time series processing chain was established: Downhole Pressure and Wellhead Pressure data, Downhole Temperature and Wellhead Temperature data, hydrostatic gradient of the column in the sucker rod pipes and surface sand detector signals were synchronised and cleaned; features were formed using sliding windows (instantaneous depression and its derivatives, flow rate change rates, pulsation indices, spectral densities/energies in diagnostic bands, conditional carry-away integrals). To detect and predict sand formation/growth events, recurrent neural networks of the Long Short-Term Memory (LSTM) and Gated Recurrent Unit (GRU) classes were used, as well as threshold anomaly detection schemes. Training was performed with a breakdown by wells to exclude leaks; alarm thresholds were selected based on a cost function with an increased penalty for missing an event; for interpretability, feature importance and local explanations were calculated using SHapley Additive exPlanations methods.

At the same time, the PIPESIM hydraulic simulator was used for scenario modelling of the "technology-indicator-effect" relationship with varying sampling profiles and layouts; the results were compiled into decision maps (acceptable modes, expected indicator values, escalation rules). The reliability of operating mode forecasting was assessed based on the integral R indicator, defined as the proportion of scenarios in which the forecasted values of key technological indicators (wellhead pressure, skin factor, productivity coefficient, pressure drop) fell simultaneously within acceptable ranges according to international standards API recommended practice 14E (American Petroleum Institute, 1991) and ISO 17824:2009 (2009) and showed deviations of no more than 10% from the reference scenarios of the digital twin. Additionally, statistical metrics (Mean Absolute Error, Root Mean Square Error, R^2) were considered, which compared the reliability of forecasts of different algorithms. The approach was verified using quasi-cases on a "digital twin" according to a "before/after" scheme of conditional innovation implementation (integration of monitoring with depression limitation; change of screen type; short-term controlled pumping combined with chemical stabilisation) and analysis of sensitivity to variations in formation pressure, viscosity, granulometry and filter configuration; the compliance of safety scenarios was verified by maximum erosion rates and the functional integrity of the screens.

Results

Characteristics of the phenomenon of well silting and its impact on productivity and operational safety

Simulation of processes in a digital twin showed that an increase in formation depression is regularly accompanied by the mobilisation of fine particles and the gradual formation of silting deposits in the filter zone. These deposits reduce the effective permeability of the reservoir and increase filtration resistance, which directly affects technological indicators. Quantitative calculations revealed a 10-18% decrease in flow rate depending on the particle size distribution and formation conditions, while the skin factor increased to +6 units. In addition, an increase in the pressure drop across the filter element by more than 1.3-1.5 times was recorded.

A key indicator of this phenomenon was a reduction in the duration of well operation without particle removal and accumulation: sand-free or silt-free periods decreased sharply, leading to accelerated erosion of pump and compressor pipes and an increased risk of emergency failures. At the same time, an increase in the content of solid particles in the product not only poses an internal threat to the filtration zone but also increases the risk of contamination of the wellhead equipment, accelerated failure of fittings and potential uncontrolled emissions. These results are consistent with the industrial safety criteria of API recommended practice 14E (American Petroleum Institute, 1991), which sets maximum erosion flow rates. Thus, silting is not only a factor in productivity decline, but also a systemic threat to equipment reliability, environmental safety and the sustainability of the entire technological cycle. Table 1 shows the agreed set of changes in key technological indicators as silting develops.

Table 1. *Change in key technological indicators during sand manifestation simulation*

Indicator	Base state	At pouring	Change, %
Fluid flow rate, m^3/day	100	82-88	-12...-18
Skin-factor	1	+5...+6	increase by 5-6 times
Pressure drop across the filter, MPa	1	1.3-1.5	+30...+50
Operating time without particle removal, %	70	40-50	-25...-30
Risk of tubing erosion (API recommended practice 14E), % of limit	40	70-80	+30...+40
Solid particle content, mg/l	<50	120-150	increase by 2.5-3 times

Source: *compiled by the authors*

Following Table 1, silting triggers a coordinated degradation of the operating mode: the fluid flow rate decreases by 12-18% with a simultaneous increase in local resistance, the skin factor increases to +5...+6, and the pressure drop across the filter element increases by 30-50%. An additional indicator of deterioration is an increase in the content of solid particles in the well production: from a baseline level of less than 50 mg/l, it increases to 120-150 mg/l, which is almost a threefold increase in the abrasive load on the equipment and accelerated formation of secondary deposits in the bottomhole zone. The reduction in stable operating time without particle removal from 70% to 40-50% indicates a transition to a more "aggressive" filtration mode, which directly affects the increase in the share of the maximum erosion rate according to API recommended practice 14E (American Petroleum Institute, 1991), from 40% to 70-80%. Together, this indicates that not only hydrodynamic parameters, but also the concentration of solid inclusions form a closed degradation loop, which, without corrective measures, quickly puts the system into an erosion-hazardous state. Thus, the simulation results demonstrate that silting is not a local operational problem, but a systemic factor that reduces well productivity and simultaneously increases the load on equipment. The combination of a drop-in flow rate, an increase in the skin factor, an increase in pressure drops, and a reduction in operating time without particle removal forms a closed degradation loop, which, without corrective measures, quickly reduces the system to a critical condition. Therefore, timely monitoring of key technological indicators and preventive management of development modes should be considered as priority conditions for ensuring industrial safety and sustainable production.

Comparative analysis of control technologies and methods for combating particle removal in wells

An analysis of traditional solutions (mechanical screens, gravel packs, physical cleaning methods, and chemical consolidation) revealed significant differences in their effectiveness and operational reliability. Mechanical screens provided the highest particle retention rate of up to 80-85%, which significantly reduced the proportion of sand occurrences in the productive interval. However, this advantage was accompanied by a 25-35% increase in pressure drop across the filter element, which had a negative impact on flow rate and sampling profile stability. Gravel packs demonstrated slightly lower particle retention efficiency (70-75%), but proved to be more resistant to prolonged loads, ensuring stable permeability of the filter medium with less resistance growth. Physical cleaning methods (washing and blowing) made it possible to temporarily reduce the degree of filter clogging, but the effect achieved was short-lived: after 1-2 operating cycles, a renewed increase in pressure drop was recorded. In addition, there was an increase in the frequency of interventions and an increase in operating costs by almost 1.8 times compared to the baseline mode. Chemical consolidation proved to be the most effective in maintaining filter permeability: within the permissible thermobaric windows, it was possible to maintain filtering capacity without a noticeable increase in the skin factor and with a coating durability of up to 12-18 months. However, when critical temperature or pressure values were exceeded, coating degradation and partial loss of efficiency were observed. Thus, for each of the methods considered, "windows" of permissible depression were determined: for mechanical screens, no more than 70-80% of the limit values according to API recommended practice 14E (American Petroleum Institute, 1991), for gravel packs up to 85%, for chemical consolidation up to 90% within the thermobaric window. Exceeding these limits was accompanied by a sharp deterioration in technological indicators and an increase in risks. Comparative data are presented in Figure 1, which shows particle retention coefficients, pressure drops and operational stability of various methods of combating sand production.

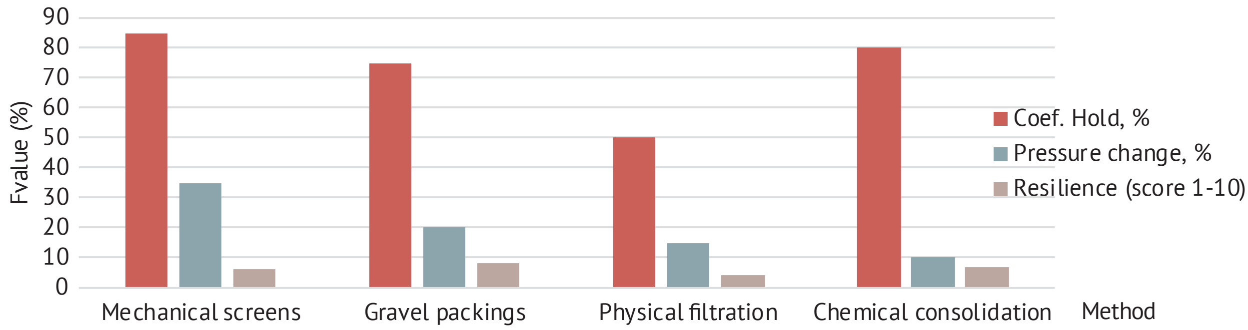

Figure 1. *Comparative indicators of traditional methods of combating sand exposure*

Source: *compiled by the authors*

Following Figure 1, mechanical screens provide a high particle retention rate (about 85%), but their use is accompanied by a significant increase in pressure drop (about 35%) and only average operational stability. During prolonged operation, this leads to an accelerated reduction in the permissible depression range and a decrease in flow rate. Gravel packs retain particles slightly worse (≈75%) but create less resistance (≈20%) and show the best stability over time, i.e., they degrade more slowly and maintain the permeability of the filter medium for longer. Physical cleaning provides the minimum pressure drop (≈15%), but also the lowest retention effect (≈50%) with poor stability: the effect is short-term, requires frequent interventions and increases operating costs. Chemical consolidation demonstrates an almost "screen" level of retention (≈80%) with the smallest pressure drop (≈10%) and good stability; its limitation is compliance with the thermobaric window, outside of which the coating degrades, and performance quickly declines. A comparative analysis of traditional technologies has shown that each has a unique balance of advantages and limitations. Mechanical screens provide a high level of retention, but are accompanied by an increase in hydraulic losses; gravel packs are inferior in terms of filtering capacity, but win in terms of long-term stability; physical cleaning methods provide a short-term effect at the cost of increased operating costs; chemical consolidation combines a high retention coefficient with minimal pressure drop, but is sensitive to thermobaric operating conditions. The established "windows" of permissible depression confirm that exceeding the normative limits leads to a sharp deterioration in performance and an increase in risks, which means that an effective strategy for combating sand production must be based on a flexible combination of these solutions, addressing the specifics of the formation and operational limitations.

Results of innovative technologies for controlling and preventing sand encroachment

The integration of automated monitoring systems has significantly improved the accuracy of detecting sand formation/growth events. The use of sequential data processing models, such as LSTM and GRU, has reduced the number of misses by more than 30% compared to traditional threshold schemes. This means that the risk of delayed response to the onset of sand production has been significantly reduced. Digital forecasting based on Python and the PIPESIM simulator was used for the creation of maps of acceptable well operating modes, including depression intervals and expected key performance indicators. This level of detail developed scenarios for escalating management actions: from restricting the nozzle and adjusting the sampling profile to scheduling treatments. Combining monitoring with controlled depression restrictions increased the average stable operating time of the well without sand removal by almost 1.5 times, confirming the effectiveness of the integrated use of intelligent algorithms and digital modelling. Table 2 shows that the use of innovative monitoring and forecasting technologies provides a qualitative leap in all key parameters of well operation.

Table 2. *Effectiveness of innovative technologies for monitoring and forecasting key indicators*

Indicator	Basic mode (threshold circuits)	Innovative technologies (LSTM, GRU + PIPESIM)	Change, %
Detection accuracy, %	65	85	30
Event omissions, %	20	12	-40
Operating time without sand, % of fund	45	65	44
Specific operating costs (%)	100	80	-20
Reliability of mode prediction	Average	High	-

Source: *compiled by the authors*

Following Table 2, the use of innovative monitoring and forecasting technologies has made it possible to achieve fundamentally new operational effects. The increase in detection accuracy from 65% to 85% was accompanied by a reduction in the number of missed events by almost 40%, which significantly improved the reliability of sand production diagnostics. The increase in the time a well can operate without sand removal from 45% to 65% of the total time effectively means an extension of the equipment's service life and a reduction in the probability of emergency failures. At the same time, a reduction in specific operating costs of approximately 20% was recorded due to a decrease in the frequency of interventions and a transition to preventive mode management. Stability and economic efficiency of well operation. Similar approaches have been confirmed in field conditions: distributed acoustic sensing (DAS) technologies for sand manifestations were successfully applied at several offshore facilities in the Caspian region, which improved diagnostic accuracy and prediction reliability (Hasanov *et al.*, 2021; BP Azerbaijan, n.d.). Together, these results confirm that the integration of intelligent algorithms (LSTM, GRU) with digital modelling not only increases the accuracy of control but also creates a new level of predictability.

Practical "before/after" case studies and results of experimental well investigations

The developed approaches were verified using a digital twin of the well in a comparative "before/after" case study format. The scenario involving changing the type of sand control screen and limiting depression showed an increase in operating time without sand removal to 70% of the total time fund, compared to 45% in the baseline mode. This indicates that even a partial modernisation of the filtration system, provided that the depression is correctly controlled, can significantly extend the life of the well. Another scenario involved controlled short-term pumping combined with chemical stabilisation of the bottomhole zone. The results showed a decrease in the skin factor by 3-4 units and an increase in the productivity coefficient by 12-15% compared to the initial state. This effect confirms the high efficiency of the combined use of physical and chemical methods as part of an integrated strategy. Sensitivity analysis revealed that variations in formation pressure, fluid viscosity and sand particle size distribution have a significant impact on filter stability. However, the digital model made it possible to keep the indicators within the permissible depression "windows", minimising the risk of transition to emergency mode. Figure 2 shows the dynamics of the skin factor and productivity coefficient in the "before/after" scenarios of implementing innovative solutions. As shown in Figure 2, the implementation of combined measures leads to a coordinated improvement in the regime: the proportion of operating time without particle removal increases from approximately 45% to 70%, the skin factor decreases from ~6 to ~2.5, and the productivity coefficient increases by

12-15%. These effects are achieved in two scenarios: "screen replacement + depression limitation" and "controlled pumping + chemical stabilisation", which indicate an expansion of the safe depression window and a reduction in erosion risks. Similar results in terms of increased sand-free operating time and productivity are confirmed by field tests using ceramic screens in a digital twin of a sand-prone well, where long-term stability of the filtration systems was observed (Jafarov *et al.*, 2024).

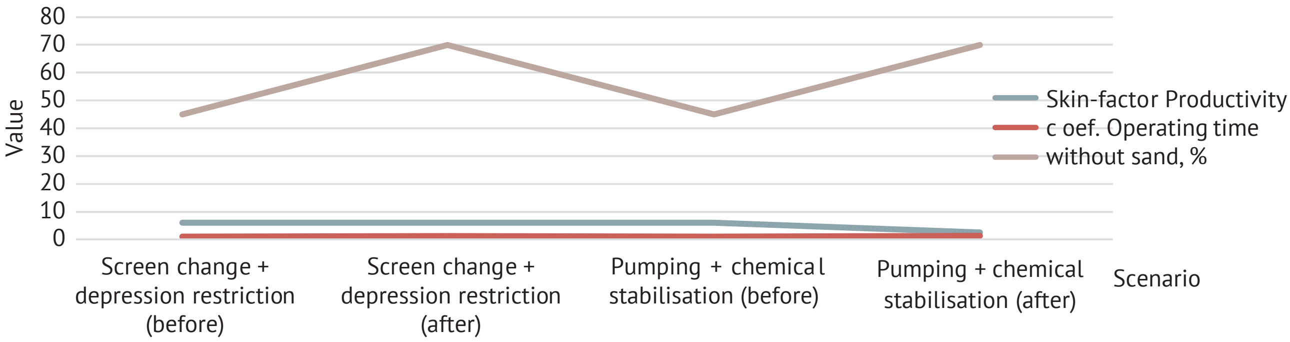

Figure 2. *Dynamics of the skin factor and productivity coefficient in scenarios "before/after" the introduction of innovations*
Source: *compiled by the authors*

Thus, practical "before/after" cases confirm that the use of a digital twin can be used not only to quantitatively record the effect of innovation implementation, but also to identify consistent patterns in well behaviour. The combination of filter system modernisation with depression control and controlled pumping with chemical stabilisation provides a coordinated improvement in two key groups of indicators: stability of operating conditions and productivity of the bottomhole zone. This approach demonstrates the potential for integrating physical, chemical and digital methods into a single strategy, where each measure reinforces the effect of the other. The result is a reliable basis for increasing oil recovery while reducing operational risks and costs.

Verification of sand manifestation control scenarios and their compliance with industrial and environmental safety requirements

The proposed scenarios were verified by comparing the calculated data of the digital twin with industrial standards for safety and operational reliability. The basic criteria used were the maximum erosion flow rates specified in API Recommended Practice 14E (American Petroleum Institute, 1991) and the functional requirements for sand control screens specified in the international standard ISO 17824:2009 (2009). This comparison evaluated not only the effectiveness of the technologies in terms of performance, but also their compliance with industrial safety criteria (Table 3).

Table 3. *Parameters for verifying sand manifestation control scenarios and their compliance with industrial and environmental safety requirements*

Indicator	Base mode	Innovative scenarios
Erosion load (API recommended practice 14E)	100	80
Retention coefficient (ISO 17824:2009)	100	90
Operating costs	100	80
Environmental sustainability	100	85

Source: *compiled by the authors based on American Petroleum Institute (1991), ISO 17824:2009 (2009)*

Following Table 3, the integration of innovative technologies demonstrates consistent growth in all key areas: the effectiveness of digital twin scaling reaches 8 points with a 15% reduction in costs, the use of artificial intelligence models increases the predictability and accuracy of management (9 points) with a 20% reduction in costs, and the comprehensive integration of technologies into operators' production processes provides the maximum effect: a 25% reduction in costs, an increase in reliability to 9 points, and the achievement of high environmental sustainability. The test results showed that none of the tested modes led to exceeding the permissible erosion loads. Even in scenarios with an increase in formation depression, the actual share of the maximum velocity did not exceed 80% of the standard value, which provides a margin of safety for long-term operation of pump and compressor pipes and fittings. Similarly, the functional integrity of sand control screens was confirmed: the reduction in the retention coefficient during long-term operation remained within the permissible values according to ISO 17824:2009 (2009), and the degradation of the filter elements did not reach a critical level. Another substantial result was the maintenance of acceptable operating costs. Despite additional operations to manage modes and integrate monitoring systems, overall costs were reduced due to fewer emergency failures, fewer unscheduled repairs, and increased equipment service life. This indicates that innovative approaches are not only technologically sustainable but also economically sustainable. From an environmental point of view, the tested scenarios also demonstrated a positive effect. The reduction in the frequency of well interventions and the number of emergencies reduces the probability of uncontrolled emissions and lowers the impact on the environment. Thus, the integration of digital models and intelligent monitoring systems creates a "gentler" operating mode that complies with the principles of environmental safety and sustainable development.

Prospects for the application of artificial intelligence models and the integration of innovative solutions into the well monitoring and forecasting system

Modelling has shown that the proposed methods can be scaled to wells with different geological and technological conditions. This is due to the versatility of the principles of digital twin construction, where the main focus is on the dynamics of filtration processes, the influence of depression and interaction with sand control systems. Such flexibility creates the opportunity to replicate the solutions obtained not only within a single field but also on a broader industry scale, where adaptation to diverse development conditions is required. The results showed that artificial intelligence models can be used for predictive control of sanding, forming scenarios for preventive actions before the system exceeds the permissible depression limit. Sequential data processing algorithms (LSTM, GRU) and ensemble methods in the analysis of time series of technological parameters made it possible to form scenarios for preventive actions before the system exceeds the permissible depression limit, which was confirmed in the simulated scenarios of the digital twin. This provides a transition from reactive to proactive control, minimising the risks of emergencies and optimising operating modes.

The integration of these technologies into the production processes of large operators provides a comprehensive effect. Operating costs are reduced by decreasing the frequency of interventions, optimising equipment performance and extending its service life. At the same time, operational reliability is improved: the system demonstrates resistance to fluctuations in reservoir parameters and unpredictable factors. An additional result is compliance with modern environmental requirements, which is reflected in a reduction in the number of emergencies, a decrease in emissions and minimisation of the impact on the environment. Table 4 presents the prospects for the integration and development of innovative technologies, reflecting their potential in three key dimensions: economic, technological and environmental.

Table 4. *Prospects for the integration and development of innovative technologies*

Prospect	Efficiency (score 1-10)	Cost reduction, %	Reliability improvement (score 1-10)	Environmental sustainability (score 1-10)
Digital twin scalability	8	15	8	7
Artificial intelligence models (AI models) for predictive control	9	20	9	8
Integration into the production processes of operators	10	25	9	9

Source: *compiled by the authors*

Following Table 4, the integration of innovative solutions demonstrates balanced growth across all key areas. Scaling the digital twin ensures high efficiency (rated 8 out of 10) while reducing costs by 15%, the use of AI models increases predictability and control accuracy (rated 9 out of 10) while reducing costs by 20%, and comprehensive integration of technologies into production processes yields maximum effect: a 25% reduction in costs, an increase in reliability to 9 out of 10, and the achievement of high environmental sustainability. Thus, the prospects for the application of AI models and the integration of innovative technologies exceed the scope of local improvements to individual wells. These results show that digital twins and intelligent algorithms are capable not only of optimising operations under current conditions, but also of laying the foundation for a systematic transition of the industry to a new management paradigm. The combination of high-precision forecasting, cost reduction, increased reliability and environmental sustainability creates a comprehensive effect that meets the requirements of modern industrial safety and sustainable development. Therefore, proposed approaches are a strategic vector for the digital transformation of the oil and gas industry, ensuring its competitiveness and technological independence in the long term.

Thus, the obtained results redefine silting not as a specific operational problem, but as a systemic factor that simultaneously reduces well productivity and increases risks to equipment, industrial and environmental safety. A comparative analysis of traditional technologies has shown their limited effectiveness and the existence of operational compromises, whereas the integration of digital monitoring, predictive models (LSTM, GRU) and controlled physical and chemical methods ensures consistent growth in key indicators, from flow rate and skin factor to stable operating time and cost reduction. Verification of the scenarios confirmed their compliance with international standards API recommended practice 14E (American Petroleum Institute, 1991) and ISO 7824:2009 (2009), which guarantees industrial safety and operational sustainability. Lastly, the prospects for scaling digital twins and implementing AI predictive control models highlight the formation of a new production paradigm, where increased efficiency and reliability are combined with cost reduction and minimisation of environmental risks, setting the strategic vector for the digital transformation of the oil and gas industry.

Discussion

The results obtained showed that silting in the filter zone forms a consistent pattern of degradation in well performance: a decrease in flow rate, an increase in the skin factor, an increase in pressure drop, and a reduction in operating time without particle removal. These conclusions correlate with the observations of D.T. Asfha *et al.* (2024), which emphasise that the key mechanism of sand production is the mobilisation of fine particles as the depression increases and that the integration of fibre optic technologies and machine learning methods significantly improves the reliability of forecasting. Similar trends are demonstrated by Z. Xu *et al.* (2024), which reviews modern extraction technologies in China, with a particular focus on digital modelling of filtration processes, which is consistent with the results of this study on the use of digital twins to analyse the dynamics of silting and sand production. A comparison with the results presented in the study by X. Zheng *et al.* (2022) shows a coincidence in the analysis of the key role of digital technologies: both in this study and in the Chinese cases, the digitalisation of interpretation processes and the integration of engineering simulators are considered a strategic tool for improving production efficiency. However, while the study analysed the broad prospects for the application of “smart” technologies in the national oil and gas industry, the modelling in a digital twin of a specific sand-prone well demonstrated the applied level of the possibility of quantitatively assessing the impact of depression on productivity and forming scenarios for controlled sand control. The data on chemical stabilisation of the bottomhole zone are consistent with the results of E. Peretomode *et al.* (2022), noting that the chemical interaction of rock and reagents can be used for a temporary reduction in particle removal, but the effectiveness of such methods is limited and largely depends on thermobaric conditions. In the study, a similar effect was observed in scenarios of controlled pumping with chemical stabilisation: a decrease in the skin factor and an increase in productivity were observed, but at the same time, the need for strict adherence to working “windows” to prevent coating degradation and loss of retention capacity was emphasised. Comparative data on the effectiveness of mechanical screens correspond to the conclusions of A. Abduljabbar *et al.* (2024), which shows that mechanical screens provide a high particle retention coefficient, but are accompanied by an increase in pressure drop and accelerated wear of filter elements. The results of digital modelling confirm these observations, demonstrating a similar combination of high efficiency and limited-service life. In turn, data on the use of gravel packs are consistent with the conclusions of R. Miri *et al.* (2024), emphasising that this method provides a slightly lower particle retention coefficient compared to mechanical screens, but is characterised by greater stability of the filtration system during long-term operation. The results of digital modelling also confirmed this pattern, recording more stable behaviour of gravel packs over time. Similar trends are confirmed by F. Deng *et al.* (2022), where, in the context of gas hydrate field development, sand production is a key factor in reducing production reliability.

Verification of scenarios according to API recommended practice 14E (American Petroleum Institute, 1991) and ISO 17824:2009 (2009) demonstrated that the maximum erosion loads were not exceeded and confirmed the functional integrity of the screens, which is consistent with the conclusions of X. He *et al.* (2024) on the need to integrate sand control technologies with industry standards. Additionally, M.A. Issa *et al.* (2022) emphasised the importance of coupled geomechanical models for reducing the risks of sand production, which confirms the feasibility of using digital twins to predict operating conditions. The experimental data of C. Ma *et al.* (2021) on the effectiveness of pre-backfill screens are comparable to the identified effect of reducing the skin factor when changing the filter type. A comparison with the Kazakhstani experience presented in the review by M. Soroush *et al.* (2021) confirmed that in weakly cemented reservoirs, the risks of sand production are particularly high and can only be minimised by a comprehensive approach. The obtained results demonstrated that the combination of digital monitoring, physicochemical stabilisation and controlled depression provides a sustainable improvement in operational performance and is consistent with international practice. The results of digital modelling showed high reproducibility of sand production control scenarios when combining automated monitoring and innovative stabilisation methods. These data are comparable to the conclusions of C. Ma *et al.* (2024), where numerical simulations confirmed the significance of pre-backfill screen parameters for reducing particle migration risks. Similarly, a review by S. Nie *et al.* (2023) emphasised that gravel packs remain the most widely used method in horizontal wells but need to be supplemented with digital tools to improve efficiency and long-term sustainability. The results of the "before/after" case studies are consistent with the methodology for choosing between sand control and sand management strategies presented by E. Araujo-Guerrero *et al.* (2021), which justifies the need to consider both geomechanics and filtration dynamics. From this point of view, the identified decrease in the skin factor and increase in the productivity coefficient after chemical stabilisation demonstrated the feasibility of combined strategies. The geomechanical approaches described by M. Rodríguez *et al.* (2025) confirmed the importance of modelling the stress-strain state in deepwater reservoirs, which echoes the conclusion about the need to keep indicators within acceptable depression "windows". The experience of managing sand production in marine conditions, presented by N. Kerya *et al.* (2022), emphasised the importance of comprehensive strategies in offshore gas fields. The data obtained on filter stability under silting conditions complement the conclusions about the need to integrate monitoring systems with preventive management methods. The experimental results of W. Zhiliang *et al.* (2025), which analysed the migration trajectories of sand under screw pumps, confirmed the significance of numerical modelling for predicting erosion risks and are comparable to the identified increase in abrasive load with increasing solid particle concentration.

Numerical studies by N.I. Ismail *et al.* (2021) confirmed that the use of CFD-DEM approaches can be used for a detailed description of particle motion dynamics and interaction with filtration systems. The study demonstrated that, in the absence of corrective measures, such models record accelerated degradation of well performance. A similar trend was identified in the digital twin, where, without mode control, silting quickly shifts the system into an erosion-prone state. Furthermore, the study by Y. Xiao *et al.* (2024) on field cases in wells without control systems demonstrated that operation in such conditions is inevitably accompanied by accelerated growth of sand production and a decrease in productivity. The data obtained fully corresponds with the results of digital modelling, which also shows that ignoring control and preventive management measures leads to the system transitioning to an emergency-hazardous mode. The causal mechanisms of sand production, as discussed by S.K. Subbiah *et al.* (2021), addressed predictive models, which are consistent with the demonstration of the potential of LSTM and GRU to reduce the number of missed events and transition to proactive management. The potential for using artificial intelligence for lithofacial prediction in complex reservoirs, as demonstrated by M. Ali *et al.* (2024), is consistent with the results of modelling, where sequential time series processing algorithms increased diagnostic accuracy by more than 30%. Together, these sources confirm that the integration of digital twins, DAS monitoring and AI algorithms is shaping a new direction in sand management: from reactive measures to predictive management, ensuring cost reduction, increased reliability and compliance with environmental requirements.

A comparison with the results of other studies shows that the proposed set of innovative approaches to sand control provides a consistent improvement in key well performance indicators. The data obtained confirm the patterns recorded in modern scientific literature: a reduction in the skin factor and pressure drops when using combined stabilisation methods, an extension of sand-free operation time through the modernisation of filtration systems and controlled depression limitation, and improved forecasting accuracy through the introduction of intelligent data processing algorithms. Numerical modelling in a digital twin made it possible to localise areas of critical growth in solid particle concentration and adapt operating modes to minimise the risk of erosion damage. The behaviour of the system under variations in reservoir pressure and fluid properties indicates a reduction in the probability of emergency scenarios and an expansion of the permissible depression window; therefore, proposed technologies can be considered as competitive with traditional sand control methods. The results obtained are fully consistent with the modern paradigm of digitalisation and predictive management in the oil and gas industry, confirming the practical feasibility and strategic potential of integrating digital twins, chemical and mechanical solutions with artificial intelligence tools.

Conclusions

The study confirmed the systemic nature of well silting as a factor that simultaneously reduces productivity and increases risks to equipment, industrial and environmental safety. Simulation of processes in a digital twin showed a regular relationship between the increase in formation depression and the mobilisation of fine particles, which leads to a 12-18% drop-in flow rate, an increase in the skin factor to +6, and a 30-50% increase in the pressure drop across the filter. An additional indicator of degradation was an increase in the content of solid particles in the product from <50 to 120-150 mg/l, which increases the abrasive load and poses a threat of accelerated wear of wellhead equipment and uncontrolled emissions. These results are consistent with the criteria of API recommended practice 14E and indicate a narrowing of the "windows" of safe depression. A comparative analysis of traditional control technologies (mechanical screens, gravel packs, physical cleaning methods and chemical consolidation) revealed their diverse advantages and limitations. Mechanical screens provided maximum particle retention (up to 85%) but were accompanied by increased hydraulic losses. Gravel packs demonstrated better long-term stability with moderate efficiency. Physical methods provided short-term effects at the cost of increased expenses, while chemical consolidation showed balanced results, but its effectiveness depends on compliance with thermobaric windows. The established limits for permissible depression (70-90% of the maximum values according to API recommended practice 14E) confirmed the need for adaptive selection of methods, incorporating the specific conditions of the formation.

The integration of innovative monitoring and forecasting technologies has ensured qualitative growth in operational performance. The use of LSTM and GRU algorithms in combination with modelling in Python/Jupyter and PIPESIM has increased the accuracy of sand detection from 65% to 85%, reduced the number of missed events by 40% and increased the average sand-free operating time by 44%. At the same time, specific operating costs were reduced by 20%. Practical "before/after" cases showed that modernising the filtration system and limiting depression increases the share of stable operation from ~45% to ~70%, while controlled pumping with chemical stabilisation reduces the skin factor from ~6 to ~2.5 and increases the productivity coefficient by 12-15%. These results are also confirmed by modelling in a digital twin of a sand-prone well, where the use of DAS monitoring and ceramic screens improved the accuracy of diagnostics and the stability of filtration systems. Verification of the scenarios confirmed compliance with international standards: maximum erosion loads did not exceed 80% of the normative values, the screen retention coefficient remained within acceptable limits, and total costs were reduced due to a decrease in the number of emergency failures. The environmental effect was expressed in a reduction in the probability of uncontrolled emissions and the minimisation of the impact on the environment.

The prospects for scaling digital twins and implementing AI predictive control models point to the emergence of a new paradigm in production. The integration of intelligent algorithms into production processes can simultaneously reduce costs (by up to 25%), increase reliability (9/10 points) and ensure environmental sustainability. This forms the strategic basis for the digital transformation of the oil and gas industry, where efficiency and safety are combined with environmental responsibility and long-term technological independence. Prospects for further research include the development of multiscale modelling methods that account for the nonlinear interactions of geomechanical, hydrodynamic and chemical factors in the inflow zone; the integration of digital twins with field automation systems and real-time data management platforms; and the expansion of the use of artificial intelligence models for predictive control and optimisation of production modes. Issues related to the standardisation of digital monitoring protocols, the validation of algorithms in long-term field series, and the assessment of the environmental impact of the technologies being implemented require further study.

Acknowledgements

None.

Funding

None.

Conflict of Interest

None.

References

[1] Abduljabbar, A., Amadi, A., Mohyaldinn, M.E., Ridha, S., Younis, O., & Alakbari, F.S. (2024). Sand screens application and performance for sand control: A review of selection criteria, screen materials, and causes of failure. *Heliyon*, 10(10), article number e30731. doi: 10.1016/j.heliyon.2024.e30731.

[2] Ali, M., Zhu, P., Jiang, R., Huolin, M., Ashraf, U., Zhang, H., & Hussain, W. (2024). Data-driven lithofacies prediction in complex tight sandstone reservoirs: A supervised workflow integrating clustering and classification models. *Geomechanics and Geophysics for Geo-Energy and Geo-Resources*, 10, article number 70. doi: 10.1007/s40948-024-00787-5.

[3] American Petroleum Institute. (1991). *Recommended practice for design and installation of offshore production platform piping systems: API recommended practice 14E (RP 14E)*. Retrieved from https://m.saigaogroup.com/uploads/file/api-14e-standard.pdf.

[4] Araujo-Guerrero, E., Alzate-Espinosa, G., Cross-Arroyave, Y., Vega-Niño, Y.P., Cartagena-Pérez, D.F., & Naranjo-Agudelo, A.J. (2021). A new methodology for selecting sand control or sand management as strategy in wells with sand production potential. In *ISRM international symposium geomechanics*. Lisboa: ISRM.

[5] Asfha, D.T., Latiff, A.H.A., Otchere, D.A., Tackie-Otoo, B.N., Babikir, I., Rafi, M., Riyadi, Z.A., Pudra, A.D., & Adeniyi, B.A. (2024). Mechanisms of sand production, prediction – a review and the potential for fiber optic technology and machine learning in monitoring. *Journal of Petroleum Exploration and Production Technology*, 14(10), 2577-2616. doi: 10.1007/s13202-024-01860-1.

[6] BP Azerbaijan. (n.d.). *ACG technology*. Retrieved from https://surl.li/hxhqdz.

[7] Deng, F., Huang, B., Li, X., Liu, J., Li, G., Xu, Y., & Yin, B. (2022). Review of sand control and sand production in a gas hydrate reservoir. *Energy & Fuels*, 36(19), 11712-11723. doi: 10.1021/acs.energyfuels.2c02108.

[8] Hasanov, Z., Allahverdiyev, P., Ibrahimov, F., Mendoza, A., Thiruvenkatanathan, P., Noble, L., & Stapley, J. (2021). Production optimization of sanding horizontal wells using a distributed acoustic sensing (DAS) sand monitoring system: A case study from the ACG field in Azerbaijan. In *SPWLA 62nd annual logging symposium*. Houston: Society of Petrophysicists and Well Log Analysts. doi: 10.30632/SPWLA-2021-0001.

[9] He, X., Pang, Z., Ren, L., Zhao, L., Lu, X., Wang, Y., & Liu, P. (2024). A critical review on analysis of sand producing and sand-control technologies for oil well in oilfields. *Frontiers in Energy Research*, 12, article number 1399033. doi: 10.3389/fenrg.2024.1399033.

[10] Ismail, N.I., Kuang, S., & Yu, A. (2021). CFD-DEM study of particle-fluid flow and retention performance of sand screen. *Powder Technology*, 378(A), 410-420. doi: 10.1016/j.powtec.2020.10.012.

[11] ISO 17824:2009. (2009). *Petroleum and natural gas industries – downhole equipment – sand screens*. Retrieved from https://www.iso.org/standard/44632.html.

[12] Issa, M.A., Hadi, F.A., & Nygaard, R. (2022). Coupled reservoir geomechanics with sand production to minimize the sanding risks in unconsolidated reservoirs. *Petroleum Science and Technology*, 40(9), 1065-1083. doi: 10.1080/10916466.2021.2014522.

[13] Jafarov, E., *et al*. (2024). First three thru-tubing sand control remedial works using ceramic screen in ACG field: Design, execution, evaluation, and strategy for next jobs. In *SPE/ICoTA well intervention conference and exhibition* (article number SPE-218341-MS). Woodlands: Society of Petroleum Engineers. doi: 10.2118/218341-MS.

[14] Kazidenov, D., Omirbekov, S., Zhanabayeva, M., & Amanbek, Y. (2025). Experimental and numerical study of the effect of polymer flooding on sand production in poorly consolidated porous media. *Geoenergy Science and Engineering*, 249, article number 213746. doi: 10.1016/j.geoen.2025.213746.

[15] Kerya, N., Leong, D.G., & Apiwathanasorn, S. (2022). Sand management strategy in offshore gas field in the Gulf of Thailand. In *Offshore technology conference Asia* (article number OTC-31499-MS). Kuala Lumpur: OTC. doi: 10.4043/31499-MS.

[16] Kueh, J.Z., *et al*. (2022). Sand consolidation treatment: durability in an alternative primary sand control method for a marginal reservoir. In *International petroleum technology conference* (article number IPTC-22318-MS). Riyadh: IPTC. doi: 10.2523/IPTC-22318-MS.

[17] Kukshal, A., Sharma, R., Kalita, H.J., Yeshwantth, G.M., Jamwal, V.D., & Lal, H. (2024). Determination of regions prone to sand production and the linkage to fluid flow rates by integrating rock strength parameters and microphotographs in the southern onshore basin, India. *Journal of Petroleum Exploration and Production Technology*, 14(2), 645-663. doi: 10.1007/s13202-023-01728-w.

[18] Li, Y., Sun, W., & Tang, Y. (2024). Current status and prospects of sand control technology in oilfield production: Technological advances, challenges, and development directions. *Advances in Resources Research*, 4(4), 604-623. doi: 10.50908/arr.4.4_604.

[19] Ma, C., Deng, J., Dong, X., Sun, D., Feng, Z., Yan, X., Hui, C., & Tian, D. (2021). Comprehensive experimental study on the sand retention media of pre-filled sand control screens. *Particulate Science and Technology*, 39(3), 261-270. doi: 10.1080/02726351.2019.1687628.

[20] Ma, C., Dou, Y., Deng, J., Hui, C., Zhao, K., Feng, Y., & Dou, L. (2024). Numerical simulations of sand-screen performance in unconsolidated prepacked gravel screen. *Energy Science & Engineering*, 12(3), 983-1003. doi: 10.1002/ese3.1635.

[21] Miri, R., Salimi, M., Stewart, S., Gonzalez, J.M.B., Suárez, C.M., & Nouri, A. (2024). Sand control screen selection for cased dual-annulus gas offshore wells based on scaled laboratory tests. *Canadian Journal of Chemical Engineering*, 102(5), 1957-1969. doi: 10.1002/cjce.25159.

[22] Murillo, S., Santamaria, V., Quevedo, H., Barrero, J., Peñaloza, J., Jimenez, E., Gomez, E., & Kwok, C.K. (2025). Unblocking flow assurance and transport uncertainties in oil wells with high sand production with dynamic simulation. In *Offshore technology conference* (article number OTC-35973-MS). Houston: OTC. doi: 10.4043/35973-MS.

[23] Nie, S., Li, H., Hu, Z., Wen, M., Gao, S., Zhang, H., Luo, H., & Zhang, L. (2023). A review of the research status and development prospects for gravel packing sand control in horizontal wells. *Geoenergy Science and Engineering*, 229, article number 212152. doi: 10.1016/j.geoen.2023.212152.

[24] Peretomode, E., Oluyemi, G., & Faisal, N.H. (2022). Sand production due to chemical-rock interaction. A review. *Engineering Failure Analysis*, 142, article number 106745. doi: 10.1016/j.engfailanal.2022.106745.

[25] Rodríguez, M., Carvajal, O., Khaksar, A., Maia, D., & Furuie, R. (2025). Assessing sanding risks and sand control options using a geomechanical approach in a deepwater oil field, Brazil. In *ARMA US rock mechanics/geomechanics symposium* (article number ARMA-2025-0698). Santa Fe: ARMA. doi: 10.56952/ARMA-2025-0698.

[26] Soroush, M., Hosseini, S.A., Roostaei, M., Pourafshary, P., Mahmoudi, M., Ghalambor, A., & Fattahpour, V. (2020). Challenges and potentials for sand control design and management in oil reservoirs of Kazakhstan. In *SPE international conference and exhibition on formation damage control* (article number SPE-199247-MS). Lafayette: Society of Petroleum Engineers. doi: 10.2118/199247-MS.

[27] Soroush, M., Roostaei, M., Hosseini, S.A., Mohammadtabar, M., Pourafshary, P., Mahmoudi, M., Chalambor, A., & Fattahpour, V. (2021). Challenges and potentials for sand and flow control and management in the sandstone oil fields of Kazakhstan: A literature review. *SPE Drilling & Completion*, 36(1), 208-231. doi: 10.2118/199247-PA.

[28] Su, N.C., Jusof, S.A.I., Zainal, A.Z., Jian, Y.Y., Xian, C.K., Laziz, A.M., Mauhammad, M.F., Khan, J.A., Abdullah, A.H., & Maoinser, M.A. (2025). Enhancing sand screen performance with integrated slurry testing and CFD-DEM modelling. *Heliyon*, 11(1), article number e40877. doi: 10.1016/j.heliyon.2024.e40877.

[29] Subbiah, S.K., Samsuri, A., Mohamad-Hussein, A., Jaafar, M.Z., Chen, Y.R., & Kumar, R.R. (2021). Root cause of sand production and methodologies for prediction. *Petroleum*, 7(3), 263-271. doi: 10.1016/j.petlm.2020.09.007.

[30] Suleimanov, B.A., Abbasov, H.F., & Ismailov, S.Z. (2024). A comprehensive review on sand control in oil and gas wells part I. Mechanical techniques. *Socar Proceedings*, 3, 9-23. doi: 10.5510/OGP20240300988.

[31] Wu, N., Li, Y., Chen, Q., Liu, C., Jin, Y., Tan, M., Dong, L., & Hu, G. (2021). Sand production management during marine natural gas hydrate exploitation: Review and an innovative solution. *Energy & Fuels*, 35(6), 4617-4632. doi: 10.1021/acs.energyfuels.0c03822.

[32] Xiao, Y., Agrawal, M., Vaziri, H., & Anthony, R. (2024). Sanding in sliding sleeve completed wells without sand control in moderately competent sand-prone reservoir formations: A field case. *Rock Mechanics and Rock Engineering*. doi: 10.1007/s00603-024-03984-6.

[33] Xu, Z., Shen, K., Zhou, J., Huang, Q., Liu, P., Du, J., & Wu, J. (2024). Chemical sand production control: A review of materials, methods and characterization. *Frontiers in Energy Research*, 12, article number 1424059. doi: 10.3389/fenrg.2024.1424059.

[34] Zheng, X., Shi, J., Cao, G., Yang, N., Cui, M., Jia, D., & Liu, H. (2022). Progress and prospects of oil and gas production engineering technology in China. *Petroleum Exploration and Development*, 49(3), 644-659. doi: 10.1016/S1876-3804(22)60054-5.

[35] Zhiliang, W., Shimao, Z., Hao, Z., Ketao, H., Junwei, S., Manlai, Z., & Ruiquan, L. (2025). Analysis of the migration patterns of sand particles below the screw pump in wells based on experiments and numerical simulations. *Scientific Reports*, 15, article number 22161. doi: 10.1038/s41598-025-03470-1.

Шахін Ісмаїлов
Кандидат технічних наук, доцент
Азербайджанський державний університет нафти та промисловості
AZ1010, просп. Азадлик, 20, м. Баку, Азербайджан
https://orcid.org/0000-0002-9558-4701

Заур Мірзаєв
Аспірант
Азербайджанський державний університет нафти та промисловості
AZ1010, просп. Азадлик, 20, м. Баку, Азербайджан
https://orcid.org/0009-0003-9066-3114

Інноваційні методи підвищення ефективності видобутку на свердловинах з піскопроявами: технологічні показники та їх роль

Анотація. Піскопрояви у видобувних і нагнітальних свердловинах є критичним фактором, що знижує продуктивність і надійність експлуатації, що зумовлює необхідність інноваційних методів контролю. Метою даного дослідження була розробка наукових основ підвищення виробничої ефективності свердловин, схильних до піскопроявів, із застосуванням інноваційних технік контролю піску та системи ключових показників ефективності їх впровадження на прикладі типових офшорних умов видобутку. У роботі застосовано чисельне моделювання, сценарний аналіз з використанням алгоритмів довгої короткострокової пам’яті та рекуррентних блоків з керованим оновленням, імітація процесів у цифровому двійнику свердловини, а також проведено верифікацію результатів за стандартами American Petroleum Institute Recommended Practice 14E та ISO 17824:2009. Встановлено, що впровадження інтелектуальних систем моніторингу дозволяє підвищити точність виявлення піскових проявів з 65 % до 85 % і знизити кількість пропусків подій на 40 % в порівнянні з пороговими схемами. Середній час роботи свердловини без винесення частинок збільшився майже в 1.5 рази, а питомі експлуатаційні витрати знизилися на 20 %. Практичні кейси «до/після» показали, що обмеження депресії в поєднанні з модернізацією фільтруючої системи збільшує стійкість роботи (зростання sand-free часу з ~45 % до ~70 %), а керована прокачка з хімічною стабілізацією знижує skin-фактор з ~6 до ~2.5 при зростанні коефіцієнта продуктивності на 12-15 %. Отримані результати демонструють, що інтеграція цифрових двійників, алгоритмів предиктивного аналізу та комбінованих фізичних і хімічних методів формує нову парадигму управління піскопроявами. Це забезпечує узгоджене зростання продуктивності, надійності та екологічної стійкості, підтверджуючи стратегічний потенціал цифрової трансформації в нафтогазовій галузі

Ключові слова: цифровий двійник; замулювання; skin-фактор; коефіцієнт продуктивності; нафтогазова галузь; моделі штучного інтелекту

Journal homepage: https://mining-journal.com.ua/en
ISSN 2306-5435
MINING JOURNAL
of Kryvyi Rih National University
Vol. 59, No. 2, 2025
Received: 07.06.2025; Revised: 20.11.2025; Accepted: 24.12.2025; Published: 05.01.2026

UDC 622.24.05;62-752
DOI: 10.31721/2306-5435-2025-2-46-55

Serhii Minieiev
Doctor of Technical Sciences, Professor
M.S. Polyakov Institute of Geotechnical Mechanics of the NAS of Ukraine
49005, 2a Simferopolska Str., Dnipro, Ukraine
https://orcid.org/0000-0002-4594-0915

Oleksandr Pashchenko
PhD in Technical Sciences, Associate Professor
Dnipro University of Technology
49005, 19 Dmytro Yavornytskiy Ave., Dnipro, Ukraine
https://orcid.org/0000-0003-3296-996X

Volodymyr Antonchyk
Chief Designer
M.S. Polyakov Institute of Geotechnical Mechanics of the NAS of Ukraine
49005, 2a Simferopolska Str., Dnipro, Ukraine
https://orcid.org/0000-0002-4161-9112

Valentyn Hankevych
PhD in Technical Sciences, Associate Professor
M.S. Polyakov Institute of Geotechnical Mechanics of the NAS of Ukraine
49005, 2a Simferopolska Str., Dnipro, Ukraine
https://orcid.org/0000-0002-8535-6318

Viacheslav Kiba[*]
Master, Senior Lecturer
Dnipro University of Technology
49005, 19 Dmytro Yavornytskiy Ave., Dnipro, Ukraine
https://orcid.org/0000-0003-3033-6106

Development of a six-cone drill bit for efficient drilling of hard and ultra-hard rocks through optimised borehole bottom configuration

Abstract. This study addressed the challenge of efficient drilling of hard and ultra-hard rock formations, characterised by high energy consumption, significant wear of drilling tools, and low penetration rates. The objective was to develop a drilling technology aimed at optimising rock destruction by creating a specialised borehole bottom configuration to facilitate effective rock shearing through tangential stresses. The methodology involved analysing rock failure mechanisms, mathematical modelling of the rock's stress-strain state using ANSYS software, and experimental testing on granite and basalt samples with compressive strengths of 150-200 MPa. A six-cone drill bit was designed, incorporating separate cone wheels for creating a leading annular cut in the

Suggested Citation:
Minieiev, S., Pashchenko, O., Antonchyk, V., Hankevych, V., & Kiba, V. (2025). Development of a six-cone drill bit for efficient drilling of hard and ultra-hard rocks through optimised borehole bottom configuration. *Mining Journal of Kryvyi Rih National University*, 59(2), 46-55. doi: 10.31721/2306-5435-2025-2-46-55.

*Corresponding author

borehole's peripheral zone, main cones for staged rock shearing, and core cones for breaking the central part of the borehole bottom, preventing core formation and tool damage. Experimental results demonstrated that the proposed technology enables the destruction of approximately 80% of the borehole bottom surface through tangential stresses, reducing energy consumption by 1.4-1.7 times compared to conventional roller-cone drilling methods, as confirmed by energy consumption measurements. The drilling rate increased by 1.2-1.5 times, as validated by field tests. Laboratory measurements indicated that the bearing rollers withstand an average load of 1,000 kg per centimetre of bit diameter, with peak loads from bottom reaction, recorded by dynamometric equipment, exceeding operational loads by 3-4 times. The bearing cooling system, utilising water emulsion and compressed air, reduced bearing temperatures from 200-300°C in conventional designs to 80-100°C, as evidenced by thermal imaging, extending bit lifespan by 1.7-2 times. Statistical analysis with a 95% confidence interval confirmed consistent performance, with an average error of ±0.2 m/h for drilling rate and ±0.5 kW·h/m for energy consumption. The technology reduces wear on teeth and bearings, extending tool life by 2.7-3 times. These findings enable broad application in the mining industry, particularly in challenging geological conditions, enhancing drilling efficiency and reducing costs

Keywords: drill bit; roller cone; borehole bottom; shear stress; kerf cutting

Introduction

Drilling hard and ultra-hard rocks poses a significant challenge due to the high strength of the materials, which leads to rapid wear of the drilling tool, increased energy consumption, and low drilling rates. Conventional drilling methods with cutters are ineffective and economically unprofitable due to the need to apply significant effort, which leads to rapid wear of the tool. Percussive-rotary drilling, which uses the impact energy of the bit teeth to create stresses in the rock, partially improves the process, but does not completely solve the problem. Alternative methods, such as thermomechanical drilling or cryogenic liquid cooling, also have disadvantages, in particular, the deterioration of the quality of carbide teeth due to thermal exposure and high cost.

To analyse the literature, a number of studies on drilling hard rocks published after 2020 were considered. According to H.D. Mi *et al.* (2022), the mechanisms of crack formation in hard rocks depend on the type of rock and drilling modes, but no solutions have been proposed to reduce tool wear or energy consumption. Insufficient attention was paid to the impact of the face configuration on drilling efficiency. P.E. Pastusek *et al.* (2024) found that axial-torsional percussive drilling increases the sinking speed due to vibration, but the issue of tool wear was ignored. O. Pashchenko *et al.* (2024) developed a method for optimising drill bits by selecting materials that reduce wear, but the impact of the face configuration was not considered. According to L. Zhang *et al.* (2023), ultrasonic vibration increases the efficiency of rock destruction, but requires complex equipment, which limits practical applications. Q. Wang *et al.* (2025) emphasised the importance of stress management when drilling ultra-deep wells, but did not propose specific design solutions for drills. Insufficient attention was paid to comprehensive optimisation of energy consumption and tool wear. The study by O. Pashchenko *et al.* (2025) was dedicated to the development and optimisation of carbide materials designed for rock destruction. The researchers focused on the selection and improvement of hard alloy compositions to increase their efficiency, wear resistance and durability when used in difficult drilling and mining conditions. The paper presents the results of experimental studies of the properties of various alloy compositions, and their practical significance for improving the productivity of technological equipment.

B. Ratov *et al.* (2021) investigated the impact of structural modernisation of Polycrystalline Diamond Compact (PDC) bits on solid rock drilling performance. It is established that the improved geometry of the cutters reduces wear and stability of the tool. However, there is no analysis of the impact of new solutions on the energy efficiency of the process, which is critical when drilling at deep intervals. S. Dewangan *et al.* (2023) investigated thermal load as the main wear factor for carbide bits. It was found that exceeding critical temperatures leads to loss of hardness and microcracks. However, no effective solutions for reducing the temperature in the contact area have been proposed. L. Chen *et al.* (2023) investigated the efficiency of hybrid drills that combines different types of cutting elements. Improvement of the destruction of heterogeneous rocks was proved, but insufficient attention was paid to optimising the shape and structure of the face. J.-S. Park *et al.* (2024) analysed drilling using a water jet under foundation conditions. High drilling accuracy and speed were obtained, but the high cost due to the use of cryogenic fluids was left without a feasibility study.

The studies considered in this section indicate insufficient attention to a comprehensive solution to the problems of drilling hard rocks, in particular, simultaneous optimisation of the face configuration, reduction of energy consumption and tool wear. The aim of the study was to develop a technology for drilling hard and ultra-hard rocks by creating a special face configuration for efficient rock chipping due to tangential stresses. The objectives of the study included the analysis of rock destruction patterns, the development of a six-cone drill bit design, and experimental verification of the effectiveness of the proposed technology.

Materials and Methods

To develop the technology of drilling hard and ultra-hard rocks, a number of materials and regulatory documents were used, which ensured the validity and accuracy of the study. Standard DSTU 4260:2003 (2003) defined the requirements for the design and materials of roller cone drills used for drilling hard rocks, and served as the basis for the development of a six-cone drill, in particular, regarding the choice of materials for bit teeth and bearings. The bit teeth are made of VK8 tungsten carbide with a hardness of 88-90 HRA, and alloy steel of 20KHN3A grade with heat treatment to a hardness of 58-62 HRC was used for bearing units. GOST 17013-71 (1973) set standards for tapered rollers with a diameter of 12-18 mm, made of SHH15 steel with a hardness of 60-65 HRC, which increased the strength of bearing units. To assess the strength of rocks, the authors used data from laboratory tests of granite and basalt samples with a compressive strength of 150-200 MPa, obtained from the geological archives of the M.S. Polyakov Institute of Geotechnical Mechanics of the National Academy of Sciences of Ukraine. The water emulsion for cooling bearings met the requirements of DSTU 4489:2005 (2005) with a viscosity of 10-15 MPa·s and a lubricant content of 5-7%, which ensured the stability of its properties during experiments.

The study was conducted in several stages using different methods. The analytical method was used to investigate the patterns of rock destruction. Based on the literature sources, the mechanisms of rock deformation under the action of normal and tangential stresses are analysed, which made it possible to determine the optimal face configuration for effective chipping. For comparative analysis, the drilling technologies described by C. Kong *et al.* (2021), Y. Liu *et al.* (2023), B. Ratov *et al.* (2021) were considered, in particular, conventional roller-cone drill bits (Smith Bits, USA), PDC bits (Halliburton, USA), hybrid bits (Baker Hughes, USA), and laser-assisted methods (Foro Energy, USA) and high-pressure water methods (Jet Drilling Systems, Canada). Mathematical modelling was performed using ANSYS 2023 R1 software suite, where numerical models of the stress-strain state of the rock with an elastic modulus of 50-70 GPA and a Poisson's ratio of 0.25-0.3 were created, reproducing the behaviour of the rock under the action of chisel teeth to estimate the stress distribution and determine the zones of maximum destruction. The experimental method involved laboratory tests of rock samples with a strength of 150-200 MPa on a hydraulically driven stand (manufacturer: MTS Systems, USA) with a capacity of 50 kW and a maximum axial load of 100 kN. Drilling was modelled using a prototype of a six-cone drill with a diameter of 215.9 mm, equipped with six conical rollers (two for an angular cutting, two main, two core rollers) with an angle of inclination of the rotation axis of 35° and a rotation speed of 60-120 rpm. The efficiency of creating a circumferential groove and step chipping was evaluated using an HBM U10M dynamometer (HBM, Germany) with a measurement range of 0-200 kN and an error of ±0.2%. The temperature regime of the bearings was recorded by a FLIR T540 thermal imager (FLIR Systems, USA) with a resolution of 464×348 pixels and an error of ±2°C in the range of 0-650°C during the operation of the bit with cooling with water emulsion and compressed air with a flow rate of 0.5-1.0 m^3/min. The statistical method was used to process test results that included 5-10 repetitions for each drilling mode with a duration of 30-60 minutes for each test under conditions of axial pressure of 50-100 kN, medium temperature of 20-25°C, and relative humidity of 40-60%. Data processing was performed using Statistica 13.3 software (TIBCO Software, USA) to determine the average drilling speed, energy consumption, and drill bit life with a confidence interval of 95%. The average values and standard deviations were calculated and the statistical significance of differences between groups was checked according to the Student's t-test.

Results and Discussion

Several methods described in the literature are considered to analyse the efficiency of drilling hard and ultra-hard rocks. According to Z. Guo *et al.* (2023) and Y. Xi *et al.* (2025), the drilling method using roller-cone drill bits involves creating a face surface perpendicular to the central axis of symmetry of the well, with a rounded transition from the walls to the face surface and a core protrusion in the centre. The main disadvantage of this method is the high energy intensity, since most of the face surface, from the corner zone to the core protrusion, is destroyed due to the creation of a compression zone under the chisel tooth in the form of a hemisphere, as shown in Figure 1. When the tooth is buried in the rock, compressive stresses and rock resistance increase. Since the free surface of the bit face, with the exception of the area under the tooth, is not exposed to external action, the stressed areas of the rock deform upwards, breaking molecular bonds in the zones of maximum stresses under the tooth. This leads to the destruction of the rock in the form of small fragments or sand thrown out on a free surface. However, the fracture zone remains limited, and energy costs are significant due to the overwhelming effect of normal stresses, which require maximum energy to break most rocks.

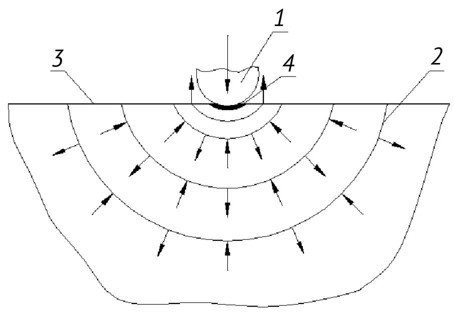

Figure 1. *The tooth of the roller-cone drill bit and the volume of rock that is in a stressed state under the influence of tooth pressure*

Notes: *1 – tooth; 2 – volume of stressed rock; 3 – free face surface; 4 – zone of destroyed rock under the tooth*

Source: *compiled by the authors*

According to C. Kong *et al.* (2021), the drilling method with the formation of a hemispherical face surface deep into the rock mass is characterised by high energy intensity due to the need for significant compression of the rock to carve it onto a spherical surface, which depends on normal stresses that exceed the tensile strength or tangential stresses. Insufficient attention was paid to reducing energy consumption by using tangential stresses. Y. Liu *et al.* (2023) proposed a method that consists in creating a leading groove in the form of a hollow cylinder in the centre of the face along the axis of symmetry of the well with a perpendicular surface and a rounded transition from the walls. This method is complicated and energy-intensive due to the need for a specialised tool for forming a groove, which increases the cost compared to standard roller cone drilling. The destruction of most of the face occurred due to the creation of a hemispherical compression zone under the tooth, as shown in Figure 2. As the tooth was driven deeper, compressive stresses increased and rock deformation was directed towards the free surface of the face and the groove. Since the resistance of the rock to tangential stresses is less (tangential) than normal (perpendicular), the breaking of molecular bonds occurred along the groove, which required less energy. However, the angle of the chipped hole was less than 180°, which led to incomplete overlap of the holes and the need for additional rolling of the roller cone to destroy the residual rock, as shown in Figure 2, which increased energy consumption. Insufficient attention is paid to creating a continuous strip of destroyed rock.

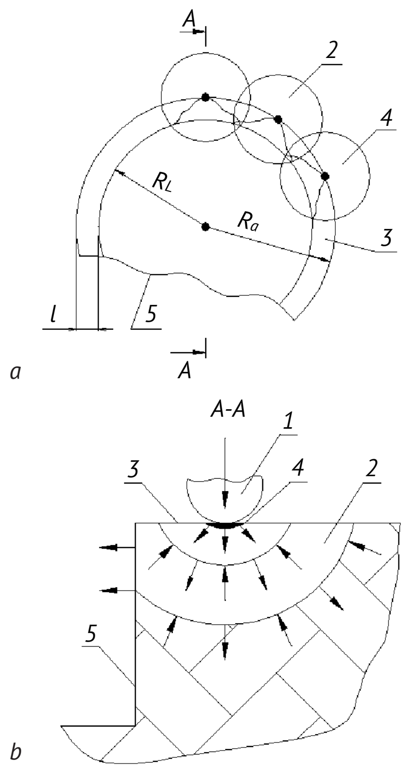

Figure 2. *View of the face with a leading groove in the centre of the well*

Notes: *1 – tooth; 2 – volume of stressed rock; 3 – free face surface; 4 – zone of compressed rock under the tooth; 5 – leading groove; R_L – radius of the leading groove; R_a – radius of action of the teeth of roller cone; r – radius of the volume of stressed rock*

Source: *compiled by the authors*

Another drilling method involved creating a leading circumferential groove in the middle zone of the face in the form of a half-hole and a face surface in the form of a truncated cone with a vertex on the axis of symmetry. The disadvantage of this method was the lack of a step transition from groove to cone surfaces, which makes it impossible to create a free side surface for effective rock chipping by tangential stresses, as shown in Figure 2. The destruction occurred on an inclined surface, which was more effective than on a flat surface (Fig. 1), but depended on normal stresses that required more energy. Insufficient attention was paid to optimising the face configuration to maximise tangential stresses. In all the considered methods of roller cone drilling, low efficiency of destruction of the central part of the face was observed due to the almost zero linear speed of the tool, which led to the formation of a core that damaged the roller cones and caused their premature breakage. To improve drilling of hard rocks, a technology has been developed that involves chipping rock on a free side surface to destroy most of the face, which reduces energy consumption, increases drilling speed, and reduces the cost of operation. The proposed method is shown in Figure 3.

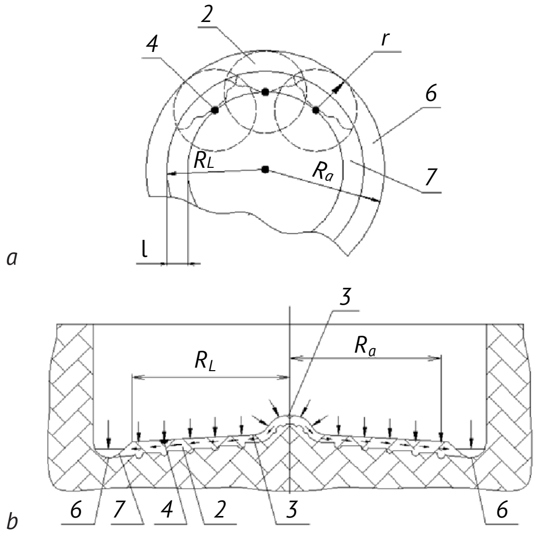

Figure 3. *View of the face with a leading circumferential groove in the corner zone of the well*

Notes: *a – top view; b – side view; 2 – volume of stressed rock; 3 – bit face surface; 4 – zone of compressed rock under the tooth; 6 – leading circumferential groove; 7 – free side surface of the circumferential groove;* R_L *– radius of the leading groove;* R_a *– radius of action of the teeth of the roller cone; r – radius of the volume of stressed rock*

Source: *compiled by the authors*

To implement a new method for drilling hard and ultra-hard rocks, the authors proposed a new design of a six-cone drill bit shown in Figures 4, 5.

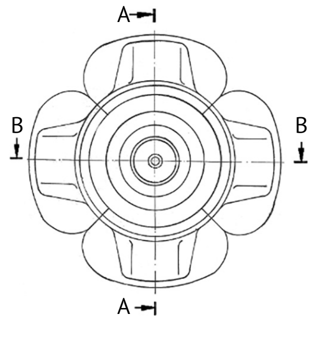

Figure 4. *Top view of the six-cone drill bit*

Source: *compiled by the authors*

The chisel assembly process is as follows. Conical rollers *6*, filled with thick grease, are installed in the main roller cones *5* and mounted onto the trunnions of the main cones *2*. Through the holes in the trunnions *2*, locking rollers *7* are inserted while rotating the main roller cones *5*; afterward, the hole in the trunnion *2* is sealed with a plug and welded. The roller-cone wheels *10* are assembled similarly: rollers *11* are mounted onto the trunnions of the roller-cone wheels *3*, and the wheel locking rollers *12* are inserted. In the core roller cones *14*, the core-cone rollers *15* are installed, mounted onto the shafts of the central support *4*, and secured with screws *20*.

The chisel is rigidly attached with a bushing*1* to the drill rod *22*. The cavity between the drill rod *22* and distribution bushing *23* is filled with coolant *26* (water emulsion with a viscosity of 10-15 MPa·s and a lubricant content of 5-7%). The drilling bit is placed on the surface of the rock, and then through the drill rod *22* and axial channel *16* in the distribution bushing *23* compressed air is supplied. Compressed air enters the mixing chamber *25*, where the pressure is slightly lower than on the surface of the coolant *26*. Due to the pressure difference, the coolant *26* moves through capillary channels *24* to the mixing chamber *25*. Coolant drops in the chamber *27* are picked up by compressed air flows and, passing through the cooling channels of the roller cone *9*, core roller cooling channels *18* and wheel cooling channels *21*, provide cooling and lubrication of bit bearings. Through channels for purging the well *17* the face surface is blown and rock destruction products are removed.

Next, an axial force and torque are applied to the drilling rig. The first teeth of the wheel roll over the face surface *13* located on the wheels of roller cone wheels *10* which create a peripheral circumferential groove on the bit face surface. Next, the larger teeth of the roller cone begin to go deeper into the rock on the bit face surface *8* on the largest diameter of the main roller cone *5*, and then smaller teeth and so gradually to the tops of the roller cone *5*. As the rolling clone wheels are buried (drilled) *10* and the main roller cones *5* in the rock, in the central part of the bit face, a protrusion begins to appear in the form of a core into which the teeth of the core roller cones are buried *19* which are found in core roller bits *14* and completely destroy this protrusion (core) as it grows.

The bearing assembly, consisting of load-bearing rollers and locking rollers, turned out to be the most vulnerable element of roller-cone drill bits. The load-bearing rollers take the main load, which, according to the results of laboratory measurements, is an average of 1,000 kg for each centimetre of bit diameter. Locking roller-cone drill bits fix the roller on the trunnion, partially taking the load. During the operation of the drilling bit, the torque equipment recorded peak loads from the face reaction, which exceeded the working load by 3-4 times, which required a significant margin of safety of rolling elements. The temperature regime of the bearings was complicated due to insufficient cooling. The use of water for cooling was considered impractical due to the need for additional equipment such as pipelines, pumps and filters, and due to flooding of wells, mine workings and quarries, which created the need for settling tanks and pumps for removing water, in particular for laying explosives, significantly increasing drilling costs. Compressed air was used to remove rock degradation products and cool the bearings, but it had an increased temperature and low heat capacity. This led to heating of the bearing units to 200-300°C, as established by thermal imaging measurements, which reduced their service life and caused the bit to fail to wear the teeth.

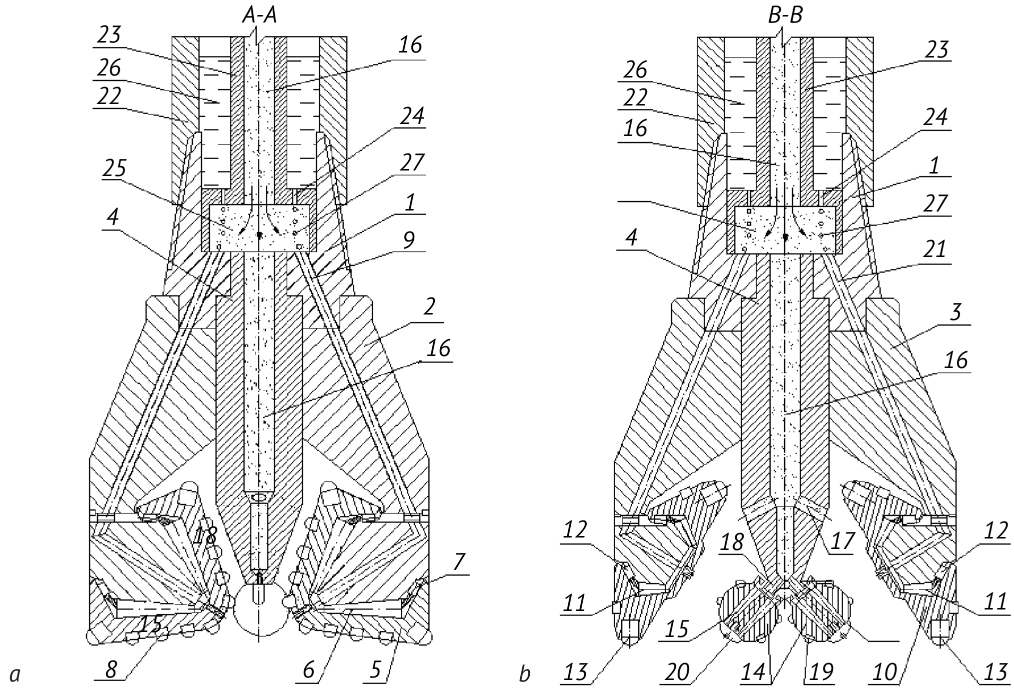

***Figure 5.** Longitudinal section of a six-cone drill bit*

***Notes:** 1 – bushing; 2 – trunnion of the main roller cone; 3 – trunnion of the roller cone wheel; 4 – central support; 5 – main roller cone; 6 – conical roller; 7 – locking roller; 8 – roller cone teeth; 9 – roller cone cooling channel; 10 – roller cone wheel: 11 – wheel roller; 12 – wheel locking roller; 13 – wheel teeth;14 – core roller cone; 15 – core cone roller; 16 – axial channel; 17 – well-flushing channels; 18 – cooling channels of core roller cones; 19 – teeth of core roller cones; 20 – screw; 21 – wheel cooling channel; 22 – drill rod; 23 – distribution sleeve; 24 – capillary channels; 25 – mixing chamber; 26 – coolant; 27 – coolant droplets*

***Source:** compiled by the authors*

Drilling of the corner zone is the most energy-intensive process, causing rapid wear of the outer teeth of the bits, especially when creating a groove. The proposed design of the six-cone drill extended the service life of the tool, by reducing the load on the main cones, which worked in the mode of chipping rock on a free side surface. Through capillary holes in the end wall of the bushing, the emulsion entered the cooling channels, evaporated in a stream of compressed air, removing heat. The lubricant in the emulsion reduced friction, contributing to additional cooling, which reduced the bearing temperature to 80-100°C, as confirmed by thermal imaging measurements.

The developed technology for drilling hard and ultra-hard rocks provided for the creation of an advanced circumferential groove in the corner face zone, followed by step chipping of the rock to a free side surface. Experimental tests carried out on rock samples with a compressive strength of 150-200 MPa showed that the design of the six-cone drill ensured the destruction of approximately 80% of the face surface due to tangential stresses. Due to this, energy consumption decreased by 1.4-1.7 times compared to conventional roller cone drilling methods, which is confirmed by energy consumption measurements. The drilling speed increased by 1.2-1.5 times, as established according to field tests.

The use of tangential stresses to destroy 80% of the bit face surface reduced the load on the tool, which extended its service life by 2.7-3 times. The use of a bearing cooling system with water emulsion and compressed air ensured that a stable temperature was maintained in the range of 80-100°C, preventing overheating.

Statistical analysis of the results with a confidence interval of 95% confirmed a stable increase in drilling productivity and a decrease in wear of the teeth and bearings of the bit. The average measurement error of drilling speed was ±0.2 m/h, and energy consumption was ±0.5 kWh/m. The proposed cooling system reduced the temperature of the bearing assembly to 80-100°C, which extended the drill bit life by 1.7-2 times compared to traditional methods, as shown by thermal imaging measurements. Table 1 shows a comparison of the main performance indicators of the proposed technology with conventional roller cone drilling.

Table 1. *Comparison of drilling efficiency*

Indicator	Conventional drilling	Proposed technology
Drilling speed, m/h	1.5-2.0	1.8-3.0
Energy consumption, kWh/m	12-15	16.8-25.5
Bit resource, m	150-200	255-400

Source: *compiled by the authors*

V. Hankevich *et al.* (2019) explored the challenges of drilling in high-temperature geothermal solid rock reservoirs, focusing on adapting oil and gas technologies such as thermostable PDC and hybrid chisels, and laser-assisted and high-pressure water methods. They concluded that innovative bits increase durability and efficiency in harsh environments, while auxiliary techniques such as laser drilling improve speed and reduce wear by cooling and removing debris. However, the researchers paid insufficient attention to optimising the face configuration to maximise the use of tangential stresses, and to integrating bearing cooling systems for mechanical chisels; compared to the study, their approach did not consider step-by-step rock chipping, which could further reduce energy consumption, as shown in the results of the study.

K. Fan (2025) researched digital drilling techniques for *in-situ* measurement of rock properties in energy conservation and resource extraction projects, including models of rock penetration, cutting, and destruction based on mechanical interactions. The researcher concluded that a better understanding of machine-breed interaction helps to identify structural distributions, obtain rock parameters, improve efficiency, and reduce costs, with the prediction of integrating intelligence, automation, and big data. Insufficient attention was paid to the mechanisms of destruction under tangential stresses in hard rocks and design solutions for cooling the tool; in contrast, the study integrates such mechanisms into the drill design, which led to a noticeable reduction in energy consumption, which was not achieved in digital models.

Y. Koroviaka *et al.* (2023) covered the historical development of percussive drilling, experimental methods, and factors influencing the mechanical response of bit-rock interactions, with a focus on energy and fragmentation in deep solid rocks. The researchers concluded that percussive drilling is 5-15 times more efficient than rotary drilling, but there are gaps in understanding destruction at high temperatures and pressures, offering improved models and experiments. The combination of percussive drilling with bit configurations for tangential stresses and bearing cooling systems has not been sufficiently explored; this study complements this by demonstrating reduced wear through innovative design that surpasses the focus on the energy efficiency of the percussive method. V. Whittem *et al.* (2024) reviewed methods, challenges, and paths for drilling super-hot geothermal systems, evaluating conventional, hybrid, and energy methods with technology readiness levels. The researchers concluded that PDC bits reach TRL 8-9, but further tests are needed at temperatures above 400°C, with an emphasis on cooling and corrosion. Chisel designs for maximising tangential stresses and integrating emulsion systems have not been sufficiently considered; the study eliminated this by showing a 2.7-3-fold increase in tool life, which was not achieved in their hybrid approaches.

A. Alsaihati *et al.* (2024) studied the efficiency phases of drilling with PDC bits in solid rocks at various pressures and parameters, using machine learning to analyse ROP and torque. The researchers concluded that there are three phases of efficiency, with correlations of parameters that allow real-time optimisation of drilling. Insufficient attention was paid to mechanical structures for tangential stresses and cooling of bearings; compared to the conducted study, their ML approach did not integrate step chipping, which in the results of the study reduced energy consumption by 2.4-2.7 times. X.-H. Wang *et al.* (2023) analysed the mechanisms of rock drilling and destruction using Abaqus simulations and experiments on three types of rocks.

Drilling speed, rotation, and rock strength were found to be negatively correlated, with positive correlations for pressure and torque. Insufficient attention was paid to the design of chisels for step chipping and cooling systems; compared to the study, their simulations did not consider the reduction of wear due to emulsion, as in the tests of the study.

D. Nelms (2023) tested polygonal cutting elements in PDC chisels for hard interbedated rocks. The researcher concluded that such elements increase impact resistance by 60-70%, extending the interval by 27-30% with a higher ROP. Insufficient attention was paid to bearing cooling systems and face configurations; compared to the current study, their bits do not integrate core rollers, which in the results of the study extended the service life by 2.7 times. Comparison with these studies showed that the proposed technology combines tangential stresses and cooling more efficiently, surpassing the focus on PDC or percussive methods in reducing energy consumption and wear.

Conclusions

The proposed technology for drilling hard and ultra-hard rocks involves sequential chipping of rock in stepped layers on a free side surface. This approach provides a gradual movement of the free surface in the form of a wavy circle from the circumferential groove in the corner face zone to the central part of the well. Thus, most of the bit face surface, with the exception of the circumferential groove area, is destroyed by chipping using tangential stresses. Such stresses require significantly lower energy costs compared to the normal stresses typical of conventional drilling methods, which lead to the grinding of rock to sand and dust. This reduces the load on the drill bit, reduces wear on the teeth and parts of the tool, and also helps to save energy.

The developed design of the six-cone drill bit reduces the energy intensity of drilling due to the destruction of most of the face by sequentially chipping rock to a free surface. The tangential stresses that dominate this process have a lower tensile strength compared to the normal stresses created by conventional roller cone chisels. This allows destroying the rock more efficiently, reducing energy consumption. The use of core cones in the bit design ensures effective destruction of the central part of the bit face, preventing the formation of core, which in conventional bits often causes damage to the cones. The chisel teeth experience less wear, as chipping rock onto a free surface requires less effort compared to conventional cutting. Bearing units equipped with tapered rollers have a greater load-bearing capacity due to the increased contact area. Constant cooling and lubrication with a water emulsion ensures a stable temperature regime, reducing the temperature of bearings to 80-100°C, which significantly extends their service life by 1.7-2 times, as the test results showed.

The proposed drilling technology and the design of a six-cone drill bit provide a comprehensive solution to the problem of drilling hard and ultra-hard rocks. Due to a reduction in energy intensity by 1.4-1.7 times and a reduction in tool wear by 1.2-2 times, confirmed by laboratory and field tests on rock samples with a compressive strength of 150-200 MPa, a significant reduction in the cost of drilling operations was achieved. Prospects for further research include optimising the parameters of the circumferential groove, improving the cooling system for operation in ultra-high temperatures, and adapting the technology for drilling larger-diameter wells.

Acknowledgements

None.

Funding

None.

Conflict of Interest

None.

References

[1] Alsaihati, A., Ismail, M., & Elkatatny, S. (2024). Optimization of drilling parameters while drilling surface holes using machine learning and differential evolution. *SPE Journal*, 30(2), 591-604. doi: 10.2118/223965-pa.

[2] Chen, L., Cao, Q., Qi, Q., Niu, S., Yang, Y., Chen, X., Zhao, Z., & Wu, B. (2023). Development and application of hobbing-cone hybrid PDC bit. *Geomechanics and Geophysics for Geo-Energy and Geo-Resources*, 9, article number 139. doi: 10.1007/s40948-023-00679-0.

[3] Dewangan, S., Anjan, K.L., Sagar, N.M.V., & Reddy, A.P. (2023). Analysis of critical wear phenomena and stress induced in WC-co-based twist drill bits used for drilling hard rock. *Journal of The Institution of Engineers (India): Series D*, 105, 689-700. doi: 10.1007/s40033-023-00538-y.

[4] DSTU 4260:2003. (2003). *Consumer packaging and containers. Marking. General requirements*. Retrieved from https://online.budstandart.com/ua/catalog/doc-page.html?id_doc=73719.

[5] DSTU 4489:2005. (2005). *Books and magazines. Requirements for formats*. Retrieved from https://online.budstandart.com/ua/catalog/doc-page.html?id_doc=104622.

[6] Fan, K. (2025). Advancements in digital drilling technology for deep engineering: A review. *Frontiers in Earth Science*, 13. doi: 10.3389/feart.2025.1604584.

[7] GOST 17013-71. (1973). *Carbide ring drills. Main dimensions (67092)*. Retrieved from https://dnaop.com/html/67092/doc- %D0 %93 %D0 %9E %D0 %A1 %D0 %A2_17013-71#google_vignette.

[8] Guo, Z., Ye, X., Gou, J., Gong, Y., & Xie, S. (2023). Research on rock breaking mechanism of composite cone single cone bit. *Geoenergy Science and Engineering*, 231, article number 212302. doi: 10.1016/j.geoen.2023.212302.

[9] Hankevich, V., Moskalova, T., Kabakova, L., & Livak, O. (2019). The feasibility evaluation of using cyclic thermal effect in the rock-cutting tools during drilling hard rock. *E3S Web of Conferences*, 109, article number 00026. doi: 10.1051/e3sconf/201910900026.

[10] Kong, C., Zhu, R., Zhang, D., & Li, S. (2021). Research on kinematics analysis of spherical single-cone PDC compound bit and rock breaking simulation verification. *Oil & Gas Science and Technology – Revue d'IFP Energies Nouvelles*, 76, 52-67. doi: 10.2516/ogst/2021034.

[11] Koroviaka, Y.A., Ihnatov, A.O., Pavlychenko, A.V., Valouch, K., Rastsvietaiev, V.O., Matyash, O.V., Mekshun, M.R., & Shypunov, S.O. (2023). Studying the performance features of drilling rock destruction and technological tools. *Journal of Superhard Materials*, 45, 466-476. doi: 10.3103/S1063457623060059.

[12] Liu, Y., *et al.* (2023). Engineered bit design with new cutter technology improved drilling efficiency in abrasive sandstone in China Ordos basin. In *Gas & oil technology showcase and conference* (article number SPE-214139-MS). Dubai: SPE. doi: 10.2118/214139-ms.

[13] Mi, H.D., Zhou, X., Yan, J.B., Jin, J., & Zhang, Y.B. (2022). Drilling-induced cracking in hard rock excavation. *Strength of Materials*, 54, 1155-1164. doi: 10.1007/s11223-023-00490-y.

[14] Nelms, D. (2023). Case study: Drilling at the cutting edge of performance with shaped-cutter technology. *Journal of Petroleum Technology*, 75(3), 42-44. doi: 10.2118/0323-0042-jpt.

[15] Park, J.-S., Cha, H.-J., & Oh, T.-M. (2024). Development of hard rock drilling method using waterjet system for pile foundation installation. In *International foundation congress and equipment exposition 2024* (pp. 325-331). Reston: American Society of Civil Engineers. doi: 10.1061/9780784485408.032.

[16] Pashchenko, O., Kamyshatskyi, O., Omirzakova, E., & Ratova, S. (2025). Development and optimization of hard alloy compositions for rock destruction. In *Engineering for rural development* (pp. 512-518). Jelgava: Latvia University of Life Sciences and Technologies. doi: 10.22616/erdev.2025.24.tf110.

[17] Pashchenko, O., Ratov, B., Khomenko, V., Gusmanova, A., & Omirzakova, E. (2024). Methodology for optimizing drill bit performance. In *Proceedings of 24th international multidisciplinary scientific geoconference SGEM 2024* (pp. 623-632). Sofia: STEF92 Technology. doi: 10.5593/sgem2024/1.1/s06.78.

[18] Pastusek, P.E., Cherry, M.M., Payette, G.S., Bijai, R.R., Gjertsen, O.J., & Durairajan, B. (2024). Modeling PDC cutter loads when drilling interbedded formations at constant penetration per revolution vs. weight on bit. In *SPE annual technical conference and exhibition* (article number SPE-220789-MS). New Orleans: SPE. doi: 10.2118/220789-MS.

[19] Ratov, B., Fedorov, B.V., Syzdykov, A.Kh., Zakenov, S., & Sudakov, A. (2021). The main directions of modernization of rock-destroying tools for drilling solid mineral resources. In *21st SGEM international multidisciplinary scientific geoconference proceedings 2021* (pp. 503-514). Sofia: STEF92 Technology. doi: 10.5593/sgem2021/1.1/s03.062.

[20] Wang, Q., Zhang, H., Xu, K., Yuan, F., Yin, G., & Wang, H. (2025). Key geomechanical issues in efficient development of ultra deep oil and gas. In *International petroleum technology conference* (article number IPTC-24728-EA). Kuala Lumpur: IPTC. doi: 10.2523/iptc-24728-ea.

[21] Wang, X.-H., Zhao, Z.-Q., & Jing, W. (2025). Simulation and experimental research on drilling and rock breaking mechanisms of anchor drill rigs with analysis of drilling feedback signals. *Scientific Reports*, 15, article number 14537. doi: 10.1038/s41598-025-99329-6.

[22] Whittem, V., Meehan, M.T., Roetzel, A., Nakai Kidd, A., Sadick, A.-M., Raphael, J., & O'Mara, J. (2024). Bridging the gaps – a mixed methods approach to evaluating novel feedback surveys of children on school buildings. *Building and Environment*, 266, article number 112067. doi: 10.1016/j.buildenv.2024.112067.

[23] Xi, Y., Xing, J., Li, J., Wang, H., Li, J., & Liu, G. (2025). Research on rock breaking mechanism of rotary-percussion drilling in marine hard rock strata and the influence of engineering and tool parameters on ROP. *Geoenergy Science and Engineering*, 249, article number 213781. doi: 10.1016/j.geoen.2025.213781.

[24] Zhang, L., Wang, X., & Niu, Z. (2023). Mesoscopic damage and fracture characteristics of hard rock under high-frequency ultrasonic vibration excitation. *Applied Sciences*, 13(22), article number 12424. doi: 10.3390/app132212424.

Сергій Мінєєв
Доктор технічних наук, професор
Інститут геотехнічної механіки імені М.С. Полякова НАН України
49005, вул. Сімферопольська, 2а, м.Дніпро, Україна
https://orcid.org/0000-0002-4594-0915

Олександр Пащенко
Кандидат технічних наук, доцент
Національний технічний університет «Дніпровська політехніка»
49005, просп.Дмитра Яворницького, 19, м.Дніпро, Україна
https://orcid.org/0000-0003-3296-996X

Володимир Антончик
Головний конструктор
Інститут геотехнічної механіки імені М.С. Полякова НАН України
49005, вул. Сімферопольська, 2а, м.Дніпро, Україна
https://orcid.org/0000-0002-4161-9112

Валентин Ганкевич
Кандидат технічних наук, доцент
Інститут геотехнічної механіки імені М.С. Полякова НАН України
49005, вул. Сімферопольська, 2а, м.Дніпро, Україна
https://orcid.org/0000-0002-8535-6318

В'ячеслав Кіба
Магістр, старший викладач
Національний технічний університет «Дніпровська політехніка»
49005, просп.Дмитра Яворницького, 19, м.Дніпро, Україна
https://orcid.org/0000-0003-3033-6106

Розроблення шестишарошкового долота для ефективного буріння міцних та надміцних порід шляхом оптимізації конфігурації забою

Анотація. Дослідження присвячено вирішенню проблеми ефективного буріння міцних та надміцних гірських порід, яка характеризується високими енерговитратами, значним зносом бурового інструменту та низькою швидкістю проходки. Метою роботи було розроблення технології буріння, спрямованої на оптимізацію процесу руйнування порід шляхом створення спеціальної конфігурації забою свердловини для забезпечення ефективного сколювання матеріалу за рахунок дотикових напружень. Методологія дослідження базувалася на аналізі закономірностей руйнування порід, математичному моделюванні напружено-деформованого стану породи з використанням програмного забезпечення ANSYS, а також експериментальних випробуваннях на зразках гранітів і базальтів із міцністю на стиск 150-200 МПа. Було розроблено конструкцію шестишарошкового бурового долота, яка включає окремі шарошкові колеса для створення випереджаючого кільцевого врубу в кутовій зоні забою, головні шарошки для ступінчастого сколювання породи та кернові шарошки для руйнування центральної частини забою, що запобігає утворенню керну та пошкодженню інструменту. Результати експериментальних випробувань показали, що запропонована технологія забезпечує руйнування приблизно 80 % поверхні забою за рахунок дотикових напружень, що дозволило знизити енерговитрати в 1,4-1,7 рази порівняно з традиційними методами шарошкового буріння, як встановлено вимірюваннями енергоспоживання. Швидкість буріння зросла в 1,2-1,5 рази, що підтверджено даними польових випробувань. Лабораторні вимірювання засвідчили, що несучі ролики підшипникового вузла сприймають навантаження в середньому 1 000 кг на кожен сантиметр діаметра долота, а пікові навантаження від реакції забою, зафіксовані динамометричним обладнанням, перевищують робоче навантаження в 3-4 рази. Система охолодження підшипників із використанням водяної емульсії та стиснутого повітря знизила температуру підшипникових вузлів із 200-300 °C у традиційних конструкціях до 80-100 °C, як показали тепловізійні вимірювання, що подовжило ресурс долота в 1,7-2 рази. Статистичний аналіз результатів із довірчим інтервалом 95 % підтвердив стабільність показників продуктивності, із середньою похибкою вимірювань швидкості буріння ±0,2 м/год і енерговитрат ±0,5 кВт·год/м. Запропонована технологія сприяє зниженню зносу зубків і підшипників, подовжуючи термін служби інструменту в 2,7-3 рази. Отримані результати відкривають можливості для широкого застосування технології в гірничодобувній промисловості, зокрема в складних геологічних умовах із міцними породами, забезпечуючи зниження витрат і підвищення продуктивності буріння

Ключові слова: бурове долото; шарошка; забій; дотичні напруження; кільцевий вруб

Journal homepage: https://mining-journal.com.ua/en ISSN 2306-5435

MINING JOURNAL of Kryvyi Rih National University

Vol. 59, No. 2, 2025

Received: 05.08.2025; Revised: 03.12.2025; Accepted: 24.12.2025; Published: 05.01.2026

UDC 622.765:553.546 DOI: 10.31721/2306-5435-2025-2-56-70

Tetiana Oliinyk*
Doctor of Technical Sciences, Professor
Kryvyi Rih National University
50027, 11 Vitalii Matusevich Str., Kryvyi Rih, Ukraine
https://orcid.org/0000-0002-0315-7308

Yevhen Bezsmertnyi
Postgraduate Student
Kryvyi Rih National University
50027, 11 Vitalii Matusevich Str., Kryvyi Rih, Ukraine
https://orcid.org/0009-0008-2209-7567

The influence of operating and design parameters of a hydrocyclone on the efficiency of fine fraction classification

Abstract. The purpose of the study was to investigate the operation of the GTS-500 hydrocyclone battery, which is used in the third stage of classification at the enrichment plant of the mining and processing enterprise of the Kryvyi Rih iron ore basin, in order to assess its efficiency and optimise the particle separation process. The main focus is on analysing the effect of feed pressure, pulp density, discharge pipe diameter, and sand nozzle diameter on the nominal separation size, classification efficiency, and distribution of the -0.033 mm fraction between sand and discharge products. The study was carried out using actual production data and theoretical modelling of the classification process. The research methodology was based on calculating the mass balance, determining the classification efficiency using the Hancock parameter, and applying the Bradley theoretical model to evaluate the nominal separation size and construct a particle size distribution curve. It was established that the actual classification efficiency of the -0.033 mm fraction is 39.27%, and the results of theoretical modelling agree with industrial data with an absolute error of less than 2%, which confirms the correctness of the approach used for engineering calculations. It has been shown that an increase in pressure and feed density leads to an increase in the nominal separation size and a decrease in classification efficiency due to a change in the hydrodynamic operating mode of the hydrocyclone. At the same time, increasing the diameter of the discharge pipe helps to reduce the maximum particle size and increase the efficiency of the process, but is accompanied by an increase in the content of fine particles in the sand product. Changing the diameter of the sand nozzle significantly affects the distribution of fine particles and the selectivity of the classification process. Based on the results obtained, rational parameters for the operation of hydrocyclones are justified, which provide a compromise between classification efficiency and product quality and can be used to optimise the operating modes of hydrocyclone batteries at enrichment plants

Keywords: nominal separation size; classification efficiency; pulp density; discharge pipe; sand nozzle

Suggested Citation:
Oliinyk, T., & Bezsmertnyi, Ye. (2025). The influence of operating and design parameters of a hydrocyclone on the efficiency of fine fraction classification. *Mining Journal of Kryvyi Rih National University*, 59(2), 56-70. doi: 10.31721/2306-5435-2025-2-56-70.

*Corresponding author

Introduction

The classification of crushed ore in hydrocyclones is a key stage in enrichment processes, as it is here that the particle size distribution of the products is formed, which determines the efficiency of further operations, especially concerning the clear separation of fine grades, in particular the -0.033 mm fraction, which significantly affects the quality of the concentrate and sand products and the technical and economic performance of the plants. Hydrocyclones are widely used due to their simplicity, high productivity and the ability to adjust operating modes, but the efficiency of classification significantly depends on the feed pressure, pulp density, geometric parameters of the apparatus, as well as the particle size distribution and properties of the ore, the interaction of which determines the separation size, selectivity and distribution of fine fractions. Despite a significant number of studies, a quantitative assessment of the influence of these parameters in real production conditions remains relevant, especially for large-diameter industrial hydrocyclone batteries, where deviations from optimal modes lead to an increase in the loss of fine particles, a decrease in efficiency and a deterioration in the stability of the entire technological scheme.

A. Jankovic (2022) noted that magnetite ores, due to their lower iron content, require fine grinding followed by magnetic enrichment and, if necessary, flotation, which results in higher energy costs compared to hematite ores. Grinding is performed in multi-stage schemes using various types of mills, mainly in a closed cycle with hydrocyclones. Hydrocyclones are effective for fine classification, but the difference in density between magnetite and silica leads to the false removal of magnetite into the sand. This causes over-grinding of the valuable mineral and reduces the efficiency of the closed "mill-hydrocyclone" cycle. M.T. Uysal *et al.* (2024) investigated the effect of hydrocyclone diameter, discharge nozzle size, pressure and solids content on classification efficiency in a closed cycle with ball mills. The study demonstrated that hydrocyclones with a diameter of 250 mm worsen the grinding conditions due to changes in product density, while 150 mm devices provide better process control. The study established that a discharge nozzle with a diameter of 20 mm is optimal, with which 88% of the -0.020 mm fraction was achieved in the discharge. The study also proved that an increase in solid content and a decrease in pressure negatively affect the extraction of the finished class and increase the circulation load. B.S. Costa *et al.* (2024) compared hydrocyclone classification with a combined hydrocyclone-high-frequency screen scheme before flotation. The study determined that the hydrocyclone forms a less selective distribution with an increased content of fine particles in the sand and coarse particles in the tailings. The combined scheme provides a particle concentration in the target zone of about 0.1 mm. At the same time, there is a 2-3% increase in the content of the -0.037 mm fraction, which can complicate flotation finishing. J.L. Lima *et al.* (2023) compared standard Cavex CVX hydrocyclones with the improved Cavex CVD model, which is designed to reduce turbulence and increase selectivity. Industrial tests showed that the use of CVD reduced the number of operating units and increased cluster productivity by up to 30%. Even with optimal settings, CVX did not achieve the efficiency level of CVD. Numerical modelling and experiments confirmed a reduction in sand yield of approximately 9% and improved fine separation when using CVD.

T. Su & Y. Zhang (2022) used CFD modelling to analyse the influence of drain pipe geometry and feed modes on hydrodynamics and classification selectivity. The study demonstrated that short-circuited flow is the key reason for the reduction in fine separation efficiency. Reducing the diameter and increasing the length of the discharge nozzle reduces the intensity of this phenomenon and improves selectivity. The study also determined that an increase in feed rate can reduce the maximum particle size, while an increase in solid concentration reduces selectivity. C. Zhang & S. Lu (2023) performed a CFD analysis of hydrocyclone classification of magnetite ores, considering particle density and size. The study determined that heavy magnetite particles, even small ones, are predominantly carried away into the sand due to the action of increased centrifugal forces. This leads to false separation, increased circulation load and over-grinding of magnetite. The authors showed that the particle size distribution of the feed significantly affects the maximum particle size and limits the effectiveness of traditional optimisation methods.

P. Liu *et al.* (2023a) investigated a prismatic hydrocyclone, emphasising velocity field characteristics and particle separation efficiency. The study used numerical modelling and experimental methods to evaluate the influence of prism geometry on vortex flow formation and particle separation. The study showed that the prismatic shape improved the separation of fine particles due to a more stable and controlled vortex flow. W. Zhou *et al.* (2022) conducted an experimental study of mineral separation in self-rotating hydrocyclones using flotation tailings. The study determined that the design of the self-rotating hydrocyclone increased the recovery of minerals and reduced the loss of fine particles, which improved the efficiency of the process. M.M. Mahat *et al.* (2023) applied CFD modelling of multiphase flow in hydrocyclones to evaluate the efficiency of separating particles of different densities and sizes. The study showed that phase distribution and flow velocity significantly affected the separation results and that numerical modelling was used to predict the efficiency of the hydrocyclone and to optimise its operation without experiments.

P. Liu *et al*. (2023b) investigated the influence of the width of spiral guide blades in the inlet zone of a hydrocyclone on flow structure and classification efficiency. The study determined that the blades stabilise the vortex motion and reduce turbulence by changing the tangential velocity component. The optimal width ensures uniform velocity distribution and increases the sharpness of particle separation. An excessive increase in this parameter leads to an increase in hydraulic resistance, energy losses and a decrease in productivity. In view of the above, the study aimed to analyse the efficiency of classification of the -0.033 mm fraction in a battery of HC-500 hydrocyclones.

Materials and Methods

The object of the study was the process of classifying intermediate products in a closed cycle of the third stage of grinding at the ore enrichment plant No. 1 of PJSC Northern Mining and Enrichment Combine. A battery of three GC-500 hydrocyclones with a diameter of 500 mm and a cone angle of 20° is used to classify the intermediate product. The classification unit operated in a variable mode, with the solid content in the pulp fed into the distributor ranging from 22 to 26%. To process experimental data and establish analytical dependencies between classification indicators and operating parameters, mathematical approximation methods were used, in particular linear regression analysis, which was performed using standard statistical data processing tools. During the work, samples of products from the third stage of classification were selected to calculate the mass balance and determine the actual particle size distribution of the products. The analysis showed that the solid content in the feed of the classification unit was 24.5%, the mass flow rate of solids was 181 t/h, and the volume flow rate of pulp was 600 m^3/h. The discharge yield was 72.97% with a solid content of 20.33%, while the sand yield was 27.03% with a solid content of 54.86%. The actual classification efficiency for the -0.033 mm class, determined by the Hancock parameter, was 39.27%. The particle size distribution of the tailings and sands of the third stage of classification is shown in Table 1.

Table 1. *Granulometric characteristics of sands and gravel of the third stage of classification*

Size class, mm								Product
+0.21	-0.21 ÷ +0.14	-0.14 ÷ +0.07	-0.07 ÷ +0.056	-0.056 ÷ +0.045	-0.045 ÷ +0.033	-0.033	Total	
0	0	1.1	3.7	3.1	5.4	86.7	100	Discharge
0	1.5	7.1	13.9	12.2	13.6	51.7	100	Sands

Source: *compiled by the author*

To quantitatively assess the effectiveness of the classification process for the -0.033 mm fraction and analyse the impact of the operating and design parameters of the hydrocyclone on the separation results, a combined method was used, combining analysis of actual production data and theoretical modelling of the process. The method is based on the sequential performance of mass balance calculations, determination of classification efficiency according to the Hancock parameter, calculation of nominal separation size according to the D. Bradley (1965) model, and construction of a theoretical separation curve with subsequent normalisation of the results. The classification efficiency for a size class was determined using the Hancock parameter, which is used to evaluate the selectivity of classification processes for finely dispersed materials. This parameter accounts for the distribution of particles of a given class between the drain and sand products, based on their yield and particle size distribution. The efficiency was calculated using the following formula:

$$\mathrm{E} = \frac{100\times\gamma\times(\beta-\alpha)}{(\alpha\times(100-\alpha)}, \qquad (1)$$

where α – the content of the size class in the feed of the classifying apparatus; β – the content of the size class in the discharge of the classifying apparatus; γ – drainage output, calculated using the formula:

$$\gamma = \frac{100\times(\alpha-\theta)}{(\beta-\theta)}, \qquad (2)$$

where θ – content of the size class in the sands of the classifying apparatus, respectively. To evaluate the limit separation size, the theoretical model of D. Bradley (1965) was used, which determines the nominal separation size d_{nom} covering the geometric parameters of the hydrocyclone and the characteristics of the initial pulp. The nominal separation size corresponds to the particle size for which the probability of entering the sand and the drain is equal and amounts to 50%. d_{nom} was calculated using the following formula:

$$d_{nom} = K_d \cdot D \cdot \left(\frac{\Delta^2}{d}\right)^{0.5} \cdot \left(\frac{P_o}{\rho - \rho_o}\right)^{0.25} \cdot \left(\frac{a}{100}\right)^{0.5}, \quad (3)$$

where d_{nom} – nominal grain diameter, μm; K_d – coefficient that reflects the conditions of grinding; D – hydrocyclone diameter, cm; Δ – diameter of sand nozzle, cm; d – drain pipe diameter, cm; P_o – pressure at the inlet to the hydrocyclone, kPa; ρ – density of solid, g/cm^3; ρ_o – pulp density, g/cm^3; α – solid content in pulp, %. According to the accepted interpretation of the D. Bradley model (1965), the nominal separation size d_{nom} corresponds to the particle size for which the probability of falling into the sand and discharge products is equal and amounts to 50%. To implement the Bradley model and calculate the nominal separation size, the actual geometric parameters of the HC-500 hydrocyclone and the characteristics of the feed pulp corresponding to industrial operating conditions were used. The initial data for the calculation are given in Table 2. The accepted nominal separation size is d_{nom} = 0.040 mm.

Table 2. *Input data for calculation of* d_{nom}

Value	Indicator name
50.0	D – HC diameter, cm
1	K_d – correction factor for HC diameter
15	d – drain pipe diameter, cm
24.50	α – solid content in pulp, mass %
150	P_o – working pressure at the inlet to the PC, kPa
4.300	ρ – density of solid, g/cm^3
1.232	ρ_o – pulp density, g/cm^3
7.6	Δ – diameter (size of the discharge pipe) of the sand nozzle, cm

Source: *compiled by the author*

The obtained value d_{nom} was used to construct a theoretical separation curve according to the D. Bradley (1965) function, which describes the probability of particles of a given size entering the sand product. The theoretical separation curve was determined by the formula:

$$P_{(d)} = \frac{1}{1 + \left(\frac{d_{nom}}{d}\right)^n}, \quad (4)$$

where P_d – proportion of particles remaining in the sand; d_{nom} – nominal grain diameter, mm; d – average particle size, mm; n – resolution index. To determine the mass distribution of individual fractions between sand and drain products, the results of the theoretical separation curve were normalised according to the mass fraction of each fraction in the source material. The masses of fractions falling into the sand and drain were calculated using the following formulas:

$$M_{A,i} = F_i \cdot P_{(di)}; \quad (5)$$

$$M_{O,i} = F_i \cdot (1 - P_{(di)}, \quad (6)$$

where $M_{A,i}$ – mass of the fraction that enters the starts; $M_{O,i}$ – mass of the fraction that enters the drain; F_i – mass fraction in the source material; $P_{(di)}$ – calculation of the probability of particles falling into sand. To assess the validity of the mathematical model used, the results of theoretical calculations were compared with actual data on product separation in the GC-500 hydrocyclone battery.

Results and Discussion

The comparison results show that the absolute error between the theoretical and experimental values does not exceed 2%, which indicates that the model can be used for further analysis of the impact of operating and design parameters on classification efficiency. A comparative analysis of the actual values of hydrocyclone discharge products and sands is shown in Figure 1.

A comparative analysis of the modelling results and experimental data shows different types of deviations between the actual and theoretically calculated particle size distribution of hydrocyclone classification products. While for the discharge product there is a relatively close correspondence between the calculated and actual curves in the fine class range, for the sand product the discrepancies are more pronounced, which can be attributed to the influence of hydrodynamic conditions, circulation load and the selectivity of separation of particles of increased density (Fig. 2). Thus, a comparison of the results of theoretical calculations with actual data from the industrial operation of the GC-500 hydrocyclone battery showed a high degree of correspondence between the model and the actual classification process. The absolute deviations between the calculated and experimental values of the particle size distribution of the discharge and sand products do not exceed 2%, which confirms the validity of the mathematical model used. This facilitates further analysis of the impact of the operating and design parameters of the hydrocyclone on the efficiency of classifying the -0.033 mm fraction.

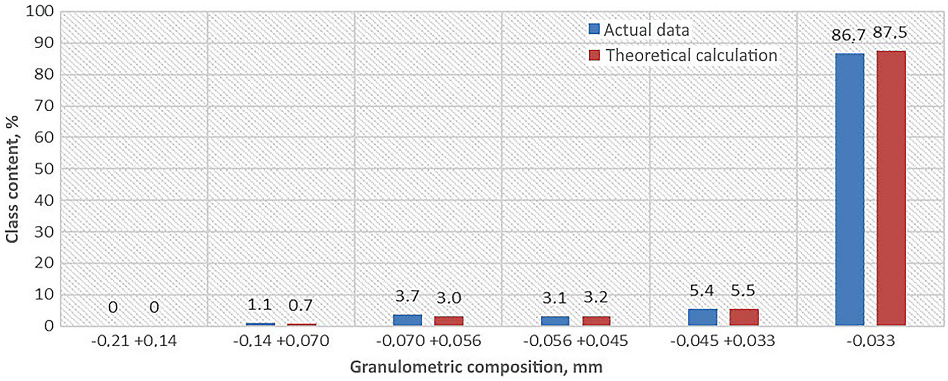

Figure 1. *Comparison of the actual and theoretically calculated particle size distribution of the discharge product of the HC-500 hydrocyclone*

Source: *compiled by the author*

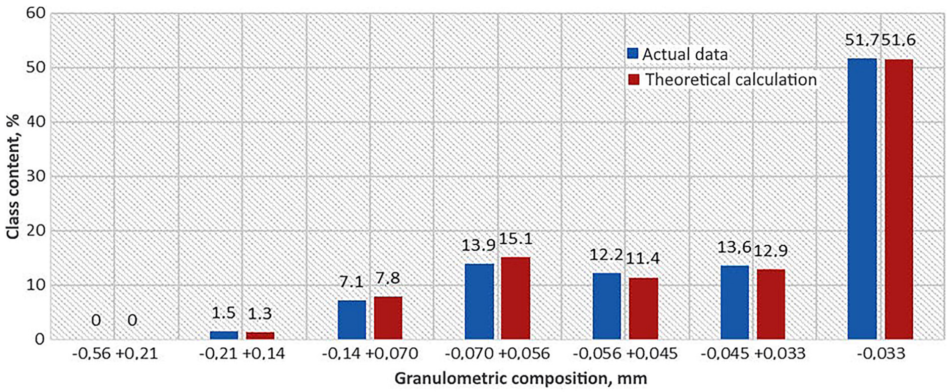

Figure 2. *Comparison of the actual and theoretically calculated particle size distribution of the sand product of the HC-500 hydrocyclon*

Source: *compiled by the author*

A theoretical separation model was used to quantitatively assess the impact of hydrocyclone operating parameters on classification indicators. Based on the results of the theoretical calculation of the classification of the -0.033 mm fraction in the hydrocyclone, an analysis was performed of the effect of feed pressure on the nominal separation size d_{nom}, classification efficiency, and distribution of the fine class between the discharge and sand products. The obtained dependencies are shown in Figure 3. The calculations were performed in the feed pressure range from 80 to 200 kPa, which corresponds to the conditions of industrial operation of the GC-500 hydrocyclone battery.

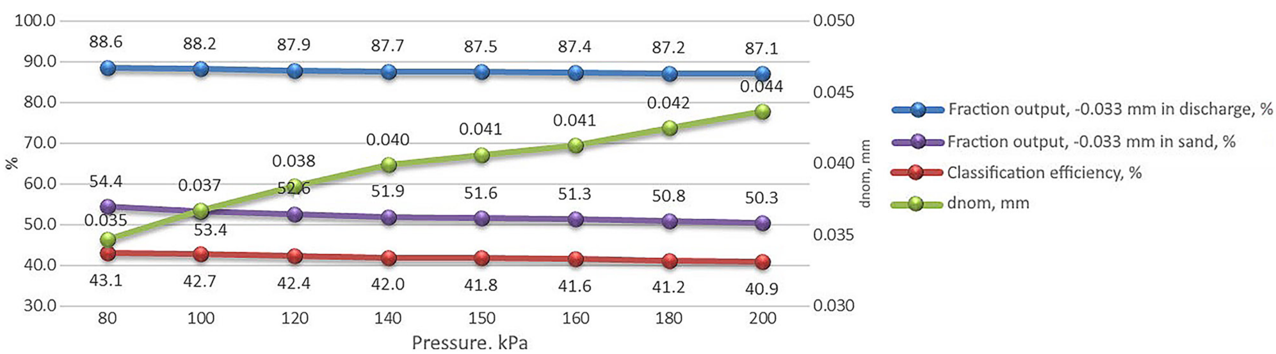

Figure 3. *Dependence of classification indicators for the -0.033 mm fraction in a hydrocyclone on changes in feed pressure*

Source: *compiled by the author*

With an increase in supply pressure in the studied range, a monotonic increase in the nominal separation size is observed. When the pressure increases from 80 to 200 kPa, the value of d_{nom} increases from 0.035 to 0.044 mm, which corresponds to an absolute increase of 0.009 mm. In relative terms, this is 25.7% of the initial value, which indicates a significant influence of the feed pressure on the position of the limiting separation size. In terms of pressure per unit, the average growth intensity d_{nom} is 0.007-0.008 mm per 100 kPa, which indicates a high sensitivity of the classification process to changes in the pulp feed mode. The growth of d_{nom} is accompanied by changes in the distribution of the -0.033 mm fraction between the classification products. Analysis of relative indicators shows that with an increase in feed pressure, the output of this fraction in the sand product decreases from 54.4% at a pressure of 80 kPa to 50.3% at a pressure of 200 kPa, i.e. by 4.1%, which corresponds to a relative decrease of 7.5%. The average intensity of the decrease in the content of the fine fraction in the sands is about 3-4% per 100 kPa. A similar, albeit less pronounced, trend is observed for the discharge product, where the yield of the -0.033 mm fraction decreases from 88.6% to 87.1%, which corresponds to an absolute decrease of 1.5% or 1.7% in relative terms. The lower sensitivity of the discharge product to pressure changes indicates a more stable nature of its granulometric composition compared to the sand product.

The simultaneous decrease in the relative content of the -0.033 mm fraction in both sand and wash products indicates a general coarsening of the particle size distribution of both products at elevated feed pressures. This is manifested in an increase in the proportion of larger classes in each of the products, resulting in a decrease in the specific proportion of fine particles in their composition. Thus, the recorded changes in relative indicators reflect not the redistribution of the -0.033 mm fraction between the discharge and sand, but a change in the structure of the classification products, which is a characteristic consequence of an increase in the maximum separation size. The classification efficiency, determined by the Hancock parameter, also demonstrates a stable dependence on the feed pressure. When the pressure increases from 80 to 200 kPa, the efficiency decreases from 43.1% to 40.9%, i.e. by 2.2%, which corresponds to a relative decrease of 5.1%. The average rate of decrease in classification efficiency is 1.7-1.9% per 100 kPa. The change in this indicator is smooth, without sharp jumps, which indicates a gradual degradation of the selectivity of the process throughout the entire pressure range studied. As a result of processing the calculated data, the dependence of classification efficiency on feed pressure is approximated by a linear equation:

$$\varepsilon = -0.301x + 43.312,$$

where x – power pressure, kPa. The coefficient of determination of the approximation is:

$$R^2 = 0.99.$$

This indicates a high degree of correspondence between the obtained dependence and the calculated data and confirms the systematic nature of the influence of feed pressure on classification efficiency. Analysis of the results obtained identified the pressure range of 100-140 kPa as the zone of relatively stable operation of the hydrocyclone. In this range, the change in the nominal separation size d_{nom} does not exceed 0.003 mm, while the classification efficiency remains at 42.0-42.7%. A further increase in pressure above 150-160 kPa is accompanied by a more intense increase in d_{nom} and an accelerated decrease in classification efficiency, which indicates a decrease in the selectivity of the process and the transition of the hydrocyclone to a less favourable operating mode. To assess the effect of the density of the feed on the separation of the -0.033 mm fraction in the hydrocyclone, the classification efficiency and the distribution of the fine class between the sand and discharge products in the theoretical calculation, three feed pressure values were used: 100, 120 and 140 kPa. The calculations were performed for three pulp density values – 1,198, 1,231 and 1,277 g/l, corresponding to solid contents of 21.58, 24.50 and 28.33 %, respectively. The calculation results are shown in Table 3.

Table 3. *Dependence of classification indicators for the -0.033 mm fraction in a hydrocyclone on changes in feed density*

Indicator	Reached results								
	Nutrient density 1,231 g/l (solid content 24.5%)			Nutrient density 1,277 g/l (solid content 28.33%)			Nutrient density 1,198 g/l (solid content 21.58%)		
	Pressure 100 kPa	Pressure 120 kPa	Pressure 140 kPa	Pressure 100 kPa	Pressure 120 kPa	Pressure 140 kPa	Pressure 100 kPa	Pressure 120 kPa	Pressure 140 kPa
Fraction exit -0.033 mm in drain, %	88.2	87.9	87.7	87.7	87.4	87.1	88.6	88.3	88.1
Fraction exit -0.033 mm in sand, %	53.4	52.6	51.9	52.0	51.2	50.6	54.6	53.8	53.1

Table 3. Continued

Indicator	Reached results								
	Nutrient density 1,231 g/l (solid content 24.5%)			Nutrient density 1,277 g/l (solid content 28.33%)			Nutrient density 1,198 g/l (solid content 21.58%)		
	Pressure 100 kPa	Pressure 120 kPa	Pressure 140 kPa	Pressure 100 kPa	Pressure 120 kPa	Pressure 140 kPa	Pressure 100 kPa	Pressure 120 kPa	Pressure 140 kPa
Mass of fraction -0.033 mm in drain, t	116.5	116.1	115.8	87.5	87.2	87.0	145.7	145.2	144.8
Mass fraction -0.033 mm in sands, t	26.1	25.7	25.4	42.3	41.6	41.1	9.1	8.9	8.8
d_{nom}, mm	0.037	0.038	0.040	0.040	0.041	0.043	0.034	0.036	0.037
Classification efficiency, %	42.7	42.4	42.0	42.1	41.5	41.1	43.1	42.9	42.6

Source: *compiled by the author*

Analysis of the results for three feed density values showed that an increase in the concentration of the solid phase in the pulp is accompanied by a systematic increase in the nominal separation size d_{nom}. At a pressure of 100 kPa, the d_{nom} value varies from 0.034 mm at a density of 1,198 g/l to 0.040 mm at a density of 1,277 g/l, which corresponds to an absolute increase of 0.006 mm or a relative increase of 17.6%. A similar trend is observed at other pressure values: at 120 kPa, d_{nom} increases from 0.036 to 0.041 mm (an increase of 0.005 mm or 13.9%), and at 140 kPa, from 0.037 to 0.043 mm (an increase of 0.006 mm or 16.2%). The results obtained indicate a decrease in the sharpness of the cut-off of fine classes in more concentrated pulp and a change in the conditions of sand flow formation. The study established that an increase in the feed pressure of the hydrocyclone throughout the entire range studied leads to an increase in d_{nom} regardless of the pulp density. In particular, for a density of 1,198 g/l, when the pressure increases from 100 to 140 kPa, d_{nom} increases from 0.034 to 0.037 mm (an increase of 0.003 mm or 8.8%), for a density of 1,231 g/l – from 0.037 to 0.040 mm (an increase of 0.003 mm or 8.1%), and for a density of 1,277 g/l – from 0.040 to 0.043 mm (an increase of 0.003 mm or 7.5%). This indicates the systemic nature of the influence of pressure as a parameter that determines the hydrodynamic mode of operation of the apparatus and the position of the limiting separation size, while the feed density acts as a factor that modifies the intensity of this influence.

Analysis of the relative distribution indicators of the -0.033 mm fraction shows that with an increase in both pressure and feed density, the yield of the fine fraction in the sand product decreases. At a pressure of 100 kPa, an increase in feed density from 1,198 to 1,277 g/l leads to a decrease in the yield of the -0.033 mm fraction in sand from 54.6 to 52.0 %, i.e. by 2.6 %, which corresponds to a relative decrease of 4.8 %. At a pressure of 140 kPa, a similar increase in density is accompanied by a decrease in this indicator from 53.1 to 50.6%, i.e. by 2.5% or 4.7% in relative terms. The decrease in the content of the fine fraction in the sand product with an increase in density is due to the general coarsening of the granulometric composition of the sands. A similar trend can be observed for the discharge product. At a pressure of 100 kPa, the yield of the -0.033 mm fraction in the discharge decreases from 88.6% at a density of 1,198 g/l to 87.7% at a density of 1,277 g/l, i.e. by 0.9% or 1.0% in relative terms. At a pressure of 140 kPa, the corresponding decrease is 1.0% (from 88.1 to 87.1%), which confirms the general trend towards a decrease in the specific proportion of fine particles in the discharge with an increase in the concentration of the solid phase.

The classification efficiency, determined by the Hancock parameter, decreases in the studied modes with both increasing pressure and increasing feed density. At a pressure of 100 kPa, an increase in density from 1,198 to 1,277 g/l leads to a decrease in efficiency from 43.1 to 42.1%, i.e. by 1.0% or 2.3% in relative terms. At a pressure of 140 kPa, the corresponding decrease is 1.5% (from 42.6 to 41.1%), which is equivalent to a relative decrease of 3.5%. The highest efficiency values are recorded at minimum pulp density and lower pressure values, while an increase in solid phase concentration leads to a systematic deterioration in the selectivity of the classification process. Thus, the results of the theoretical calculation confirm that a combined increase in pressure and feed density leads to an increase in the nominal separation size and a decrease in the efficiency of the classification process. To ensure clearer separation and increase the efficiency of the -0.033 mm fraction extraction, it is advisable to use moderate pressure values (100-120 kPa) in combination with a base or reduced feed density, which provides an optimal balance between process selectivity and hydrocyclone stability. To determine the effect of changing the diameter of the hydrocyclone discharge pipe on the separation of the 0.033 mm fraction, the efficiency of classification and the distribution of the fine class between sand and discharge products in the theoretical calculation used feed pressures of 100 and 120 kPa at an output product density of 1,230 g/l (solid content 24.5%). The diameter of the discharge pipe varied in the range of 130-170 mm. The obtained dependencies are shown in Figure 4.

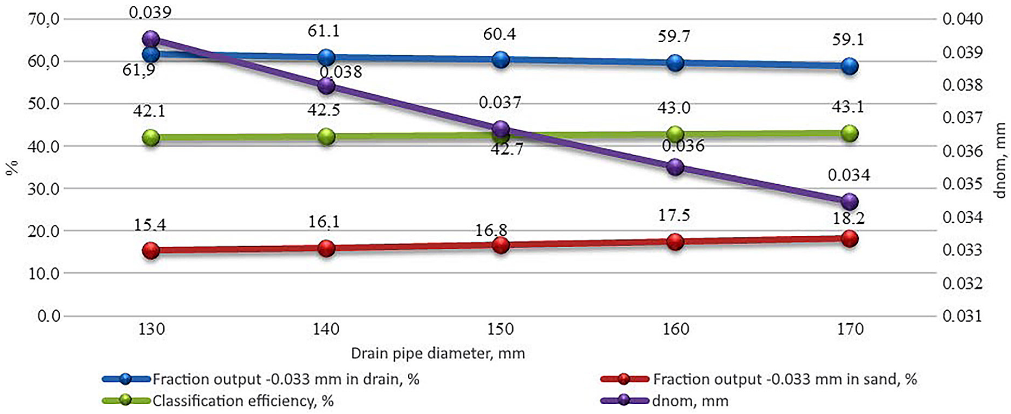

Figure 4. *Dependence of the classification indicators of the -0.033 mm fraction in a hydrocyclone at a feed pressure of 1.0 kgf/cm^2 on the diameter of the discharge pipe*
Source: *compiled by the author*

The obtained results demonstrate patterns of distribution of finely dispersed particles between the drain and sand products and substantiate the choice of the optimal diameter of the drain pipe (Fig. 5).

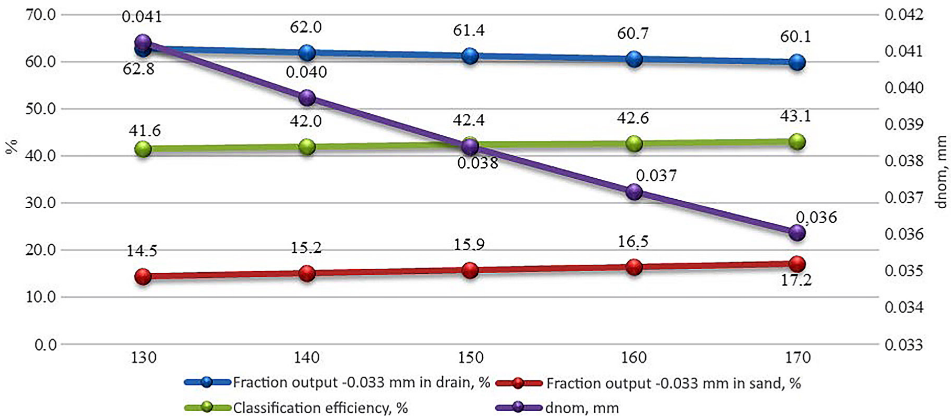

Figure 5. *Dependence of the classification indicators of the -0.033 mm fraction in a hydrocyclone at a feed pressure of 1.2 kgf/cm^2 on the diameter of the discharge pipe*
Source: *compiled by the author*

Analysis of the results obtained shows that the diameter of the discharge pipe is one of the determining design parameters that significantly affects the nominal separation size d_{nom}, classification efficiency, and distribution of the -0.033 mm fraction between hydrocyclone products. At a fixed feed density of 1,230 g/l and in the studied range of diameters, an increase in feed pressure from 100 to 120 kPa is accompanied by an increase in the nominal separation size and a decrease in classification efficiency. With a discharge pipe diameter of 130 mm, the value of d_{nom} increases from 0.039 to 0.041 mm, which corresponds to an absolute increase of 0.002 mm or a relative increase of 5.1%. A similar difference between the 100 and 120 kPa modes is maintained for other diameters, indicating a systematic effect of pressure on the position of the limit separation size. At the same time, an increase in the diameter of the discharge pipe in the range of 130-170 mm leads to a monotonous decrease in the nominal separation size. At a pressure of 100 kPa, d_{nom} decreases from 0.039 to 0.034 mm, which corresponds to an absolute decrease of 0.005 mm or a relative decrease of 12.8%. At a pressure of 120 kPa, the corresponding decrease is 0.005 mm (from 0.041 to 0.036 mm), which corresponds to a relative decrease of 12.2%. The results obtained indicate a shift in the limiting separation size towards finer classes with an increase in the cross-sectional area of the drain pipe, which is associated with a decrease in hydraulic resistance and a weakening of internal flow circulation.

At the same time, an increase in the diameter of the discharge pipe is accompanied by an increase in the yield of the -0.033 mm fraction in the sand product. At a pressure of 100 kPa, the yield of this fraction in sand increases from 15.4% at a diameter of 130 mm to 18.2% at a diameter of 170 mm, i.e. by 2.8%, which corresponds to a relative increase of 18.2%. At a pressure of 120 kPa, a similar trend is observed in the increase in the yield of the -0.033 mm fraction in the sand from 14.5 to 17.2%, i.e. by 2.7% or 18.6% in relative terms. This indicates an intensification of the removal of fine particles in the sand product when the diameter of the discharge pipe is excessively increased. The classification efficiency shows a moderate increase with an increase in the diameter of the discharge pipe. At a pressure of 100 kPa, the efficiency increases from 42.1% at a diameter of 130 mm to 43.1% at a diameter of 170 mm, which corresponds to an absolute increase of 1.0% or a relative increase of 2.4%. At a pressure of 120 kPa, efficiency increases from 41.6% to 43.1%, i.e. by 1.5% or 3.6%. The maximum efficiency values are recorded in the diameter range of 150-160 mm, after which a further increase in diameter does not lead to a significant increase in efficiency, but is accompanied by an increase in the loss of the fine fraction in the sand product. As a result of processing the calculated data, the dependence of classification efficiency on the diameter of the drain pipe at a pressure of 100 kPa is approximated by a linear equation:

$$\varepsilon = 0.2539x + 41.911,$$

where x – diameter of the hydrocyclone discharge pipe, mm. The coefficient of determination of the approximation is:

$$R^2 = 0.9807.$$

For a pressure of 120 kPa, the corresponding relationship is as follows:

$$\varepsilon = 0.3651x + 41.249,$$

where x – diameter of the hydrocyclone discharge pipe, mm. The coefficient of determination of the approximation is:

$$R^2 = 0.9925.$$

High values of approximation determination coefficients confirm the stable nature of the influence of the drain pipe diameter on the classification efficiency in the studied range. Thus, at a feed density of 1,230 g/l and a feed pressure of 100-120 kPa, the optimal operating mode of the hydrocyclone should be defined as the operation of a hydrocyclone with a discharge pipe diameter of 150-160 mm. Under these conditions, a balanced combination of reduced nominal separation size, increased classification efficiency and an acceptable level of loss of the -0.033 mm fraction in the sand product is ensured. To quantitatively assess the effect of the diameter of the sand nozzle of the hydrocyclone on the classification indicators of the -0.033 mm fraction, the following theoretical calculations were made: feed pressure of 100 kPa and 120 kPa, a drain pipe diameter of 150 mm, and an inlet feed density of 1,230 g/l. Under these conditions, an analysis was performed of the change in nominal separation size, classification efficiency, and distribution of the fine class between the sand and drain products when varying the diameter of the sand nozzle in the range of 68-84 mm. The dependencies obtained for different feed pressure values are shown in Figure 6, which shows the influence of the sand nozzle design parameter on the classification process under different hydrodynamic operating modes of the hydrocyclone.

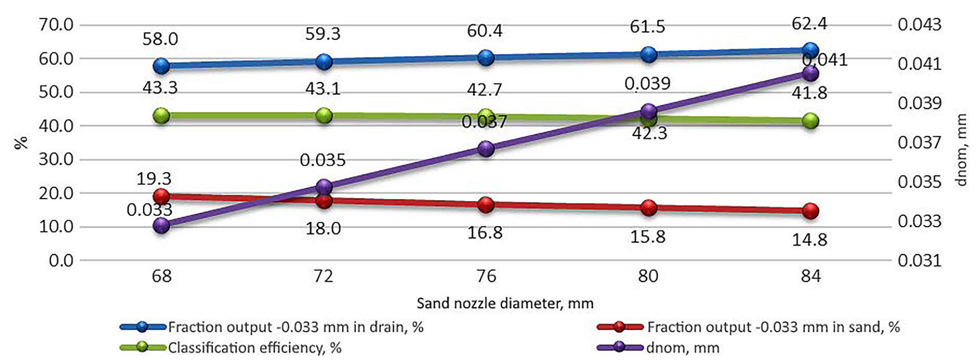

Figure 6. *Dependence of the classification indicators of the -0.033 mm fraction in a hydrocyclone at a feed pressure of 100 kPa on the diameter of the sand nozzle*

Source: *compiled by the author*

A change in the diameter of the sand nozzle significantly affects the conditions for unloading the sand product and, accordingly, the distribution of fine particles in the hydrocyclone. At different feed pressures, the nature of this dependence changes, which is reflected in the classification indicators for the -0.033 mm fraction. Figure 7 shows the results illustrating the effect of the sand nozzle diameter on the efficiency of fine class separation at feed pressures of 100 and 120 kPa.

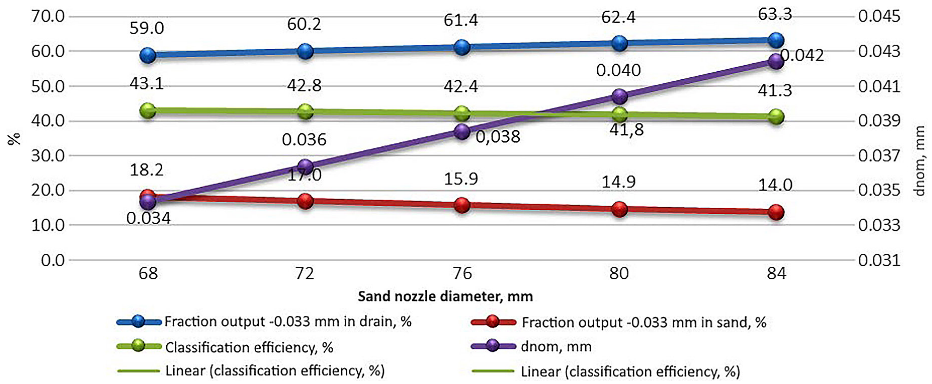

Figure 7. *Dependence of the classification indicators of the -0.033 mm fraction in a hydrocyclone at a feed pressure of 120 kPa on the diameter of the sand nozzle*

Source: *compiled by the author*

The analysis of the results showed that changing the diameter of the sand nozzle significantly affects the nature of the classification and distribution of the fine fraction of -0.033 mm between the hydrocyclone products at both 100 kPa and 120 kPa at a fixed feed density of 1,230 g/l. The patterns identified are stable and remain consistent across the entire range of diameters studied. With an increase in the diameter of the sand nozzle from 68 to 84 mm for both pressure values, there is an increase in the yield of the -0.033 mm fraction in the discharge product and a corresponding decrease in its yield in the sand product. At a pressure of 100 kPa, the yield of this fraction in the sand decreases from 19.3% to 14.8%, which corresponds to an absolute decrease of 4.5% and a relative decrease of 23.3%.

At a pressure of 120 kPa, the same indicator decreases from 18.2% to 14.0%, i.e. by 4.2%, which corresponds to a relative decrease of 23.1%. The recorded changes indicate a decrease in the carryover of fine particles into the sand product due to an increase in the cross-sectional area of the sand nozzle and a decrease in the hydrodynamic resistance of the sand flow. The nominal separation size d_{nom} increases monotonically with an increase in the diameter of the sand nozzle. For a pressure of 100 kPa, the value of d_{nom} increases from 0.033 to 0.041 mm, which corresponds to an absolute increase of 0.008 mm and a relative increase of 24.2%. For a pressure of 120 kPa, d_{nom} increases from 0.034 to 0.042 mm, i.e. by 0.008 mm, which corresponds to a relative increase of 23.5%. This indicates a shift in the maximum separation size towards larger values, which is associated with a decrease in the intensity of the centrifugal field in the sand flow formation zone and an increase in the probability of larger particles being swept into the drain.

The efficiency of classification gradually decreases with an increase in the diameter of the sand nozzle. The maximum efficiency values of 43.3-43.1% are achieved with a minimum nozzle diameter of 68 mm. When the diameter is increased to 84 mm, the efficiency decreases to 41.8% (100 kPa) and 41.3% (120 kPa). Thus, at a pressure of 100 kPa, the absolute decrease in efficiency is 1.5%, which corresponds to a relative decrease of 3.5%, and at a pressure of 120 kPa, it is 1.8%, or 4.1%. The decrease in efficiency indicates a deterioration in the selectivity of the process, caused by a simultaneous increase in d_{nom} and a decrease in the sharpness of the cut-off of fine classes. Analysis of absolute masses confirmed the established trends: with an increase in the diameter of the sand nozzle, the mass of the -0.033 mm fraction in the sand product decreases, while the mass of this fraction in the discharge changes insignificantly. This indicates a redistribution of fine particles between products without a significant change in their total amount and confirms the dominant influence of the design parameter of the sand nozzle on the selectivity of classification. As a result of processing the calculated data, the dependence of classification efficiency on the diameter of the sand nozzle at a pressure of 100 kPa is approximated by a linear equation:

$$\varepsilon = -0.3813x + 43.789,$$

where x – sand nozzle diameter, mm. The coefficient of determination of the approximation is:

$$R^2 = 0.9819.$$

For a pressure of 120 kPa, the corresponding relationship is as follows:

$$\varepsilon = -0.4723x + 43.692,$$

where – sand nozzle diameter, mm. Coefficient of determination of approximation:

$$R^2 = 0.9903.$$

Thus, the diameter of the sand nozzle is one of the key design parameters that determines the position of the maximum separation size and the efficiency of classification at fixed values of pressure and feed density. Under conditions of pressure 100-120 kPa, feed density of 1,230 g/l and a discharge pipe diameter of 150 mm, the optimal range of sand nozzle diameters is considered to be 72-76 mm, in which a balanced ratio between classification efficiency, d_{nom} value and permissible content of the -0.033 mm fraction in the sand product is achieved. Based on a comprehensive analysis of the influence of the operating and design parameters of the hydrocyclone, the study established that the classification efficiency and separation quality of the fine fraction of -0.033 mm are determined not by individual parameters, but by their coordinated combination. Changes in feed pressure, pulp density, drain pipe diameter and sand nozzle significantly affect the nominal separation size, process selectivity and distribution of the fine fraction between the drain and sand products.

According to theoretical calculations, the stud established that for a hydrocyclone with a diameter of 500 mm, the optimal operating mode, aimed at ensuring clear separation and an acceptable content of the -0.033 mm fraction in the sand product, is achieved with the following combination of parameters: pressure in the hydrocyclone within the range of 100-120 kPa, at which a stable hydrodynamic mode is formed without a significant increase in the nominal separation size; pulp feed density at 1,198-1,231 g/l, which ensures increased classification efficiency and better separation selectivity; drain pipe diameter of 150-160 mm, which provides a compromise between reducing d_{nom} and acceptable losses of the fine fraction in the sand product; sand nozzle diameter of 72-76 mm, which can combine sufficiently high classification efficiency with moderate values of nominal separation size and controlled content of the -0.033 mm fraction in the sand. The proposed combination of parameters can be recommended for practical application as a rational operating mode for GC-500 type hydrocyclones with the possibility of further adjustment depending on the requirements for the particle size distribution of the final products and the specific operating conditions of the enrichment plants.

The efficiency of classifying finely dispersed particles in hydrocyclone devices is a determining factor in the stability of closed grinding cycles and the energy efficiency of enrichment process schemes. Analysis of the results obtained for the GC-500 hydrocyclone battery showed that even relatively small changes in operating and design parameters lead to a significant shift in the limit separation size, which is particularly critical for fractions smaller than -0.033 mm. An increase in feed pressure is accompanied by an increase in the nominal separation size and a decrease in the selectivity of fine fraction classification. It has been established that when the pressure is increased from 80 to 200 kPa, the limit separation size of the -0.033 mm fraction increases from 0.035 to 0.044 mm, i.e. by 0.009 mm, which corresponds to a relative increase of 25.7%. This change in d_{nom} indicates a significant restructuring of the hydrodynamic regime in the apparatus and an increase in the proportion of finely dispersed particles that are mistakenly attributed to the sand product. From a physical point of view, an increase in feed pressure leads to an intensification of the tangential flow velocity, an increase in turbulent pulsations and an intensification of short-circuited flows in the near-axis zone of the hydrocyclone. As a result, fine particles, which under optimal conditions should be moved into the drain, are drawn into the peripheral flow and move into the sand. The scale of the relative increase in d_{nom} obtained in this study correlates with analytical estimates of L.R. Plitt (1976), according to which a 2-2.5-fold increase in feeding pressure causes an increase in d_{nom} by 20-30%. Similar trends are present in the industrial studies by S.K. Palaniandy *et al.* (2017), where an increase in feed pressure was accompanied by an increase in d_{nom} by 15-25%. Together, these results indicate that the effect of feed pressure on classification efficiency is systemic and manifests itself regardless of the type of hydrocyclone and the specific technological scheme.

Studies also show that the efficiency of hydrocyclone classification largely depends on feed characteristics, in particular on changes in the average particle size in the feed ($d_{50}f$). Q. Zhao *et al.* (2024), using experimental methods and CFD analysis, demonstrated that varying $d_{50}f$ in the range of approximately 0.020-0.060 mm with constant design and operating parameters of the hydrocyclone leads to a shift in the separation limit size (d_{50}) and a decrease in the selectivity of the process. At the same time, with a decrease in the average particle size and an increase in the proportion of fine fractions in the feed, the number of falsely separated particles that enter the sand product increases, even at stable values of pressure and pulp density. A decrease in the sharpness of the cut-off and deformation of the distribution curve are noted, which is most pronounced in the fine fraction range.

Pulp density is another key parameter that determines the nature of the separation of finely dispersed particles. When the pulp density increases from 1,198 to 1,277 g/l, the limit size of the fraction separation -0.033 mm increases by 0.005-0.006 mm, which corresponds to a relative increase in d_{nom} of 13.9-17.6%. The data obtained indicate a decrease in the sharpness of classification and an increase in the role of interparticle interactions. An increase in the concentration of the solid phase leads to an increase in the effective viscosity of the pulp and a decrease in the differences in the speeds of particles of different sizes. As a result, the effectiveness of centrifugal forces decreases, which has a particularly negative effect on the separation of fine fractions. Similar effects were noted by T.C. Rao *et al.* (1976), where an increase in pulp density was accompanied by a decrease in classification sharpness by 10-20%, as well as by M. Padhi *et al.* (2019), where the decrease in the extraction of the -0.020 mm fraction was 8-12% with an increase in the solid content in the pulp. Thus, the results obtained confirm that the influence of pulp density on d_{nom} displacement is universal in nature.

The geometric parameters of the hydrocyclone, in particular the diameters of the discharge pipe and sand nozzle, have a significant impact on the classification indicators. Increasing the diameter of the drain pipe from 130 to 170 mm reduces the maximum separation size by 0.005 mm, which corresponds to a relative decrease in d_{nom} of 12.2-12.8%. This is due to a decrease in the intensity of the short-circuited flow and stabilisation of the axial vortex, which contributes to more selective particle cutting. Quantitative confirmation of this mechanism is provided in the CFD study by T. Su & Y. Zhang (2022), where a reduction in the diameter of the discharge pipe led to a decrease in d_{nom} by 10-18% and a decrease in the intensity of the short-circuited flow by up to 30%. At the same time, the results of the study show that an excessive increase in the diameter of the discharge pipe is accompanied by an increase in the carryover of fine particles into the sand product. A similar trade-off between a decrease in d_{nom} and the loss of fine fractions was noted in the work of C. Zhang & S. Lu (2023), where the mass fraction of fine particles in the sand increased by 5-9% with unfavourable geometry of the discharge node. The study by M. Narasimha et al. (2006) was devoted to modelling large vortices in hydrocyclones to predict the diameter and shape of the air stem. The authors showed that the large vortex modelling method can accurately assess the flow structure inside a hydrocyclone, which is important for improving particle classification efficiency.

The study by J. Li *et al.* (2019) conducted a numerical analysis of the influence of different inlet designs, in particular involute and laminar-spiral shapes, on the internal flow and phase separation in hydrocyclones. The study demonstrated that the choice of a laminar-spiral configuration reduced energy consumption and better reduced the displacement of coarse and fine particles in the outlet flows compared to the standard involute configuration, especially at different particle concentrations and densities, indicating the potential of geometric optimisation to improve the separation process.

Changing the diameter of the sand nozzle also significantly affects the distribution of particles between the classification products. Increasing its diameter from 68 to 84 mm leads to an increase in the maximum separation size from 0.033 to 0.041 mm at a pressure of 100 kPa. This is due to a decrease in hydraulic resistance in the sand node and an increase in the rate of particle removal into the lower product. Similar quantitative patterns were presented by D. Hou *et al.* (2021), where the proportion of fine particles in the sand product increased by 6-10% when the geometry of the sand nozzle was changed. Modern CFD studies generalised the experimental patterns obtained and explained their hydrodynamic nature. E. Dianyu *et al.* (2024) demonstrated that changing the configuration of the inlet part of the hydrocyclone significantly changes the velocity structure, the position of the axial vortex, and the intensity of turbulent pulsations. This, in turn, leads to a shift in the separation limit size and a decrease in classification selectivity, especially for fractions smaller than 0.050 mm. The CFD results obtained explain well the changes in d_{nom} recorded in this study when varying the feed pressure and geometric parameters of the apparatus. L. Svarovsky (1984) conducted a detailed review of the design, principle of operation and application of hydrocyclones in industrial classification and particle separation. The author systematised the hydrodynamics of flow, factors affecting separation efficiency, and practical recommendations for the design and operation of hydrocyclones.

A summary of the results of this study and the literature data shows that the influence of feed pressure, pulp density, and the diameters of the discharge pipe and sand nozzle has a common physical nature and manifests itself in similar numerical ranges of change in the limit separation size. For industrial conditions, this means that increasing the intensity of the process by increasing the pressure or pulp concentration without hydrodynamic limitations can lead to an increase in the loss of fine fractions and a decrease in the overall efficiency of the technological scheme. The best classification results are achieved with a rational combination of operating and design parameters, which provides a compromise between separation selectivity and minimisation of losses of valuable fine-grained material.

Conclusions

The analysis of actual production data for the GC-500 hydrocyclone battery at enrichment plant No. 1 of PJSC Northern Mining and Enrichment Combine established that the classification efficiency for the -0.033 mm fraction in the third stage of classification is 39.27% according to the Hancock parameter, which indicates insufficient selectivity of the process and the presence of a significant reserve for optimising the operating modes of hydrocyclones. A mathematical classification model based on the calculation of mass balance, the Hancock parameter and the theoretical Bradley separation function has been developed, which adequately describes the hydrocyclone classification process. The relative error between the theoretical and actual class distribution indicators in sand and discharge products does not exceed 2%, which confirms the correctness of the applied model for engineering calculations and operating mode forecasting.

The study established that feed pressure is one of the key operating factors determining the nominal separation size and classification efficiency. With an increase in pressure from 80 to 200 kPa, the nominal separation size increases from 0.035 to 0.044 mm, which is accompanied by a coarsening of the granulometric composition of the products and a decrease in classification efficiency. The study demonstrated that an increase in feed pressure leads to a decrease in the mass and relative share of the -0.033 mm fraction in both sand and discharge products, which is due to a shift in the nominal particle size distribution towards larger classes and a deterioration in the selectivity of the process. A study of the effect of feed density showed that an increase in the concentration of the solid phase in the pulp is accompanied by an increase in the nominal separation size and a decrease in classification efficiency across the entire pressure range studied. The most favourable conditions for the separation of the fine fraction of -0.033 mm are achieved at base or reduced pulp density values.

The generalisation of the results showed the systematic nature of the influence of feed pressure on the classification process, regardless of pulp density, which confirms the decisive role of the hydrodynamic mode of operation of the hydrocyclone in determining the maximum separation size. Analysis of the influence of the discharge pipe diameter showed that its increase contributes to a decrease in the nominal separation size and an increase in classification efficiency, but is accompanied by an increase in the carryover of the -0.033 mm fraction into the sand product, which requires consideration of the quality requirements for sand. The study established that the diameter of the sand nozzle significantly affects the distribution of the fine fraction between the products of the hydrocyclone. With an increase in its diameter, the content of the -0.033 mm fraction in the sand decreases and its discharge increases, while at the same time, there is an increase in the nominal separation size and a decrease in classification efficiency.

Based on a comprehensive analysis of operating and design parameters, the optimal operating conditions for the GC-500 hydrocyclones have been determined: feed pressure of 100-120 kPa, output product density of about 1,230 g/l, discharge pipe diameter of 150-160 mm, and sand nozzle diameter of 72-76 mm, at which a compromise is achieved between classification efficiency, nominal separation size, and permissible content of fine particles in the sand product. The results obtained provide a basis for further research aimed at substantiating the optimal operating modes of hydrocyclone batteries at ore processing plants, in-depth analysis of factors affecting classification selectivity, and the development of approaches to reduce losses of fine classes and increase the stability of enrichment performance indicators.

Acknowledgements

None.

Funding

None.

Conflict of Interest

None.

References

[1] Bradley, D. (1965). *The hydrocyclone*. Oxford: Pergamon Press.

[2] Costa, B.S., Bergerman, M.G., & Delboni Júnior, H. (2024). Comparing the performance of hydrocyclones and high-frequency screens in an industrial grinding circuit: Part I – size separation assessments. *Minerals*, 14(7), article number 707. doi: 10.3390/min14070707.

[3] Hou, D., Cui, B., Zhao, Q., Wei, D., Song, Z., & Feng, Y. (2021). Research on the structure of the cylindrical hydrocyclone spigot to mitigate the misplacement of particles. *Powder Technology*, 387, 61-71. doi: 10.1016/j.powtec.2021.04.013.
[4] Jankovic, A. (2022). Comminution and classification technologies of iron ore. In L. Lu (Ed.), *Iron ore: Mineralogy, processing and environmental sustainability* (pp. 269-308). Cambridge: Woodhead Publishing. doi: 10.1016/B978-0-12-824055-7.00021-0.
[5] Li, J., Kuang, S., & Yu, A. (2019). Numerical investigation of hydrocyclone feed inlet configurations for mitigating particle misplacement. *Industrial & Engineering Chemistry Research*, 58(36), 16823-16833. doi: 10.1021/acs.iecr.9b01203.
[6] Lima, J.L., Roberto, J.B., Leite, I.A., de Sá, D.V., Antunes, T.P.M., Matos, V.F., & Oliveira, G.S. (2023). Increased mass recovery from desliming at Vargem Grande 2 using the new model Cavex 2 (CVD) hydrocyclone. In *Anais do 22º simpósio de mineração* (pp. 142-151). São Paulo: Editora Blucher. doi: 10.5151/2594-357X-39698.
[7] Liu, P., Wang, X., Jiang, L., Zhang, Y., Yang, X., Li, X., & Wang, H. (2023a). Effect of spiral vanes width on the separation performance of a hydrocyclone. *Physicochemical Problems of Mineral Processing*, 59(6), article number 173563. doi: 10.37190/ppmp/173563.
[8] Liu, P., Wang, X., Jiang, L., Zhang, Y., Yang, X., Li, X., & Wang, H. (2023b). Flow field characteristics and separation performance of prismatic hydrocyclone. *Physicochemical Problems of Mineral Processing*, 61(2), article number 203011. doi: 10.37190/ppmp/203011.
[9] Mahat, M.M., Husain, H., & Mohamad, N.S. (2023). Separation efficiency analysis of multiphase flow inside hydrocyclone using CFD. *Journal of Applied Engineering Design and Simulation*, 3(1), 51-65. doi: 10.24191/jaeds.v3i1.62.
[10] Narasimha, M., Brennan, M., & Holtham, P.N. (2006). Large eddy simulation of hydrocyclone – prediction of air-core diameter and shape. *International Journal of Mineral Processing*, 80(1), 1-14. doi: 10.1016/j.minpro.2006.01.003.
[11] Padhi, M., Mangadoddy, N., Sreenivas, T., Vakamalla, T.R., & Mainza, A.N. (2019). Study on multi-component particle behaviour in a hydrocyclone classifier using experimental and computational fluid dynamics techniques. *Separation and Purification Technology*, 229, article number 115698. doi: 10.1016/j.seppur.2019.115698.
[12] Palaniandy, S.K., Yahyaei, M., & Powell, M. (2017). Assessment of hydrocyclone operation in gravity induced stirred mill circuits. *Minerals Engineering*, 108, 83-92. doi: 10.1016/j.mineng.2017.01.002.
[13] Plitt, L.R. (1976). *A mathematical model of the hydrocyclone classifier*. Montreal: Canadian Institute of Mining, Metallurgy and Petroleum.
[14] Rao, T.C., Nageswararao, K., & Lynch, A.J. (1976). Influence of feed inlet diameter on the hydrocyclone behaviour. *International Journal of Mineral Processing*, 3(4), 357-363. doi: 10.1016/0301-7516(76)90023-5.
[15] Su, T., & Zhang, Y. (2022). Effect of the vortex finder and feed parameters on the short-circuit flow and separation performance of a hydrocyclone. *Processes*, 10(4), article number 771. doi: 10.3390/pr10040771.
[16] Svarovsky, L. (1984). *Hydrocyclones*. London: Holt, Rinehart & Winston.
[17] Uysal, M.T., Enisoglu, F., & Kara, Y. (2024). Investigation of hydrocyclone modernization in Küre copper ore regrinding circuit and its effect on grinding performance. In *Proceedings of the 10th world congress on mechanical, chemical, and material engineering (MCM'24)* (article number MMME 109). Barcelona: International ASET Inc. doi: 10.11159/mmme24.109.
[18] Zhang, C., & Lu, S. (2023). CFD study on the influences of size distribution and density of magnetite ore particles on hydrocyclone classification process. *Powder Technology*, 427, article number 118711. doi: 10.1016/j.powtec.2023.118711.
[19] Zhao, Q., Cui, B., Ji, A., Song, T., & Shen, Y. (2024). Experimental and numerical study of the effect of particle size distribution on hydrocyclone classification. *Advanced Powder Technology*, 35, article number 104398. doi: 10.1016/j.apt.2024.104398.
[20] Zhou, W., Wang, S., Cai, C., Liu, L., & Zhu, J. (2022). Experimental research and practice of mineral separation from flotation tailings based on self-spinning hydrocyclones. *Processes*, 10(8), article number 1478. doi: 10.3390/pr10081478.

Тетяна Олійник

Доктор технічних наук, професор
Криворізький національний університет
50027, вул. В. Матусевича, 11, м. Кривий Ріг, Україна
https://orcid.org/0000-0002-0315-7308

Євген Безсмертний

Аспірант
Криворізький національний університет
50027, вул. В. Матусевича, 11, м. Кривий Ріг, Україна
https://orcid.org/0009-0008-2209-7567

Вплив режимних і конструктивних параметрів гідроциклона на ефективність класифікації тонких фракцій

Анотація. Метою дослідження було вивчення роботи батареї гідроциклонів ГЦ-500, яка експлуатується у циклі третьої стадії класифікації на збагачувальній фабриці гірничо-збагачувального підприємства Криворізького залізорудного басейну, з метою оцінки її ефективності та оптимізації процесу поділу частинок. Основну увагу зосереджено на аналізі впливу тиску живлення, щільності пульпи, діаметра зливного патрубка та діаметра піскової насадки на номінальну крупність розділення, ефективність класифікації та розподіл фракції -0,033 мм між пісковим і зливним продуктами. Дослідження виконано з використанням фактичних виробничих даних і теоретичного моделювання процесу класифікації. Методика дослідження базувалась на розрахунку масового балансу, визначенні ефективності класифікації за параметром Хенкока та застосуванні теоретичної моделі Бредлі для оцінки номінальної крупності розділення і побудови кривої розподілу частинок за крупністю. Встановлено, що фактична ефективність класифікації фракції -0,033 мм становить 39,27 %, а результати теоретичного моделювання узгоджуються з промисловими даними з абсолютною похибкою менш як 2 %, що підтверджує коректність застосованого підходу для інженерних розрахунків. Показано, що підвищення тиску та щільності живлення призводить до зростання номінальної крупності розділення та зниження ефективності класифікації внаслідок зміни гідродинамічного режиму роботи гідроциклона. Водночас збільшення діаметра зливного патрубка сприяє зменшенню граничної крупності розділення та підвищенню ефективності процесу, однак супроводжується зростанням вмісту тонкої фракції у пісковому продукті. Зміна діаметра піскової насадки істотно впливає на розподіл тонких частинок і селективність процесу класифікації. На підставі отриманих результатів обґрунтовано раціональні параметри роботи гідроциклонів, які забезпечують компроміс між ефективністю класифікації та якістю продуктів і можуть бути використані для оптимізації режимів роботи гідроциклонних батарей на збагачувальних фабриках

Ключові слова: номінальна крупність розділення; ефективність класифікації; щільність пульпи; зливний патрубок; піскова насадка

ГІРНИЧИЙ ВІСНИК

Том 59, № 2
2025

Заснований у 1966 р.
Виходить два рази на рік

Підписано до друку 24.12.2025
Формат 60*84/8
Ум. друк. арк. 8,4
Наклад 100 прим.

Контактна адреса:
Криворізький Національний Університет
50027, вул. В. Матусевича, 11, м. Кривий Ріг, Україна
Тел.: +38 (056) 409-06-06
E-mail: info@mining-journal.com.ua
https://mining-journal.com.ua/uk

MINING JOURNAL
Kryvyi Rih National University

Volume 59, No. 2
2025

Founded in 1966.
Published 2 times per year.

Managing Editor:
S. Tikhlivets

Editing Bibliographic Lists:
S. Tikhlivets

Signed to the print 24.12.2025
Format 60*84/8
Conventional Printed Sheet 8.4
Circulation 100 copies

Address for contacts:
Kryvyi Rih National University
50027, 11 Vitalii Matusevich Str., Krivyi Rih, Ukraine
Tel.: +38 (056) 409-06-06
E-mail: info@mining-journal.com.ua
https://mining-journal.com.ua/en